

BEHAVIOR OF ONE-WAY SLABS REINFORCED
WITH DEFORMED WIRE AND DEFORMED WIRE FABRIC

by

John P. Lloyd

Clyde E. Kesler

Prepared as a Part of an Investigation

Conducted by

THE ENGINEERING EXPERIMENT STATION

THE DEPARTMENT OF THEORETICAL AND APPLIED MECHANICS

UNIVERSITY OF ILLINOIS

in Cooperation With

THE WIRE REINFORCEMENT INSTITUTE

April 28, 1969

Urbana, Illinois 61801

ACKNOWLEDGMENT

The investigation reported here was conducted as a project of the Engineering Experiment Station at the University of Illinois in the Department of Theoretical and Applied Mechanics, under the sponsorship of the Wire Reinforcement Institute.

The authors express their gratitude to all who contributed to the success of this investigation.

TABLE OF CONTENTS

1. SUMMARY AND CONCLUSIONS.	Page 1
1.1 Flexural Cracking	2
1.2 Splices	3
1.3 Anchorage and Shear	4
1.4 Flexural Strength	6
2. INTRODUCTION	8
2.1 Statement of the Problem.	8
2.2 Objective and Scope	8
2.3 Notation.	9
3. EXPERIMENTAL PROGRAM	13
3.1 Specimens	13
3.2 Designation of Specimens.	13
3.3 Materials	14
3.3.1 Concrete	14
3.3.2 Reinforcement.	14
3.4 Experimental Procedure.	15
4. FLEXURAL CRACKING.	16
4.1 Background.	16
4.1.1 Problem.	16
4.1.2 Factors Which Affect Cracking.	16
4.1.3 Proposed Methods of Estimating Crack Widths.	19
4.2 Experimental Results.	21
4.2.1 Crack Formation.	21
4.2.2 Crack Spacings and Widths.	22
4.3 Discussion of Results	22
4.3.1 Crack Spacing.	22
4.3.2 Maximum Crack Widths	23
4.3.3 Average Crack Widths	24
4.4 Summary and Conclusions	25
5. SPLICES.	26
5.1 Background.	26
5.1.1 Problem.	26
5.1.2 Present Design Approaches.	26

TABLE OF CONTENTS (Continued)

	<u>Page</u>
5.2 Experimental Results.	27
5.2.1 General.	27
5.2.2 Deformed Wires and Deformed Bars	28
5.2.3 Deformed Wire Fabric	28
5.3 Discussion of Results	29
5.3.1 Deformed Wires and Deformed Bars	29
5.3.1.1 Type of Failure	29
5.3.1.2 Analysis of Deformed Wire and Deformed Bar Splices	30
5.3.2 Deformed Wire Fabric	31
5.3.2.1 Type of Failure	31
5.3.2.2 Analysis of Deformed Wire Fabric Splices.	31
5.3.3 Discussion	32
5.3.3.1 General	32
5.3.3.2 Influence of Longitudinal Overhang on Splice Strength	34
5.3.3.3 Influence of the Number of Transverse Wires in Lap on Splice Strength	34
5.4 Splice Design Considerations.	35
5.4.1 General.	35
5.4.2 Deformed Wire.	37
5.4.3 Deformed Wire Fabric	38
5.5 Summary and Conclusions	39
6. ANCHORAGE AND SHEAR.	41
6.1 Background.	41
6.1.1 Problem.	41
6.1.2 Factors Which Affect Anchorage and Shear	41
6.1.3 Present Design Approaches.	42
6.2 Experimental Results.	43
6.2.1 General.	43
6.2.2 Development of Diagonal Cracks	44
6.2.3 Anchorage and Splitting.	45
6.3 Discussion of Results	46
6.3.1 General.	46

TABLE OF CONTENTS (Concluded)

	<u>Page</u>
6.3.2 Analysis of Diagonal Tension.	47
6.3.3 Analysis of Anchorage and Splitting	48
6.3.4 Discussion.	51
6.3.4.1 Diagonal Tension	51
6.3.4.2 Anchorage and Splitting.	52
6.3.4.3 Smooth Wire Fabric	53
6.4 Anchorage Design Considerations.	54
6.4.1 General	54
6.4.2 Deformed Wires.	55
6.4.3 Deformed Wire Fabric.	56
6.5 Summary and Conclusions.	57
7. FLEXURAL STRENGTH	58
7.1 Background	58
7.1.1 Problem	58
7.1.2 Present Design Approaches	60
7.2 Experimental Results	60
7.3 Discussion of Results.	61
7.4 Conclusions.	62
LIST OF REFERENCES.	64
APPENDIX A1 PULL-OUT TESTS	64
A1.1 General.	64
A1.2 Specimens.	65
A1.3 Experimental Procedure	66
A1.4 Experimental Results	66
A1.5 Discussion of Results.	68
A1.6 Conclusions.	70
APPENDIX A2 MEANS OF CRACK CONTROL IN THE BUILDING CODE.	72
APPENDIX A3 EXAMPLES OF SPLICE DESIGNS	75
TABLES.	115
FIGURES	

LIST OF TABLES

	<u>Page</u>
TABLE 1	OUTLINE OF CRACK CONTROL SPECIMENS 75
TABLE 2	OUTLINE OF SPLICE SPECIMENS. 77
TABLE 3	MIX PROPORTIONS. 85
TABLE 4	CONCRETE PROPERTIES OF CRACK CONTROL SLABS 86
TABLE 5	CONCRETE PROPERTIES OF SLABS WITH SPLICES. 87
TABLE 6	STRENGTH AND GEOMETRY OF BARS. 89
TABLE 7	STRENGTH AND GEOMETRY OF DEFORMED WIRE 90
TABLE 8	STRENGTH PROPERTIES OF FABRIC. 91
TABLE 9	CRACK SPACING IN CONSTANT MOMENT REGION. 92
TABLE 10	CRACK WIDTHS IN SLABS AT THE LEVEL OF REINFORCEMENT. . . 93
TABLE 11	CRACK WIDTHS IN SLABS AT THE EXTREME TENSILE FIBER . . . 95
TABLE 12	EQUATIONS FOR MAXIMUM CRACK WIDTH. 96
TABLE 13	RESULTS OF STATIC TESTS OF SLABS WITH SPLICES. 97
TABLE 14	OUTLINE OF ANCHORAGE SPECIMENS 100
TABLE 15	SPECIMENS WHICH FAILED IN THE SHEAR SPAN 105
TABLE 16	RESULTS OF DIAGONAL TENSION ANALYSIS 108
TABLE 17	RESULTS OF ANCHORAGE ANALYSIS. 109
TABLE 18	SPECIMENS WHICH FAILED IN FLEXURE. 111
TABLE A.1	PROPERTIES OF CONCRETE 112
TABLE A.2	PULL-OUT DATA. 113
TABLE A.3	ULTIMATE BOND STRESS 114

LIST OF FIGURES

		<u>Page</u>
Fig. 1	Typical Deformed Wires.	115
Fig. 2	Average Stress-Strain Curves for Deformed Bars. . .	115
Fig. 3	Average Stress-Strain Curves for Deformed Wires . .	116
Fig. 4	Average Stress-Strain Curves for Deformed Wires . .	116
Fig. 5	Average Stress-Strain Curves for Longitudinal Wires from Fabric	117
Fig. 6	Average Stress-Strain Curves for Longitudinal Wires from Fabric	117
Fig. 7	Typical Deformed Wires.	118
Fig. 8	Maximum Crack Widths at the Extreme Tensile Face. .	118
Fig. 9	Maximum Crack Widths at the Level of Reinforcement.	119
Fig. 10	Average Crack Widths at the Extreme Tensile Face. .	119
Fig. 11	Average Crack Widths at the Level of the Reinforcement	120
Fig. 12	Effectiveness of Laps in Slabs Reinforced with Deformed Wire and Deformed Bars	120
Fig. 13	Effectiveness of Laps in Slabs Reinforced with Deformed Wire Fabric.	120
Fig. 14	Bond Stress Coefficient Obtained with Splices of Deformed Wires and Deformed Bars.	121
Fig. 15	Splice Details.	121
Fig. 16	Comparison of Measured and Calculated Effectiveness	122
Fig. 17	Influence of Longitudinal Overhand on Splice Effectiveness	122
Fig. A.1	Pull-Out Specimens.	123
Fig. A.2	Test Setup.	123
Fig. A.3	Stress-Slip Curves for Specimens with D10 Longitudinal Wire	124
Fig. A.4	Stress-Slip Curves for Specimens with Unbonded D10 Longitudinal Wire and D4 Transverse Wire.	124
Fig. A.5	Stress-Slip Curves for Specimens with D10 Longitudinal Wire and D4 Transverse Wire.	124
Fig. A.6	Stress-Slip Curves for Specimens with D19 Longitudinal Wire	125
Fig. A.7	Stress-Slip Curves for Specimens with Unbonded D19 Longitudinal Wire and D9 Transverse Wire.	125

LIST OF FIGURES (Concluded)

	<u>Page</u>
Fig. A.8 Stress-Slip Curves for Specimens with D19 Longitudinal Wire and D9 Transverse Wire	125
Fig. A.9 Stress-Slip Curves for Specimens with D21 Longitudinal Wire.	126
Fig. A.10 Stress-Slip Curves for Specimens with Unbonded D21 Longitudinal Wire and D7 Transverse Wire	126
Fig. A.11 Stress-Slip Curves for Specimens with D21 Longitudinal Wire and D7 Transverse Wire	126
Fig. A.12 Stress-Slip Curves for Specimens with D29 Longitudinal Wire.	127
Fig. A.13 Stress-Slip Curves for Specimens with Unbonded D29 Longitudinal Wire and D11 Transverse Wire.	127
Fig. A.14 Stress-Slip Curves for Specimens with D29 Longitudinal Wire and D11 Transverse Wire.	127
Fig. A.15 Shear Area per Inch Necessary for 70,000 psi at Various Embedment Lengths (18)	128
Fig. A.16 Relationship Between Shearing Area per Inch and Ultimate Bond Stress	128
Fig. A.17 Maximum Crack Widths at the Extreme Tensile Fiber versus Z	129

1. SUMMARY AND CONCLUSIONS

A thorough understanding of the crack control, splicing and anchorage characteristics of reinforcement is essential for safe and economical designs. The investigation reported here was conducted to obtain this information for deformed wire fabric. Information concerning deformed wire was also obtained.

Sixty-three slabs reinforced with either deformed wires, deformed bars or deformed wire fabric were tested. All fabrics met or exceeded pertinent ASTM specifications except that some fabric was intentionally supplied with low weld shear strengths. The slabs were 2 ft wide, 5 or 7 in. deep and simply supported on a 6-ft span. Two equal, symmetrically placed loads were continuously applied until failure occurred.

The results of tests were analyzed and compared to results obtained in other studies using smooth wire fabric and deformed bars. The findings and design recommendations or considerations for the various phases are as follows:

1.1 Flexural Cracking

Twenty-three slabs reinforced with deformed bars, deformed wires or deformed wire fabric were tested to determine crack controlling characteristics of each type of reinforcement. Crack spacings and crack widths, both at the level of the reinforcement and at the extreme tensile fiber, were obtained for calculated steel stresses of 30,000, 40,000, 50,000 and 60,000 psi. No apparent difference existed in the crack spacings for the various styles of reinforcement. The maximum crack widths at the extreme tensile fiber and at the level of the reinforcement were compared to the crack widths predicted by equations which were developed by Gergely and Lutz (5)*.

At the extreme tensile fiber:

$$w'_{\max} = 0.076 \sqrt[3]{t_b A} Rf_s \times 10^{-6}$$

* Numbers in parentheses refer to entries in the list of references.

At the level of the reinforcement:

$$w_{\max} = \frac{0.076 \sqrt[3]{t_s A}}{1 + 2t_s/3h_1} f_s \times 10^{-6}$$

where:

- w'_{\max} = maximum crack width at the extreme tensile fiber, in.
- w_{\max} = maximum crack width at the level of the reinforcement, in.
- t_b = thickness of concrete cover measured from the extreme tensile fiber to the center of the wire or bar located closest thereto, in.
- t_s = side cover measured from center of outer bar or wire, in.
- A = average effective concrete area around a reinforcing bar, sq in.
- $R = h_2/h_1$
- h_2 = distance from the extreme tensile fiber to the neutral axis, and
- h_1 = distance from the centroid of the tensile reinforcement to the neutral axis.

Crack widths at the level of the reinforcement obtained by Atlas et al (7) in an earlier study of the crack control characteristics of smooth wire fabric were also considered. It was found that the Gergely and Lutz equations correctly predicted the width of cracks in slabs reinforced with deformed wire and smooth and deformed wire fabrics. Statistical analyses indicated that, at the 0.95 level, for similarly placed reinforcement there was no significant difference between the widths of cracks obtained with deformed bars, deformed wires, deformed wire fabric and smooth wire fabric. The low weld shear strengths in some of the fabric did not have an adverse effect on the width of cracks.

It may be concluded that:

1. Deformed wire, deformed wire fabric, deformed bars and smooth wire fabric, with transverse wire spacings as great as 12 in., control cracks equally well in one-way slabs of the type tested when the reinforcement is similarly placed, and

2. The equations developed by Gergely and Lutz correctly predict maximum crack widths in one-way slabs of the type tested here.

1.2 Splices

Forty slabs containing splices of deformed bars, deformed wires and deformed wire fabric were tested. It was found that the strength of a splice was limited by either a bond failure or a shearing failure of the concrete between the lapped layers of the reinforcement.

Expressions were developed which relate the strength of a splice to the strength of the concrete, the strength of welds, bond, and lap geometry. These expressions were modified to permit a designer to determine the necessary length of lap when wire and fabric just meet minimum ASTM specifications.

For deformed wires the necessary length of lap is given by

$$\ell = 0.045 D f_y / \sqrt{f'_c}$$

where:

ℓ = length of lap, in.

D = nominal diameter of the wire, in.

f_y = yield strength of reinforcement, psi, and

f'_c = compressive strength of concrete, psi

For deformed wire fabric the length of the lap must be

$$\ell = 0.045 D (f_y - 20,000 \text{ N}) / \sqrt{f'_c}$$

where:

ℓ = length of lap, in.

f_y = yield strength of reinforcement, psi

N = number of pairs of transverse wires in lap (see Fig. 15), and

f'_c = compressive strength of concrete, psi.

When a reinforcement to be spliced has a close lateral spacing, a bond splitting failure can occur. For this reason, the ACI Building Code (1) increases the lap length 20 per cent in splices where the reinforcement is spaced closer than 12 diameters. The splice lengths obtained from the two preceding equations already include the 20 per cent increase and, therefore may be reduced one-sixth when the reinforcement has a lateral spacing greater than 12 D .

To prevent splitting of the concrete the distance between outermost transverse wires must be

$$\ell_s = p d \left[\frac{f_y}{3.5 \sqrt{f'_c}} - \frac{8 \ell_o}{D} \right] \text{ or } \frac{A_w}{S_\ell} \left[\frac{f_y}{3.5 \sqrt{f'_c}} - \frac{8 \ell_o}{D} \right]$$

where:

ℓ_s = distance between outermost transverse wires in lap, in.

p = reinforcement ratio

d = effective depth of reinforcement, in.

f_y = yield strength of reinforcement, psi.

f'_c = compressive strength of concrete, psi.

ℓ_o = total length of longitudinal overhang in lap, in.,

D = nominal diameter of reinforcement, in.

A_w = area of individual wire to be spliced, sq in.

S_ℓ = spacing of wires to be spliced, in.

or if $f_y = 70,000$ psi and $f'_c = 3000$ psi,

$$\ell_s = p d (360 - 8 \ell_o / D) \text{ or } \frac{A_w}{S_\ell} (360 - 8 \ell_o / D)$$

The above splice equations are based on ultimate strength design concepts. They express the splice length required when the calculated ultimate moment fully develops the yield strength of the steel, in many cases an excess amount of steel will exist at the location of a splice and the yield strength of the reinforcement need not be developed to resist the imposed loading; in such cases, the splice length may be reduced by replacing the yield strength, f_y , in the above equations by the calculated steel stress, f_s , or by multiplying the lengths given by the above equations by the ratio of the design stress to the yield strength. The latter method is approximate and conservative for fabric reinforcement and compatible with the techniques used for deformed bars in the ACI Building Code.

1.3 Anchorage and Shear

Fifteen of the 63 slabs tested in the crack control and splicing studies failed in the shear span. The slabs were intentionally subjected

to high shears and anchorage stresses. It was found that the ACI-ASCE Committee 326 expression for diagonal tension strength* provided a conservative estimate of the shear strength of slabs reinforced with deformed wire and deformed wire fabric.

The results indicated that depending on the spacing of longitudinal wires and the location of transverse wires in the anchorage zone, anchorage was limited by bond or bond plus weld strengths or the shearing strength of the concrete. Expressions were developed to determine the development length, L'' , necessary to develop a desired steel stress, f_s , for reinforcements just meeting minimum ASTM specifications.

For deformed wire reinforcement, the development length must be at least

$$L'' = 0.03 f_y D / \sqrt{f'_c}$$

where:

L'' = development length, in.

f_y = yield strength of reinforcement, psi.

D = nominal diameter of reinforcement, in., and

f'_c = compressive strength of concrete, psi.

For deformed wire fabric the development length must be at least

$$L'' = 0.03 D (f_y - 20,000 \text{ N}) / \sqrt{f'_c}$$

where:

L'' = development length, in.

D = nominal diameter of reinforcement, in.

f_y = yield strength of reinforcement, psi.

N = number of welds in the development length which are at least 2 in. from the critical section, and

f'_c = compressive strength of concrete, psi.

$$*V = b d \sqrt{f'_c} \left[1.9 + (2500 \text{ psi}) \frac{p V d}{M \sqrt{f'_c}} \right] \text{ but not } > 3.5 b d \sqrt{f'_c}, \text{ where}$$

b = width of beam, in.; d = effective depth of beam, in.; f'_c = compressive strength of concrete, psi; p = steel ratio; V/M = ratio of shear to moment at the section considered, in.

When the wires being developed are 12 D or further apart, the lengths given by the two preceding equations may be reduced by one-sixth.

To prevent splitting anchorage type failures in the concrete the development length for both the deformed wire and the deformed wire fabric must be at least

$$L'' = \frac{p d f_y}{5.25 \sqrt{f'_c}} \quad \text{or} \quad \frac{A_w f_y}{5.25 S_\ell \sqrt{f'_c}}$$

where:

L'' = development length, in.

p = reinforcement ratio

d = effective depth of reinforcement, in.

f_y = yield strength of reinforcement, psi.

A_w = area of individual wire to be spliced, sq in., and

S_ℓ = spacing of wires to be spliced, in.

When ultimate strength design procedures are used but the design stress is less than the yield strength the actual design stress may be substituted in these equations.

1.4 Flexural Strength

The results of 11 slabs which failed either by crushing of the concrete or by tensile failure of the reinforcement were studied. It was found that the experimental strengths were approximately equal to the strength predicted by Eq 16-1 of the ACI Building Code if, in computations,

$$M_u = \phi [A_s f_y (d - \frac{A_s f_y}{1.7 f'_c b})] \times 10^{-3}$$

where:

M_u = ultimate moment, in.-kips.

ϕ = capacity reduction factor.

A_s = area of tensile reinforcement, sq in.

f_y = yield strength of the reinforcement, psi.

d = effective depth, in.

f'_c = compressive strength of concrete, psi.

b = width of compressive face of flexural member, in.

the ultimate tensile strength of the reinforcement is used in place of the yield strength. A design ultimate moment calculated by Eq 16-1 with a yield strength of 70,000 psi will provide a conservative estimate of the strength of a member reinforced with deformed wires or deformed wire fabric.

2. INTRODUCTION

2.1 Statement of the Problem

In the United States the "ACI Building Code Requirements for Reinforced Concrete", is incorporated in most municipal building codes. The ACI Building Code (1)* specified the minimum requirements for design and construction which will lead to safe and serviceable structures. When a new construction material such as deformed wire fabric is marketed, code writing bodies must determine, normally from experimental results, what minimum requirements shall apply for its use.

The proper design of reinforced concrete members involves a number of considerations, one of which is adequate flexural strength. The fact that deformed wire fabric is composed of high strength, cold-drawn wires does not pose any special difficulties so far as flexural strength is concerned. However, other design considerations such as control of flexural cracks, splices, and anchorage are directly related to the bonding characteristics or shear weld strengths of the reinforcement or both. Since deformed wire fabric neither conforms to the deformation requirements of deformed bars nor to the weld strength requirements of smooth wire fabric, it is necessary to undertake a research program to develop information so that present design concepts could be extended to include this product.

2.2 Objective and Scope

The objective of this program is to determine the crack control, splicing, anchorage, and flexural strength properties of deformed wire and deformed wire fabric used to reinforce one-way concrete slabs. It is intended, whenever possible, to compare these properties with the properties of deformed bars and smooth wire fabric reinforcement by means of tests and the study of earlier research results. It is also intended to study the applicability of current or proposed design procedures to slabs reinforced with deformed wire and deformed wire fabric; when appropriate alternate design procedures will be suggested.

This study is based upon the results from tests of 63 one-way flexural slabs of normal weight concrete reinforced with deformed wire,

*Numbers in parentheses refer to entries in the List of References.

deformed wire fabric and deformed bars. The results from a limited number of pull-out tests of deformed wire and deformed wire fabric samples are also given.

This report is organized as follows: Chapter 3 contains various details concerning the entire program; Chapters 4, 5, 6 and 7 are sufficiently complete in themselves that the reader may if he desires consider separately the various studies; and Chapter 1 contains a brief summary of the results obtained in each of the studies.

2.3 Notation

The symbols used in this report are:

- A = effective tension area of concrete surrounding the tension reinforcing bars or wires and having the same centroid as that of the reinforcement, divided by the number of bars or wires, sq in.
- A_e = effective area of concrete in tension, sq in.
- A_s = area of tensile reinforcement, sq in.
- A_w = area of a longitudinal wire, sq in.
- a = length of shear span defined as the distance between a concentrated load and the nearest reaction, that is, length of a region of constant shear, in.
- b = width of slab, in.
- c_{ave} = average distance between cracks, in.
- c = distance between cracks, in.
- c_{max} = maximum distance between two cracks at "limiting stage," in.
- c_{min} = minimum distance between two cracks at "limiting stage," in.
- D = nominal diameter of reinforcement, in.
- d = effective depth of reinforcement, in.
- E_s = elastic modulus of steel, psi.
- f'_c = compressive strength of concrete, psi.
- f_f = steel stress at failure, psi.
- f_s = steel stress, calculated by elastic cracked section theory, psi.
- f'_s = ultimate tensile strength of reinforcement, psi.

f_t	= tensile strength of concrete, psi.
f_v	= shear strength of concrete, psi.
f_w	= weld strength of fabric, psi.
f_y	= yield strength of reinforcement, psi.
h_1	= distance from the centroid of the reinforcement to the neutral surface, in.
h_2	= distance from the extreme tensile face to the neutral surface, in.
$j d$	= internal moment arm, in.
K	= factor relating the maximum internal crack width at the steel to the tensile strength of the concrete, bond and the elastic modulus of the steel.
K_1	= constant in crack width expression.
k_1	= factor relating the depth of the rectangular stress block to the strength of the concrete.
L''	= development length, in.
ℓ	= length of lap; also anchorage length, in.
ℓ_o	= total length of longitudinal overhang in lap, in.
ℓ_s	= distance between outermost transverse wires in lap, in.
M_{max}	= maximum moment in shear span considered, in.-kips.
M_{test}	= ultimate moment applied to slab, in.-kips.
M_y	= yield moment, in.-kips.
N	= number of pairs of transverse wires in lap; also number of welds along a longitudinal wire in anchorage length, ℓ .
p	= reinforcement ratio.
p_e	= A_s/A_e
p_w	= area of the tensile reinforcement divided by the product of the width of the web and the effective depth.
R	= h_2/h_1
S_ℓ	= spacing of longitudinal wires, in.
S_t	= spacing of transverse wires, in.

- t_b = thickness of concrete cover measured from the extreme tensile fiber to the center of the nearest wire or bar, in.
 t_s = side cover measured from the center of the outer wire or bar, in.
 U_u = ultimate bond stress, psi.
 V = vertical shear, kips.
 V/M = ratio of shear to moment at section considered, in.
 V_{cr} = vertical shear causing formation of critical diagonal tension crack, kips.
 V_t = ultimate vertical shear, kips.
 V_u = ultimate vertical shear, kips.
 v = nominal shearing stress, psi.
 v_u = ultimate nominal shearing stress, psi.
 w_{max} = maximum crack width at the level of the reinforcement, in.
 \bar{w}_{max} = maximum internal crack width at the steel, in.
 w'_{max} = maximum crack width at the extreme tensile fiber, in.
 X = horizontal distance between support and tip of diagonal tension crack, in.
 X_1 = variable relating bond to splice effectiveness.
 X_2 = variable relating shear strength of concrete to splice effectiveness.
 Y = effectiveness, the ratio of experimental moment to the calculated moment at yield, M_{test}/M_y .
 α = bond stress coefficient.
 α' = factor reflecting the distribution of bond along the reinforcement between cracks.
 β = constant relating shear strength of concrete to $\sqrt{f'_c}$.
 σ_B = stress in steel at inclined crack developed by bond, ksi.
 σ_S = stress in steel at inclined crack developed by shear strength of concrete, ksi.
 σ_t = stress in steel at inclined crack at failure, ksi.

π = 3.14

ϕ = capacity reduction factor.

Σo = sum of reinforcement perimeters, in.

3. EXPERIMENTAL PROGRAM

3.1 Specimens

Sixty-three slabs have been tested to study the control of flexural cracking, splice strength, anchorage strength and flexural strength. All slabs were 76 in. long, 24 in. wide and either 5 or 7 in. deep. The 7-in. depth was used for some slabs reinforced with large steel percentages. All slabs were simply supported on a 6-ft span. Slabs which were 5 in. deep were loaded 12 in. from the supports; slabs which were 7 in. deep were loaded either 12 or 18 in. from the supports to obtain additional information about anchorage.

Reinforcement was supported on 3/4 in. square wooden blocks of appropriate height, 3/4 to 1-5/16 in., to obtain the desired cover. Deformed wire fabric was placed with the transverse wires above the longitudinal wires. Splices were fabricated with equal lengths of longitudinal overhang at both ends of the splice. The splices were normally located at the middle of the slab, but in a few cases to provide the desired anchorage condition, the centers of the splices were shifted as much as 2 in. toward one end of the slab. Reinforcement was wired in place with 14 gage annealed wire.

For the purposes of description and designation, the slabs are divided into two major groups; those slabs used to study flexural cracking are in one group and the slabs used to study splice strength are in the other group. Details of the crack control and splice slabs are given in Tables 1 and 2, respectively.

3.2 Designation of Specimens

As shown in Tables 1 and 2, slabs are designated by a combination of three letters and a number. The first letter identifies the phase of the investigation in which the specimen was tested; i.e. "C" refers to the crack control phase, and "S" refers to the splicing phase. If the slab was reinforced with deformed bars, the remaining two letters in the designation are "DB". Slabs reinforced with deformed wire are identified with a "W" followed by a code letter designating the manufacturer, while slabs reinforced with deformed wire fabric are identified by a "F" followed by the manufacturer's code letter. The number which follows the three letters serves to identify a particular slab in the crack control and splicing studies.

3.3 Materials

3.3.1 Concrete

Some of the concrete used in this investigation was obtained from a local ready mix plant and the remainder was mixed in the laboratory. Type I portland cement and aggregates meeting relevant ASTM specifications were used for all concrete. The ready mix concrete contained sand from a local source and Indiana gravel; the concrete mixed in the laboratory contained Wabash sand and gravel.

The mix proportions are given in Table 3 and the properties of concrete for individual slabs used in the crack control and splicing phases of the program are given in Tables 4 and 5, respectively.

3.3.2 Reinforcement

The #3, #4, and #5 deformed bars were supplied by one manufacturer; the #2 deformed bars were supplied by another manufacturer. The #2 bars were a special order; the other deformed bars exceeded the ASTM Standard Specification for Deformed Billet-Steel Bars for Concrete Reinforcement with 60,000 psi Minimum Yield Strength, A 432-65, and the ASTM Standard Specification for Minimum Requirements for the deformations of Deformed Steel Bars for Concrete Reinforcement, A 305-65. A summary of strength properties and geometry of the bars is given in Table 6.

Fabric styles were chosen to give a wide range of sizes and steel percentages. In order that various types of deformations could be included in the program, the deformed wire fabric was supplied by five different manufacturers in Canada and the United States. A quantity of deformed wire used as the longitudinal reinforcement in the fabric was also supplied by each manufacturer. All deformed wires contained deformations on 4 lines. The deformed wires supplied by four of the manufacturers contained either a "dimple" or "square-edged" deformation. One manufacturer supplied wire which was deformed prior to drawing; deformations consisted of numerous transverse ribs at the base of the longitudinal grooves. The grooves had a twist of approximately 5 deg per in. Typical deformed wires are shown in Fig. 1.

The deformed wires exceeded the requirements of ASTM Standard Specification for Deformed Steel Wire for Concrete Reinforcement, A 496-64, for material to be used in the fabrication of deformed welded wire fabric. The deformed wire fabric exceeded the requirements of ASTM Standard

Specification for Welded Deformed Steel Wire Fabric for Concrete Reinforcement, A 497-64, except that five of the fabric styles, 6x6:D7xD4, 6x12:D7xD4, 4x3:D29xD11, 4x6:D29xD11, and 4x12:D29xD11 did not meet the weld shear strength requirements. Low weld strengths were especially requested for some of the fabric in order that the results from the anchorage and splicing phases of the program would be meaningful. Summaries of the strength properties of the deformed wire and the deformed wire fabric are given in Tables 7 and 8, respectively. The tensile properties of the deformed wires represent the average of 3 or 5 tests; the tensile properties of the deformed wire fabric represent the average of 2, 3, 4, or 5 tests. The weld strengths represent the average of 4 to 10 tests.

Typical stress-strain diagrams for the reinforcement are shown in Figs. 2 through 6.

3.4 Experimental Procedure

All slabs and control specimens were cast in steel forms in accordance with pertinent ASTM specifications. The slabs, control cylinders and modulus of rupture beams were removed from the forms after 24 hours and cured in a 100 per cent relative humidity chamber at 70 F for 6 days. After removal from the moist room, specimens were stored in the laboratory until the time of testing.

Slabs were tested as schematically shown in Fig. 7. The slabs were simply supported on a 6-ft span and loaded either 12 or 18 in. from the supports. The load was applied through a hydraulic system and maintained constant while readings were being taken. At each increment of loading the crack pattern on the slab was marked, indicating the length of each crack and the load level.

Loading was applied in one or two kip increments, depending on the slab thickness, steel percentage, and length of the shear span, until all the cracks had developed; larger load increments were then applied until failure occurred. Steel stresses were measured with bonded electrical resistance strain gages. Crack widths were measured at the level of the reinforcement and at the extreme tensile fiber at loads which produced measured steel strains corresponding to stresses of 20,000, 30,000, 40,000, 50,000 and 60,000 psi, except that in a few of the early tests crack widths were not measured at a stress of 60,000 psi. Crack widths were not measured in a few of the later slabs which contained splices.

4. FLEXURAL CRACKING

4.1 Background

4.1.1 Problem

Cracking of reinforced concrete is expected and cannot be economically eliminated utilizing our current design procedures. Control of cracks is one of the important considerations in design and construction. Cracks of excessive widths are potential sources of danger where corrosion is a possibility and may permit leakage in a hydraulic structure. Furthermore, visible cracks may be objectionable aesthetically.

Because the widths of cracks are related to steel stress, allowable stresses for high strength reinforcements are dictated, in part, by permissible crack widths. This study concerns the crack controlling properties of deformed wire and deformed wire fabric.

4.1.2 Factors Which Affect Cracking

As load is applied to an uncracked reinforced concrete flexural member, the load is resisted almost entirely by the concrete until the tensile strength of the concrete is reached. The formation of initial cracks occur at apparently random locations in a member; the tensile strain in the concrete at cracking is normally 0.0001 to 0.0002. The initial cracking appears to be almost entirely dependent on the strength of the concrete; certain other variables such as mix proportions, curing conditions, and ambient conditions may also play a minor role in this cracking. For mesh types of reinforcement such as smooth and deformed wire fabrics, it appears that initial cracks may form without regard for the location of transverse wires, but that initial cracks which do form between transverse wires often intercept a transverse wire and follow it.

With the formation of cracks, the state of stress is altered appreciably. The tensile forces formerly carried by concrete are transferred to the steel, thereby, shifting the neutral surface toward the compressive face and increasing the compressive stresses in the concrete. Cracking tends to "release" the concrete from the longitudinal tensile strains associated with bending deformations, slippage between the concrete and steel occurs at crack interfaces, and cracks develop a finite width.

As cracking continues, the position of new cracks becomes less random. During this stage of cracking, cracks show a marked preference to form at the location of transverse wires with mesh styles of reinforcement. Eventually, a "limiting stage" is reached where further increases in load will not increase the number of cracks but only increase the width of existing cracks. This limiting stage has been given detailed attention by many investigators.

At the location of a crack, there is a transfer of stress by means of bond into and out of the concrete between adjacent cracks. As a result of this transfer, high tensile stresses are present in the concrete at the level of the reinforcement; the extreme tensile fiber may actually be in a state of compression (2, 3). The amount of stress which can be transferred into the concrete between two cracks a distance "c" apart is related to the bonding characteristics of the reinforcement. Realizing that crack formation is subject to unavoidable experimental scatter, it can be assumed that there is some nominal minimum crack spacing, c_{min} , and that if two cracks have formed $2c_{min}$ or farther apart, sufficient stress can be transferred into the concrete to produce a new crack. The tensile force which is transferred from the steel to the concrete has commonly been equated to the strength of the concrete as follows:

$$c_{min} U_u \alpha' \Sigma o = A_e f_t$$

where:

c_{min} = minimum crack spacing.

α' = factor reflecting the distribution of bond stress along the reinforcement between adjacent cracks.

U_u = ultimate bond stress.

Σo = sum of reinforcement perimeters.

A_e = effective area of concrete in tension.

f_t = tensile strength of the concrete.

Letting c_{max} equal $2c_{min}$,

$$c_{max} = \frac{2A_e f_t}{\alpha' U_u \Sigma o} \quad (1)$$

This expression requires that A_e , the effective tensile area of the concrete, be defined and the influence of nonuniform stresses over A_e and flexural tensile stresses be ignored. Equation 1 can be simplified by letting

$$\Sigma o = 4 A_s / D \text{ and } p_e = A_s / A_e$$

where:

A_s = area of tensile reinforcement.

D = nominal reinforcement diameter.

p_e = effective reinforcement ratio.

Equation 1 becomes

$$c_{\max} = \frac{f_t}{2 \alpha' U_u} \frac{D}{p_e} \quad (2)$$

The maximum internal width of crack at the steel may be obtained by expressing the difference between the elongation of the steel and concrete over the length c_{\max} . The C.E.B. general theory (4), considers A_e to be an area of concrete with a width equal to the tensile face of the beam or slab and a depth equal to twice the distance between the centroid of the tensile steel and the extreme tensile fiber and considers the longitudinal elongation of the concrete to be negligible. With these assumptions the maximum internal crack width can be expressed as,

$$\bar{w}_{\max} = K \frac{D}{p_e} f_s \quad (3)$$

where:

\bar{w}_{\max} = maximum internal crack width at the steel.

$K = f_t / (2 \alpha' U_u E_s)$

f_s = tensile stress in the reinforcement.

E_s = elastic modulus of the steel.

Certain modifications have been made in Eq 3 so that it may better represent the experimental data, but most of these expressions indicate that D/p_e and f_s are the major parameters influencing maximum internal crack width. Gergely and Lutz (5) note that Broms has conducted

tests with specimens having a constant A_e but various bar diameters, D . There was found to be little difference in crack widths for varying D/p_e values. Also Hognestad (6) has presented results indicating that \bar{w}_{\max} is nearly proportional to D/p_e for old-type deformed bars but is independent of D/p_e for bars conforming to ASTM A 305. The old-style deformed bars had widely spaced deformations and possessed inferior bonding properties compared to the A 305 deformed bars. In view of Hognestad's results it is not surprising that D/p_e was found to influence crack width in slabs reinforced with smooth wire fabric (7). These studies also clearly show that the closer the reinforcement is spaced the better the crack control.

The crack width at the extreme tensile fiber which has received much attention in recent years is more easily measured than the width of an internal crack and can be important aesthetically or when concrete deterioration and steel corrosion are considered. This crack width is primarily related to the location of the neutral surface and the concrete cover for a given internal crack width at the steel.

4.1.3 Proposed Methods of Estimating Crack Widths

Although it may be possible to develop crack width expressions which correlate well with selected test results, it is desirable that a general expression be available which correctly estimates crack width for a large range of critical variables; such a general expression would allow designers to provide proper restrictions on actual crack widths in structures. Equation 3 has been modified so that it may better represent the experimental data; for example, Efsen and Krenchel (8) proposed the following expression for the average crack spacing.

$$c_{\text{ave}} = 1.8 \text{ in.} + D/p_e$$

If c_{\max} is assumed to be equal to $1.5 c_{\text{ave}}$, the following expression for \bar{w}_{\max} results,

$$\bar{w}_{\max} = (2.7 + 0.19 D/p_e) f_s / K_1 \quad (4)$$

where:

$$K_1 = 47.5 \times 10^6 \text{ psi.}$$

A similar equation for values of p_e between 0.02 and 0.20 has been proposed by C.E.B. (9).

$$\bar{w}_{\max} = (4.5 + 0.4/p_e) D f_s / K_1 \quad (5)$$

where:

$$K_1 = 47.5 \times 10^6 \text{ psi for deformed bars and } 29.7 \times 10^6 \text{ psi for smooth bars.}$$

These expressions are concerned with the internal crack width at the steel; many recent researchers have investigated the maximum width of cracks at the level of the reinforcement on the edge of a beam, w_{\max} , and the maximum crack width at the extreme tensile fiber, w'_{\max} , which can be related to \bar{w}_{\max} by a magnification factor, R . The factor, R , may be taken equal to h_2/h_1 , where h_2 is the distance between the neutral surface and the extreme tensile fiber and h_1 is the distance between the neutral surface and the centroid of the tensile reinforcement.

Gergely and Lutz (5) have analyzed the results from six crack control investigations. They applied various crack control parameters, as proposed by numerous investigators and modifications thereof, to crack widths obtained experimentally. They found that no one expression provided a "best fit" for all data, but that the following expressions were reasonably accurate for all the data.

At the extreme tensile fiber:

$$w'_{\max} = 0.076 \sqrt[3]{t_b} A R f_s \times 10^{-6} \quad (6)$$

At the level of the reinforcement:

$$w_{\max} = \frac{0.076 \sqrt[3]{t_s} A}{1 + 2t_s/3h_1} f_s \times 10^{-6} \quad (7)$$

where:

t_s = side cover measured from the center of outer bar or wire, in.

t_b = thickness of concrete cover measured from the extreme tensile fiber to the center of the wire or bar located closest thereto, in.

A = average effective concrete area around a reinforcing bar, sq in.

$$R = h_2/h_1$$

h_1 = distance from the centroid of the tensile reinforcement to the neutral surface, in.

h_2 = distance from the extreme tensile fiber to the neutral surface, in.

4.2 Experimental Results

4.2.1 Crack Formation

Cracking initiated when the measured steel strain was between 0.00009 and 0.00013. In the slabs reinforced with deformed wire, cracks initially developed at apparently random locations. As the number of cracks increased, the new cracks tended to be located such as to develop a uniform spacing. In those slabs reinforced with deformed welded wire fabric, there was a preference for cracks to form at the transverse wires, although it was not unusual for cracks to develop between them.

Slabs contained three or four electrical resistance strain gages bonded to the reinforcement in the region of constant moment. Slabs reinforced with small percentages of reinforcement showed wide variations in measured steel strains as the first cracks formed. A gage on the longitudinal reinforcement near a crack would often indicate a strain 0.0006 higher than gages located away from the crack. When the maximum measured steel strain reached about 0.0013, the continued cracking had eliminated most of this strain variation along the reinforcement. Slabs containing more than about 0.7 per cent of reinforcement were found to have nearly uniform steel strains at the various stages of crack formation.

The formation of cracks in slabs reinforced with deformed bars appeared nearly identical to those in slabs reinforced with comparable percentages of deformed wire.

Two slabs containing a high steel percentage, CWA 13 and CFA 22 did not contain shear reinforcement and failed in the shear span before the calculated steel stress reached 60,000 psi. The absence of shear reinforcement was desirable to permit the study of anchorage behavior. Slab CFA 23 which was tested late in the program contained shear reinforcement to insure a flexural mode of failure and supply additional crack control data.

4.2.2 Crack Spacings and Widths

Average crack spacings were calculated by dividing the length of the constant moment region by the number of flexural cracks observed at the level of the reinforcement. Average crack spacings are presented in Table 9 for various calculated steel stresses. Cracks which did not extend to the level of the reinforcement were excluded from consideration.

Crack widths at calculated steel stresses were obtained by either interpolation or, in a few instances, extrapolation of the crack widths obtained at corresponding measured steel stresses. The measured crack widths on slab CFA 23, tested late in the program, were obtained at the calculated steel stresses directly. A summary of average and maximum crack widths, both at the level of the reinforcement and at the extreme tensile surface, are given in Tables 10 and 11. As before, cracks which did not extend to the level of the reinforcement were excluded from consideration.

4.3 Discussion of Results

4.3.1 Crack Spacing

Although not usually considered of direct importance, a knowledge of crack spacing in slabs and beams permits a qualitative estimate of crack width. After cracking has initiated in a member under increasing load, it has been found that at a given steel stress, the presence of a large number of closely spaced cracks results in small crack widths. Crack spacing and crack width can be affected by the geometry and surface characteristics of the reinforcement, both of which are quite different for deformed wires and deformed bars. However, although no statistical analysis was made of the information on crack spacing given in Table 9, there does not appear to be any significant difference in crack spacings for slabs reinforced with deformed wires and deformed bars.

When used in slabs, the ACI Building Code permits smooth wire fabric to be considered as deformed bars if the transverse wires are spaced not more than 12 in. apart and are not more than six gages different in size than the longitudinal wires. Because of the tendency for flexural cracks to form at a transverse wire, this restriction on smooth wire fabric can be regarded as an indirect control on crack spacing and, therefore, crack width. With deformed wire fabric, there is also a

tendency for cracks to develop at transverse wires; however, the crack spacings shown in Table 9 do not seem to indicate a significant difference between the crack spacings obtained with deformed wire fabric and those obtained with either deformed wires or deformed bars.

4.3.2 Maximum Crack Widths

Several studies have attempted to determine the important parameters which affect the width of cracks in reinforced concrete. Since the maximum crack width is more important than the average crack width when durability and aesthetic values are considered, most recent work has concentrated at the determination of the important variables which control the maximum crack widths. A knowledge of these variables would suggest means by which crack widths can be controlled. Gergely and Lutz (5) analyzed the results of six investigations and developed expressions (Eqs 6 and 7) for predicting the maximum crack widths at the extreme tensile fiber and at the level of the reinforcement.

The maximum crack widths obtained in this investigation of slabs with different types of reinforcements are compared to each other, and to the results predicted by Eqs 6 and 7 in Figs. 8 and 9. In Fig. 9 measured maximum crack widths at the level of the reinforcement in slabs reinforced with smooth wire fabric (7) are compared to the other results. A statistical analysis at the 0.95 confidence level indicates that there is no significant difference in the slope of the regression lines in either of these figures. Since slabs reinforced with deformed wires only and with deformed wires having transverse wires spaced at 6 or 12 in. are considered, the results reflect the influence of transverse wire spacing varied between 6 in. and infinity. The results indicate that for this range of spacings, the transverse wire spacing does not significantly influence crack width, and further, that in one-way slabs of the type tested, deformed wire fabric, deformed wires and deformed bars control cracks equally well in similar situations. Furthermore, Eqs 6 and 7 satisfactorily predict the maximum crack widths obtained in these slabs.

While the results indicated that there was no significant difference between the crack control properties of smooth wire fabric and the other reinforcements, it should be pointed out that the smooth wire fabric considered had a light covering of rust which would have increased its bond. The smooth wire fabrics used in the study had 6, 12 and, in one case, 18 in. transverse wire spacings. In another crack control study (10)

in which low strength concrete (approximately 2200 psi cube strength) and smooth wire fabric with a 11.8-in. (30 cm) transverse wire spacing were used, it was found that fabric in a clean rustless condition produced only approximately one-half as many cracks as fabric which was severely pitted or was pitted and corroded. The maximum crack widths for the smooth rustless fabric were also about twice as great as for the pitted and the pitted and corroded fabrics.

In another phase of the same study (10), smooth fabrics with 11.8 in. (30 cm) and 3.9 in. (10 cm) transverse wire spacings and a fabric with 2 lines of flat, notch deformations and a 11.8-in. (30 cm) transverse wire spacing were considered. The nominal concrete strength was 4500 psi (cube strength). The smooth fabric with 11.8-in. transverse wire spacing had fewer and larger cracks than the other two fabrics. There was little difference in the number of cracks with the smooth fabric having closely spaced transverse wires, 3.9 in. and the "deformed" wire fabric with the larger transverse wire spacing, 11.8 in., but the smooth wire fabric had slightly smaller crack widths than the deformed wire fabric. The higher strength concrete in the latter study resulted in much smaller crack widths for the smooth wire fabric than had been obtained with the fabric in the former study.

It is believed that these results given in Ref 10 are not in direct conflict with the smooth wire fabric data obtained by Atlas et al (7) which were analyzed here, but that the use of moderate strength concrete, 3000 to 4500 psi, combined with the use of fabrics with a light coat of rust resulted in sufficient bond to be reflected in the measured crack widths.

The computed slopes and standard errors for the maximum crack width data reported here and those reported by Gergely and Lutz for the six investigations they studied are given in Table 12; it can be seen that the standard errors obtained here are comparable to those obtained by Gergely and Lutz.

4.3.3 Average Crack Widths

Average crack widths at the extreme tensile fiber and at the level of the reinforcement are shown in Figs. 10 and 11. Also data for average crack widths in slabs reinforced with smooth wire fabric (7) are shown in Fig. 11. The regression lines indicate that the different reinforcements provide similar crack control.

4.4 Summary and Conclusions

For a wide range of deformed wire sizes with different deformation patterns, a wide range of deformed wire fabric styles, some having unusually low weld strengths, and a limited number of deformed bar sizes and smooth wire fabric styles, the measured maximum and average crack widths indicate the following conclusions:

1. Deformed welded wire fabric, smooth welded wire fabric with a maximum transverse wire spacing of 12 in., deformed wires and deformed bars control the maximum crack width equally well when the reinforcements are similarly placed.

2. Equations 6 and 7 developed by Gergely and Lutz, satisfactorily predict maximum crack widths in one-way slabs of the type tested here.

5. SPLICES

5.1 Background

5.1.1 Problem

Splicing of tensile reinforcement is at times necessary to permit the transfer of tensile stress from one wire or bar or sheet of fabric to another wire or bar or sheet of fabric. The transfer of stress may be accomplished by mechanical devices or welding, but it is more economical in most cases to lap the reinforcement.

The lap splicing properties of deformed bars and smooth welded wire fabric have been investigated (11-15) and building codes have provisions regarding the splicing of these materials. However, since deformed wire does not conform to the deformation requirements for deformed bars, ASTM A 305, and the required shear weld strength for deformed wire fabric is 15,000 psi less than that required for smooth wire fabric, neither the design provisions for deformed bars nor those for smooth wire fabric are applicable to deformed wire and deformed wire fabric.

This study was concerned with developing design criteria for the lap splicing of deformed wires and deformed wire fabric.

5.1.2 Present Design Approaches

Design procedures (1) for lap splicing of deformed bars are based on a bond stress criterion. The bond stress in laps is limited to three-fourths of the permissible bond stress which is assumed to be proportional to $\sqrt{f'_c}/D$ where f'_c is the compressive strength of the concrete and D is the nominal diameter of the tensile reinforcement. Minimum required lap lengths are specified for various yield strengths; in addition, a minimum lap length of 12 in. is required. Where contact splices are spaced closer than 12 bar diameters or located closer than 6 in. or 6 bar diameters from an outside edge, the lap length must be increased 20 per cent or stirrups must be provided.

The restriction of bond stress to three-fourths of the permissible bond stress is to lessen the tendency for stress concentrations at either end of the splice to produce early splitting. Increasing the lap length for closely spaced laps has been found necessary because some minimum amount of concrete is needed between adjacent splices to fully develop bond and prevent a splitting failure in the plane of the bars.

The splice requirements for smooth wire fabric are considerably simpler. The presence of bond acting along the longitudinal wires is ignored and complete reliance is placed on the weld strengths. Lapping a pair of transverse wires at least two inches has been found sufficient (7) to develop the shear weld strength and therefore transfer 50 per cent of the yield strength. By lapping two pairs of transverse wires, such that the total distance between the outermost transverse wires in the lap is at least a transverse wire spacing plus 2 in., the full yield strength can be transferred.

5.2 Experimental Results

5.2.1 General

The ultimate loads developed by the slabs are tabulated in Table 13. The yield moment capacity for each slab is also given in Table 13.

The moment resulting from the weight of the slab is inconsequential and was excluded.

The calculated yield moments for the slabs are based upon Eq 16-1 of ACI 318-63 (1).

$$M_y = \phi A_s f_y \left(d - \frac{A_s f_y}{1.7 f'_c b} \right) \times 10^{-3} \quad (8)$$

where:

M_y = yield moment, in.-kips

ϕ = 1.00

A_s = area of tensile reinforcement, sq in.

f_y = yield strength of tensile reinforcement, psi.

d = effective depth of slab, in.

f'_c = compressive strength of concrete, psi.

b = width of slab, in.

For slabs reinforced with deformed bars, the actual yield strength of the reinforcement was used in computations; for slabs reinforced with deformed wire and deformed wire fabric the minimum specified yield strength, 70,000 psi, was used. Since the actual yield strengths of the bars were about 70,000 psi, and the deformed wire and deformed wire fabric reached the minimum yield strength at a strain of about 0.003, the experimental

strengths are therefore compared to calculated strengths which are based on similar conditions of stress and strain in the reinforcement.

The calculated yield moment was calculated for two effective depths; these effective depths are based on the distance between the extreme compressive fiber and the center of the longitudinal reinforcement at either end of the splice. Both the calculated yield moment and the effectiveness of the splice, which is the ratio of the maximum test moment to the calculated yield moment, are given in Table 13 for both effective depths.

5.2.2 Deformed Wires and Deformed Bars

Fifteen slabs reinforced with deformed wire and two slabs reinforced with deformed bars were tested. All failures occurred in the lap.

The effectiveness of splices, based on the maximum effective depth in the lap region, for slabs reinforced with deformed wires and deformed bars is plotted in Fig. 12. The effectiveness which ranged between 0.43 and 0.95 increased with increasing lap length for a given size of longitudinal wire.

The slabs which contained less than 0.4 per cent of reinforcement failed with a pull-out of the wires in the lap. The plane of failure normally occurred near the center of the lap. Examination of the tensile face of the slabs after the completion of a test revealed that splitting of the concrete normally accompanied the pull-out of the reinforcement. The degree of splitting increased with increasing reinforcement diameter.

As the percentage of reinforcement increased, the splitting became severe; in some instances the concrete was completely spalled away in the region of the lap. With large sizes of reinforcement, the plane of failure passed between the two layers of reinforcement in the lap.

5.2.3 Deformed Wire Fabric

Of 23 slabs reinforced with deformed wire fabric, there were 18 failures in the splice region, 3 failures in the shear span, and 2 flexural failures in the constant moment region caused by fracture of the wire. The test results from the slabs which failed in shear are presented to provide a conservative estimate of the splice strength but are not used in calculations.

The effectiveness of splices, based on the maximum effective depth, for slabs reinforced with deformed wire fabric is shown in Fig. 13.

The effectiveness ranged between 0.28 and 1.24. There was a general tendency for the effectiveness to increase with the length of lap; however, the influence of other variables such as longitudinal overhang and position of transverse wire in the lap were also important.

Failure of the splice normally occurred when a crack propagated between the lapped sheets of fabric. Examination of the slabs after the completion of tests revealed the presence of splitting and, in some cases, spalling of the concrete along the overhanging length of longitudinal wires beyond the last transverse wire in the lap. Three slabs, SFB 20, SFD 27 and SFE 31 did not have a lap of transverse wires; a flexural crack developed near the center of the lap and a pull-out mode of failure occurred. Flexural failure occurred in slabs SFA 18 and SFB 22 with a fracture of the longitudinal wires at the edge of the lap in the sheet of fabric with the smaller effective depth.

5.3 Discussion of Results

5.3.1 Deformed Wires and Deformed Bars

5.3.1.1 Types of Failure

Lapped splices of tensile reinforcement involves a complex interaction between the reinforcement and concrete known as bond. Building codes require that splices of deformed and smooth bars be designed on permissible bond stresses; a minimum length of lap is also normally specified.

The slabs reinforced with deformed wire were tested to evaluate the magnitude of bond stress obtainable in splices. This knowledge was needed for the interpretation of the results obtained from deformed wire fabric splices. The details of the laps were chosen to simulate the geometry of fabric laps; the longitudinal wires were placed in contact, one above another in the lap. The close proximity of the wires may have hampered consolidation of concrete and lowered the ultimate bond strength to some degree. Although splitting often accompanied failure, there was no indication that splitting initiated until the bond was fully developed and pull-out was imminent. The data have been analyzed assuming that splitting was a secondary characteristic of failure and the ultimate bond strength was obtained at failure.

5.3.1.2 Analysis of Deformed Wire and Deformed Bar Splices

The ACI Building Code specifies that the ultimate bond stress which can be developed with deformed bars which conform to the requirements of ASTM A 305 can be expressed as follows:

$$U_u = \alpha \frac{\sqrt{f'_c}}{D} \quad (9)$$

where:

U_u = ultimate bond stress, psi.

α = bond stress coefficient

f'_c = compressive strength of concrete, psi.

D = nominal diameter of reinforcement, in.

If one knows the steel stress at failure, f_f , and the length of lap, ℓ , the bond stress coefficient, α , can be determined:

$$\alpha = \frac{f_f D^2}{4 \ell \sqrt{f'_c}} \quad (10)$$

In a cracked section, the internal moment is nearly proportional to the steel stress. Therefore Eq 10 can be simplified to,

$$\alpha = \frac{Y A_w f_y}{\pi \ell \sqrt{f'_c}} \quad (11)$$

where:

Y = effectiveness, the ratio of experimental moment to the calculated moment at yield, M_{test}/M_y

A_w = area of a longitudinal wire, in.

The splice effectiveness, Y , is based upon the lower sheet of fabric in the lap. The bond stress coefficients obtained with Eq 11 are shown in Fig. 14. It was found that α increased slightly with decreasing lap length, and the bond stress coefficients obtained with deformed wires were normally less than those obtained with the two splices of deformed bars. However, the heights of deformations on the bars exceeded minimum heights more than those on the wires; if both wires and bars had the same relative

height compared to minimum specifications the difference between the bond stress coefficients might have been less.

5.3.2 Deformed Wire Fabric

5.3.2.1 Types of Failure

The transfer of stress between lapped sheets of deformed wire fabric involves bond, weld, and concrete strengths. There are two general failure mechanisms possible in a lap. If weld strengths are of a minimal nature, a pull-out type of failure may result when bond stresses and weld strengths are insufficient to transfer the necessary stress. If weld strengths are relatively high, a splitting failure may occur when the concrete is no longer capable of transmitting the stresses between the sheets of fabric. This latter type of failure was found to occur in the splices considered in this study. No weld failures occurred in the splices tested, although some of the welds were below ASTM minimum requirements.

Providing that at least one pair of transverse wires were lapped in the splice, e.g. SFD 25, failure appeared to result from a bond failure along the overhanging portion of the longitudinal wires and a shear failure of the concrete between the outermost transverse wires in the lap. If transverse wires were not lapped, e.g. SFD 27, a flexural crack formed near the center of the lap and a pull-out failure resulted.

5.3.2.2 Analysis of Deformed Wire Fabric Splices

If weld failures do not occur, the load carried by a splice is the sum of that carried by the overhanging ends, through bond, and by the concrete, in shear, included between the sheets of fabric and between the outermost transverse wires in the splice. The effectiveness, Y , of such a splice may be computed as follows:

$$Y = \frac{M_{\text{test}}}{M_y} = \alpha X_1 + \beta X_2 \quad (12)$$

where:

αX_1 = bond stress contribution

βX_2 = shear strength contribution from concrete.

Letting the bond stress be defined by Eq 9, assuming that the shear strength of the concrete is proportional to $\sqrt{f'_c}$, and assuming that

the moment in a cracked section is proportional to the steel stress, Eq 12 may be written as,

$$Y = \frac{\alpha \sqrt{f'_c} \pi \ell_o + \beta \sqrt{f'_c} \ell_s S_\ell}{A_w f_y} \quad (13)$$

where

α = bond stress coefficient.

ℓ_o = total length of longitudinal overhang in lap, in.

β = shear strength coefficient.

ℓ_s = distance between the outermost transverse wires in the lap, in.

S_ℓ = spacing of longitudinal wires, in.

Figure 15 illustrates the definition of ℓ_o and ℓ_s . Since the outermost transverse wires in slabs SFB 20, SFD 27 and SFE 31 were not lapped, ℓ_s equals zero and ℓ_o is equal to the total length of the splice.

The experimental results were applied to Eq 13 with Y based on the sheet of fabric with the smallest cover and largest effective depth, α and β were then determined by the method of least squares. Slabs which failed in the shear span or by fracture of the steel were not considered. The coefficients α and β were found to be equal to 4.95 and 3.56, respectively. Thus Eq 13 becomes:

$$Y = \frac{4.95 \sqrt{f'_c} \pi \ell_o + 3.56 \sqrt{f'_c} \ell_s S_\ell}{A_w f_y} \quad (13a)$$

The predicted effectiveness and measured effectiveness of splices are shown in Fig. 16. The standard error* was equal to 0.12.

5.3.3 Discussion

5.3.3.1 General

Equation 13a is valid only if the bond is fully developed and the weld strengths are sufficient to cause a shear failure in the

* Standard Error = $\sqrt{\frac{\sum (Y_c - Y_m)^2}{n-1}}$, where Y_c and Y_m are the calculated and measured values of splice effectiveness, respectively, and n equals the number of observations.

layer of concrete between the sheets of fabric and between the outermost transverse wires in the lap. If the weld strengths are insufficient, the strength of the splice is the sum of the load carried by the bond and that carried by the welds. For this case the effectiveness of the splice, Y , cannot exceed the following:

$$Y = \frac{4.95 \pi \sqrt{f_c'} \ell + N A_w f_w}{A_w f_y}$$

or

$$Y = \frac{4.95 \pi \sqrt{f_c'} \ell}{A_w f_y} + N \frac{f_w}{f_y} \quad (14)$$

where:

ℓ = total length of lap, in.

N = number of welds in the lap (see Fig. 15)

f_w = weld strength, psi.

For the geometry of splices tested, Eq 13a predicts lower values of effectiveness than Eq 14 for all specimens reinforced with deformed wire fabric. Therefore, it may be concluded that, for the slabs tested, the weld strengths were more than adequate. This conclusion is supported by the fact that no weld failures occurred in the splices.

If the longitudinal wires are closely spaced a shear failure may develop in the concrete prior to the full development of bond along the overhanging ends. In this case Eq 13a would predict too large an effectiveness. Any spacing of the longitudinal wires which results in greater bond capacity than shear capacity would give a lower effectiveness. Thus the spacing of longitudinal wires that results in equal bond strength and concrete shear strength in the splice is the minimum spacing to which Eq 13a applies. This minimum spacing, S_ℓ , can be computed by equating the bond strength to the shear strength as follows:

$$4.95 \sqrt{f_c'} \pi \ell_o = 3.56 \sqrt{f_c'} \ell_o S_\ell$$

$$S_\ell = 4.5 \text{ in.}$$

If S_ℓ is less than 4.5 in., the bond along the overhanging ends will not be fully developed. The strength of a splice is determined by

the shear strength of the concrete in the splice and effectiveness may be computed as follows:

$$Y = \frac{3.56 \sqrt{f_c'} \ell S_\ell}{A_w f_y} \quad (15)$$

Only one slab, SFC 19, contained deformed wire fabric with longitudinal wires spaced closer than 4 in. This slab failed in the shear span and not in the splice at an effectiveness less than that given by Eq 15. The D29xD11 fabrics used in six slabs had a 4-in. longitudinal wire spacing; both Eqs 13a and 15 predict approximately the same effectiveness for these slabs. Equation 13a appears suitable if the longitudinal wire spacing, S_ℓ , is 4 in. or greater.

The bond stress coefficient, α , was found to be 4.95 for deformed wire fabric splices; α was approximately 20 per cent less for most deformed wire laps. The difference may be caused by better consolidation of concrete around the wires in a fabric lap resulting in bond around the perimeter of each wire in the lap.

5.3.3.2 Influence of Longitudinal Overhang on Splice Strength

Slabs SFD 23, SFD 25 and SFD 29 contained similar laps except that the length of overhang beyond the outermost transverse wires in the splice varied between 0.5 and 6.0 in. Figure 17 shows how the strength of the splices increased with increasing overhang; also shown are the strengths predicted by Eq 13a. It is clear that a significant stress transfer was accomplished via bond and Eq 13a correctly reflects the influence of increasing overhang.

5.3.3.3 Influence of the Number of Transverse Wires in Lap on Splice Strength

The splice effectiveness as expressed by Eq 13a does not depend on the number of transverse wires in the lap. The data support this statement. For example slabs SFD 24 and SFD 28 both contained two pairs of transverse wires in the lap; SFD 24 contained fabric with a 3-in. spacing of transverse wires while slab SFD 28 contained fabric with a 6-in. spacing. The splice in slab SFD 28 was 60 per cent stronger than that in SFD 24; this difference is partially due to the over-all lap length, which was 14.0 in. in SFD 28 and 7.5 in. in SFD 24.

Slabs SFA 34 and SFA 37 had approximately the same total lap length, but SFA 34 contained 4 pairs of transverse wires in the lap compared to 2 pair for SFA 37. However, slab SFA 37 was stronger than SFA 34.

Viewed as a whole, the test data show no apparent trend between the number of transverse wires in the lap and the strength of the splice.

5.4 Splice Design Considerations

5.4.1 General

The above analyses are relatively complex and unsuitable for design and detailing purposes; however, both the approaches employed and the results obtained do suggest methods which may be acceptable.

While a design procedure for deformed wire could be developed directly from Eq 9 and the test results, which indicate that the bond stress coefficient, α , might be assumed equal to 4.0 (Fig. 14), and a design procedure for deformed wire fabric could be developed from Eqs 13a and 14 which are based on experimental data, such approaches would not necessarily lead to conservative designs. The results shown in Fig. 14 and given by Eqs 13a and 14 are based upon test data obtained with deformed wire and deformed wire fabric which exceeded the deformation requirements given by ASTM A 496.

Since the ultimate bond stress has been found (16) to be closely related to the shearing area, it is desirable to develop design procedures which will be applicable to reinforcement just meeting minimum deformation requirements. Some of the decisions made in developing expressions for determining the length of laps of deformed wire and deformed wire fabric might appear arbitrary but were made for the convenience of the designer. An attempt was made to develop design criteria which will be consistent with that for deformed bars.

As discussed in more detail in Section A1.5 of Appendix A1, earlier pull-out tests (16) employing a wide range of deformed wire sizes and deformation patterns indicate that the ultimate pull-out bond stress for deformed wires which just meet deformation requirements varies between about 700 psi for large wire (D31) to about 800 psi for small wire (D4). A variation of 100 psi in bond strength is not large enough to justify an elaborate design procedure reflecting the variation in

bond strength with wire size. It is desirable to use the lower pull-out bond stress of 700 psi which would be obtained with 3500 psi concrete and large deformed wires which are more likely to produce splitting.

In general, the ultimate pull-out bond stress exceeds the actual bond stress which can be developed in structural elements. A more conservative bond stress of 600 psi is assumed to be the permissible bond stress for deformed wires. Assuming that the bond stress is proportional to the $\sqrt{f'_c}$, the bond stress can be expressed with sufficient accuracy as $U_u = 10 \sqrt{f'_c}$.

Because of stress concentrations at the ends of lap splices which can cause premature splitting, the ACI Building Code (1), Sec 805(b) limits the bond stress for deformed bars in splices to three-fourths of the permissible bond stress. To guard against premature splitting at the ends of the splices containing deformed wire and deformed wire fabric reinforcements the permissible bond stress should, therefore, be reduced 25 per cent to $7.5 \sqrt{f'_c}$.

One additional feature of lap splices of the type tested, where the wires are placed one above another and are separated by a transverse wire in the case of deformed wire fabric reinforcement, requires attention. A designer will only be concerned with calculated steel stresses in the fabric having the nominal effective depth, d . Therefore, in the region of a splice, one sheet of fabric will have the assumed effective depth while the second sheet will have a smaller effective depth. For moment equilibrium, the steel stress in the sheet of the fabric with the smaller effective depth will be the highest. While it is possible to develop a design procedure using a bond stress of $7.5 \sqrt{f'_c}$ and to consider the higher stresses in the sheet of fabric with the smaller d , which represents the critical case for bond stress, it is more practical to develop a procedure which allows the designer to use the calculated stresses in the sheet of fabric with the nominal effective depth.

If a designer is concerned with a splice which must transfer the minimum yield strength of deformed wire fabric, 70,000 psi, the upper sheet of fabric cannot be expected to develop more than 80,000 psi, the minimum specified ultimate strength of the fabric. If a bond stress of $7.5 \sqrt{f'_c}$ is

required to develop the 80,000 psi stress in the upper layer of fabric in the splice, a bond stress of approximately $6.6 \sqrt{f'_c}$ will develop the 70,000 psi stress in the lower layer of reinforcement. Therefore in developing a splice design procedure, the calculated steel stress and effectiveness will be based on the reinforcement with the largest effective depth, and a permissible bond stress of $6.6 \sqrt{f'_c}$ will be assumed.

It should be noted that reduced bond stresses were automatically used in the splice analyses given in Sec 4.3.1.2 and 4.3.2.2 since the computations were based on values of effectiveness associated with the larger effective depth.

It is desirable that design expressions for deformed wire and deformed wire fabric be compatible with the expressions for deformed bars which are expected to be in the 1970 version of the ACI Building Code. Thus the splice length will be expressed in terms of the yield strength, f_y , and the compressive strength of the concrete, f'_c . Since the expressions for deformed bars are based on a lateral bar spacing of less than 12 bar diameters, a situation which may produce early splitting and perhaps incomplete development of bond, the splice length for deformed bars has been increased by 20 per cent with a reduction factor applied to the splice length in cases where the lateral bar spacing exceeds 12 bar diameters. Provisions for deformed wire and deformed wire fabric will be developed in accordance with these considerations.

5.4.2 Deformed Wire

The splice length for deformed wire can be obtained by equating the force transferred by means of bond to the total force in a wire at a critical section.

$$U_u \pi D \ell = 1.2 f_y A_w$$

Letting $U_u = 6.6 \sqrt{f'_c}$ and $A_w = \pi D^2/4$ and solving for ℓ .

$$\ell = \frac{1.2 \pi D^2 f_y}{4 \times 6.6 \sqrt{f'_c} \pi D}$$

or

$$\ell = 0.045 D f_y / \sqrt{f'_c} \quad (16)$$

where:

ℓ = length of lap, in.

D = nominal diameter of reinforcement, in.

f_y = yield strength of reinforcement, psi., and

f'_c = compressive strength of concrete, psi.

5.4.3 Deformed Wire Fabric

Equation 16 considers only the stress transferred by means of bond. If splitting is prevented each weld can transfer at least 20,000 psi. Thus for fabric, Eq 16 may be modified to

$$\ell = 0.045 D (f_y - 20,000 N) / \sqrt{f'_c} \quad (17)$$

where:

ℓ = length of lap, in.

f_y = yield strength of reinforcement, psi.

N = number of pairs of transverse wires in lap (see Fig. 15),
and

f'_c = compressive strength of concrete, psi.

To provide an expression which considers the possibility of a splitting failure of the concrete between the outermost transverse wires, Eq 13a may be employed. Replacing the bond stress, $4.95 \sqrt{f'_c}/D$, which was used in Eq 13a with $6.6 \sqrt{f'_c}$ and letting Y equal one, the distance between the outermost transverse wires, ℓ_s , may be solved for

$$\ell_s = \frac{1}{S_\ell} \left[\frac{A_w f_y - 6.6 \sqrt{f'_c} \pi D \ell_o}{3.56 \sqrt{f'_c}} \right]$$

and simplifying

$$\ell_s = p d \left[\frac{f_y}{3.56 \sqrt{f'_c}} - \frac{7.4 \ell_o}{D} \right]$$

which may be written approximately as

$$\ell_s = p d \left[\frac{f_y}{3.5 \sqrt{f'_c}} - \frac{8 \ell_o}{D} \right] \quad (18)$$

where:

ℓ_s = distance between outermost transverse wires in lap, in.

p = reinforcement ratio

d = effective depth of reinforcement, in.

f'_c = compressive strength of concrete, psi.

ℓ_o = total length of longitudinal overhang in lap, in., and

D = nominal diameter of reinforcement, in.

In some cases it will be possible to neglect the influence of variations in the strength of the concrete and to assume a concrete strength of 3000 psi which is common for floor slabs. With this assumption, Eq 18 simplifies to

$$\ell_s = p d (360 - 8 \ell_o / D) \quad (19)$$

where:

ℓ_s = distance between outermost transverse wires in lap, in.

p = reinforcement ratio.

d = effective depth of reinforcement, in.

ℓ_o = total length of longitudinal overhang in lap, in., and

D = nominal diameter of reinforcement, in.

When less than the full yield strength is to be transferred the length, ℓ_s , may be multiplied by Y , the ratio of the stress in the reinforcement to specified yield strength.

Examples of typical splices are given in Appendix A3.

5.5 Summary and Conclusions

The results of a number of pull-out tests and slabs with lapped splices indicate the following conclusions:

1. The transfer of stress between lapped sheets of deformed wire fabric in a splice zone involves a complex interaction between the concrete and the reinforcement. The strength of a lapped splice is limited by either the bond and weld strengths associated with the reinforcement or the splitting strength of the concrete between the lapped sheets of fabric.

2. The strength of a lapped splice is a function of the higher stressed sheet of fabric, that is the sheet which is closer to the neutral surface.

3. The length of a lapped splice for deformed wire may be computed from

$$\ell = 0.045 D f_y / \sqrt{f'_c} \quad (16)$$

when splitting is not a factor.

4. The length of a lapped splice for deformed wire fabric may be computed from

$$\ell = 0.045 D (f_y - 20,000 \text{ N}) / \sqrt{f'_c} \quad (17)$$

when the length of the lap is controlled by the bond and weld strength. To eliminate the possibility of splitting the concrete the distance between outermost transverse wires must be at least

$$\ell_s = p d \left[\frac{f_y}{3.5 \sqrt{f'_c}} - \frac{8 \ell_o}{D} \right] \quad (18)$$

or, if $f_y = 70,000$ psi and $f'_c = 3000$ psi,

$$\ell_s = p d (360 - 8 \ell_o / D) \quad (19)$$

5. If the wires being lapped are spaced $12 D$ or further apart the splice lengths required in 3 and 4 may be reduced by one-sixth.

6. When the splice is to be designed by ultimate strength methods for a steel stress less than the specified yield strength, the lengths required may be obtained by multiplying by the ratio of the design stress to the yield strength or simply substituting the design stress for f_y in the appropriate equations. The first method is approximate and will result in a more conservative lap than the second method.

6. ANCHORAGE AND SHEAR

6.1 Background

6.1.1 Problem

To insure ductile behavior, reinforced beams and slabs subjected to combined shear and moment are designed such that the shear strength is greater than the flexural strength; special care is taken to prevent shear and anchorage failures. Anchorage of plain and deformed bars is accomplished with embedment length, end anchorage or hooks. Hooks are not practical with welded wire fabric reinforcements, and anchorage is normally accomplished by means of embedment length and end anchorage.

It is desirable to determine whether sufficient anchorage can be achieved by means of bond with deformed wire reinforcement and bond plus weld strengths with deformed wire fabric reinforcement to permit the use of existing shear strength design procedures. It is also necessary to develop expressions which permit the designer to determine the necessary development length at critical sections which are: the face of a support, points where tension reinforcement is terminated within a span, and points of inflection.

6.1.2 Factors Which Affect Anchorage and Shear

Although diagonal tension was recognized to be a complex phenomenon influenced by a number of parameters, design procedures for shear and diagonal tension which were used in the United States through the 1950's relied on the concept that the nominal shearing stress, $v = V/bjd$, could be considered a measure of the diagonal tension; the allowable nominal shearing stress was related to the strength of the concrete, f'_c . Such a concept ignores the influence of flexural tensile stresses on diagonal tension and assumes that the strength of the concrete is the only major variable. Although their views did not prevail, a number of investigators realized the shortcomings of this approach. For example, in 1909, Talbot (17) after studying the results of 109 beams without shear reinforcement concluded:

"In beams without web reinforcement, web resistance depends upon the quality and strength of the concrete...

"The stiffer the beam, the larger the vertical shearing stress which may be developed. Short, deep beams give higher results than long slender ones, and beams with a high percentage of reinforcement than beams with a small amount of metal..."

Beginning in the late 1940's, investigators realizing the weakness of the nominal shearing stress concept conducted numerous studies to better define diagonal tension failures. A. P. Clark introduced the parameter a/d , "a" being the length of the shear span and "d" the effective depth, which conveniently expresses the influence of the length-to-depth ratio. Unfortunately, a/d has no meaning for beams under a general state of loading; the parameter was slightly modified to M/Vd which can be used under any state of loading. Investigators also considered the influence of the width-to-depth ratio, b/d , and refined the concrete parameter to $\sqrt{f'_c}$ which is considered proportional to the tensile strength of concrete.

The shear capacity of a member not only depends on the strength of concrete, M/Vd , b/d , and the reinforcement ratio, but also on the proper anchorage of the reinforcement. In regions of shear and locations in a member where a portion of the reinforcement has been terminated, there is a transfer of stress between the concrete and steel. This transfer of stress is accomplished by means of bond, hooks, and, in the case of welded fabric reinforcements, the mechanical anchorage of transverse wires in the concrete.

The bond between the concrete and the steel depends on the surface characteristics of the reinforcement and the strength of the concrete; the anchorage provided by transverse wires depends on the weld shear strength. In instances of large reinforcement ratios and cases of small concrete cover, the concrete may experience a splitting failure before the bond or weld shear strengths are fully developed.

6.1.3 Present Design Approaches

The shear and diagonal provisions of the ACI Building Code (1) are based on the recommendations of the ACI-ASCE Committee 326, Shear and Diagonal Tension (18). For specimens without shear reinforcement, the ultimate nominal shearing stress is computed by

$$v_u = V_u / bd \quad (20)$$

The shear stress, v_u , is limited to $2\phi\sqrt{f'_c}$, where ϕ is a capacity reduction factor, unless the following expression is considered:

$$v_u = \phi \left(1.9 \sqrt{f'_c} + 2500 \frac{P_w Vd}{M} \right) \quad (21)$$

where:

P_w = area of tensile steel divided by the product of the width of the web and the effective depth.

V/M = ratio of shear to moment at section considered, in.

d = effective depth, in.

The shear stress, v_u , is limited to $3.5 \phi \sqrt{f'_c}$.

The ultimate strength design provisions for the anchorage of deformed bars are covered by Sec 918 and 1800 of the ACI Building Code. The bond stress is assumed to be proportional to $\sqrt{f'_c}/D$, where D is the nominal diameter of the reinforcement.

6.2 Experimental Results

6.2.1 General

Sixty-three slabs were tested to study the crack control and splicing characteristics of deformed wire and deformed wire fabric reinforcement. Of these 63 slabs, this chapter will consider the behavior of 15 slabs which failed in the shear span and 13 slabs which did not fail in the shear span, but which contribute to an understanding of anchorage behavior. Four specimens in the splicing study and one specimen in the crack control study contained shear reinforcement and are not considered. The details of the specimens including the location of transverse wires in the shear spans are presented in Table 14.

Table 15 presents the ultimate moments developed by the slabs; these moments are compared to calculated yield and ultimate moments; brief descriptions of the external characteristics of failure are also given.

The calculated yield moments for the slabs are based upon Eq 16-1 of the ACI Building Code (1).

$$M_y = \phi A_s f_y \left(d - \frac{A_s f_y}{1.7 f'_c b} \right) \times 10^{-3} \quad (8)$$

where:

M_y = yield moment, in.-kips

ϕ = 1.00

A_s = area of tensile reinforcement, sq in.

f_y = yield strength of tensile reinforcement, psi

d = effective depth of slab, in.

f'_c = compressive strength of concrete, psi.

b = width of slab, in.

For slabs reinforced with deformed bars, the actual yield strength of the reinforcement was used in computations; for slabs reinforced with deformed wire and deformed wire fabric, the minimum specified yield strength, 70,000 psi was used. Since the actual yield strengths of the bars were about 70,000 psi, and the deformed wire and deformed wire fabric reached the minimum yield strength at a strain of about 0.003, the experimental strengths of the slabs are compared to calculated strengths which are based on similar conditions of stress and strain in the reinforcements.

The ultimate moments for slabs reinforced with deformed wire and deformed wire fabric were also calculated with Eq 8 except that f_y was replaced by f'_s , the ultimate strength of the reinforcement. The deformed bars exhibited "flat-top" stress-strain properties at yield, Fig. 2. Strain hardening was ignored in the slabs reinforced with deformed bars, and the calculated yield and ultimate moments are identical.

6.2.2 Development of Diagonal Cracks

Diagonal cracks normally developed approximately a distance equal to the effective depth from the section of applied loading; however, the location was influenced by the position of existing flexural cracks and the position of transverse wires in the shear span. Diagonal tension cracks frequently developed from a nearly vertical flexural crack with the inclination and slow growth of the crack toward the load point. In some cases, a second and critical diagonal crack formed after the first crack had become fully inclined. The second diagonal crack normally formed somewhere between the top of the inclined crack and mid-depth of the slab and propagated downward, toward the tensile reinforcement. The higher the location of this second diagonal crack, the faster the propagation of the crack. When the crack formed near mid-depth, it normally propagated slowly toward the tensile surface of the slabs; two or more increments of load were usually applied before failure occurred.

In a few cases a diagonal tension crack would form at the tensile face of the slab and propagate instantaneously to the compressive face passing through inclined flexural cracks which had formed earlier. A

transverse wire 4 to 6 in. from the support normally aided the formation of this type of crack.

6.2.3 Anchorage and Splitting

The amount of load a member can carry after the formation of a critical diagonal tension crack is difficult to estimate and is neglected for design purposes. However, it is desirable that the residual strength after the formation of the diagonal tension crack be as large as possible. In many instances this residual strength depends on the anchorage and the splitting characteristics of a member. As a diagonal crack forms, a redistribution of internal stresses occurs which increases the steel stress at the location of the diagonal tension crack. For the redistribution to be accomplished so that the member will resist additional load it is necessary that the stress in the steel be transferred to the concrete by means of bond and mechanical anchorage of any transverse wires present in the anchorage length, ℓ ; when the ultimate bond and weld strengths are insufficient to accomplish the redistribution, an anchorage failure occurs.

If the reinforcement is closely spaced or if transverse wires are present in the anchorage length, ℓ , or both, the concrete may be unable to develop the ultimate bond and weld strengths, and a splitting failure will occur. Both anchorage and splitting failures are secondary failure modes which are possible after the primary mode of failure, the formation of a diagonal tension crack, has occurred.

In deep members a third mode of failure, shear-compression, has frequently been observed. The possibility that shear-compression failures occurred was studied by careful evaluation of failure characteristics and by checking the shear-compression strength predicted by Eq 18 in Ref (19). There was not found to be any substantial evidence of shear-compression failures, and this mode of failure will not be considered further.

In a study of anchorage failures, the results indicated that appreciable bond stresses were developed with deformed wire reinforcement. Slabs CWC 10, CWE 11, and CWE 12, reinforced with deformed wire, and slabs SFC 17, CFE 20, and SFA 35, reinforced with deformed wire fabric, appeared to fail when the diagonal tension crack had slowly propagated under increasing load to a point at which the redistribution of internal stresses by means of anchorage was no longer possible. Only one

of the three slabs, CFE 20, reinforced with deformed wire fabric contained a transverse wire between the location of the diagonal crack and the outer end of the slab. The welds along the transverse wire were not broken.

Slab CWC 7, reinforced with deformed wire, and slabs SFC 19, CFD 19, CFA 22, and SFA 39, reinforced with deformed wire fabric, appeared to fail by splitting. Slab CFA 22 contained one transverse wire in the anchorage length, ℓ ; five welds along this wire were sheared off and the sixth weld was broken at the time of casting. Slab SFA 39 contained two transverse wires in the anchorage length; two of the six welds on the outer transverse wire were broken, but no welds were broken on the transverse wire closer to the point of applied load which indicates that the welds along the outer transverse wire were not broken as a pull-out type of failure occurred. These weld failures occurred in fabric which intentionally had low weld strengths. It was not possible to determine at the completion of the tests of the two slabs with the weld failures whether the welds failed at the initiation of splitting or whether the welds failed during the violent collapse of the slabs.

6.3 Discussion of Results

6.3.1 General

Many of the present design procedures have been developed experimentally from tests of structures or structural elements which are not representative of actual structures -- the specimens considered here are no exception. Two equal loads were applied to the slabs either 12 or 18 in. from the supports which purposely resulted in large moment gradients in the shear spans thus allowing severe conditions of anchorage and shear to be studied. Since bond stress is nearly proportional to the moment gradient, many slabs contained very high bond stresses. Although bond stresses were usually quite high at failure, the ultimate moments for 9 of the 15 slabs which failed in the shear span were greater than the calculated yield moments as shown in Table 15. Since the stress-strain properties of reinforcement and concrete become increasingly nonlinear as the applied moment exceeds the yield moment, the nonlinearity may have precipitated some of the shear failures; this possibility was ignored in the analysis of test data.

6.3.2 Analysis of Diagonal Tension

Although no precise method exists to calculate the diagonal tension strength of beams and slabs, tests have shown the strength to be sensitive to concrete strength, steel percentage, length-to-depth, and width-to-depth ratios. Numerous equations have been proposed by investigators which are dependent on some form of most of the above variables. Based on the results of 194 tests of beams, the ACI-ASCE Committee 326, Shear and Diagonal Tension, proposed that the total vertical shear, V , on any section should not exceed:

$$V = bd \sqrt{f'_c} \left[1.9 + (2500 \text{ psi}) \frac{p V d}{M \sqrt{f'_c}} \right] \text{ but not } > 3.5 b d \sqrt{f'_c} \quad (22)$$

where:

b = width of beam, in.

d = effective depth of beam, in.

f'_c = compressive strength of concrete, psi.

p = steel ratio.

V/M = ratio of shear to moment at section considered, in.

It was observed that beams having low ratios of $pVd/(M\sqrt{f'_c})$ often exhibited little stress redistribution after the formation of a diagonal tension crack; since such members give little or no warning of impending failure, Eq 22 is intended to predict a conservative strength for low values of $pVd/(M\sqrt{f'_c})$.

The committee noted that the diagonal tension crack normally formed approximately a distance " d " away from the point of application of the load. For convenience of analysis the following standardized expression for M/V was used.

$$\frac{M}{V} = \left(\frac{M_{\max}}{V} \right) - d \text{ but not less than } \left(\frac{M_{\max}}{V} \right) - \frac{a}{2} \quad (23)$$

where:

M_{\max} = maximum moment in the shear span considered.

V = total vertical shear in the shear span considered.

d = effective beam depth.

- a = length of shear span defined as the distance between a concentrated load and the nearest reaction, that is, length of a region of constant shear.

For the type of specimens considered here, M/V can be defined as the distance measured from the diagonal crack to the nearest support. Using both definitions of M/V , the allowable shear predicted by Eq 22 was calculated for slabs which failed in the shear span and compared with the vertical shear, V_{cr} , at the formation of the critical diagonal tension crack, and with the maximum shear, V , actually obtained; the results of the analysis are given in Table 16.

6.3.3 Analysis of Anchorage and Splitting

An anchorage failure in a slab reinforced with deformed wire, deformed wire fabric, or deformed bars is normally possible only after the formation of a diagonal tension crack and accompanying redistribution of stresses; the diagonal tension crack must therefore be considered the primary cause of failure. However, if there is sufficient anchorage by means of bond and the mechanical anchorage of transverse wires, considerable redistribution of internal stresses may occur before failure. In some instances, the concrete may be incapable of transferring sufficient stress into the reinforcement to fully develop the anchorage potential of the reinforcement. In this case a splitting failure may occur which is distinct from the splitting caused by slippage of the reinforcement or doweling forces.

In order to study anchorage and splitting quantitatively, it is necessary to determine the tensile stress in the steel at the location of a diagonal tension crack. By considering the anchorage length as a 3 hinged arch, the total tensile force in the reinforcement can be obtained by equating the external moment to the internal resisting moment.

$$T = \frac{V_t X}{jd} \quad (24)$$

where:

T = total tensile force in the reinforcement, kips.

V_t = support reaction at ultimate, kips.

X = lever arm of external loads (see figure at top of Table 17), in.

jd = level arm of internal forces, based on Eq 8, in.

The distance X was measured from photographs taken after the completion of a test. The tensile stress at ultimate, σ_t , equal to T divided by the area of the longitudinal steel, A_s , is given in Table 17 for each slab.

Having thus obtained an estimated steel stress at failure, it is desirable to consider the anchorage and splitting strength. The ACI Building Code assumes that bond strength is proportional to the $\sqrt{f'_c}$ and inversely proportional to the diameter of the reinforcement, D , and considers the shear strength of concrete to be proportional to the $\sqrt{f'_c}$. Thus letting α and β be constants relating the bond strength to $\sqrt{f'_c}/D$ and the shearing strength of concrete to $\sqrt{f'_c}$, respectively,

$$U_u = \frac{\alpha \sqrt{f'_c}}{D} \quad (25)$$

and

$$f_v = \beta \sqrt{f'_c} \quad (26)$$

Assuming that the anchorage capability of deformed wire fabric is the sum of bond and the weld strengths present in an anchorage length, ℓ , the maximum stress transferred can be expressed as:

$$\sigma_B = \left[\frac{U_u \pi D \ell}{A_w} + N f_w \right] \times 10^{-3} \quad (27)$$

where:

σ_B = ultimate stress developed via bond and transverse wires, ksi.

U_u = ultimate bond stress, psi.

D = nominal diameter of longitudinal wires, in.

A_w = area of a longitudinal wire, sq in.

N = number of transverse wires in anchorage length, ℓ .

f_w = weld shear strength, psi.

If splitting occurs, the ultimate stress transferred can be expressed as:

$$\sigma_s = \frac{f_v b \ell}{A_s} \times 10^{-3} \quad (28)$$

where:

σ_s = ultimate stress developed at splitting, ksi.

f_v = shearing strength of concrete, psi.

b = width of slab, in.

ℓ = anchorage length, in.

A_s = area of tensile reinforcement, sq in.

Substituting Eqs 25 and 26 into Eqs 27 and 28, respectively:

$$\sigma_B = \left[\frac{\alpha \sqrt{f'_c} \pi \ell}{A_w} + N f_w \right] \times 10^{-3} \quad (27a)$$

$$\sigma_s = \frac{\beta \sqrt{f'_c} b \ell}{A_s} \times 10^{-3} \quad (28a)$$

Comparing the estimated steel stresses at failure with the stresses predicted by Eqs 27a and 28a, it was found that α and β were approximately 6.0 and 5.25, respectively. Therefore Eqs 27a and 28a can be rewritten as follows:

$$\sigma_B = \left[\frac{6.0 \sqrt{f'_c} \pi \ell}{A_w} + N f_w \right] \times 10^{-3} \quad (29)$$

$$\sigma_s = \frac{5.25 \sqrt{f'_c} b \ell}{A_s} \times 10^{-3} \quad (30)$$

Equation 27 may be used to analyze the anchorage behavior of slabs reinforced with deformed bars; the bond stress may be based on the provisions of Sec 1801 of the ACI Building Code. The code specifies an ultimate bond stress of 800 psi for the concrete strengths and bar sizes encountered in the slabs reinforced with deformed bars. Therefore, Eq 27 may be rewritten as follows:

$$\sigma_B = \frac{800 \pi D \ell}{A_w} \times 10^{-3} \quad (31)$$

Equation 30 applies if a slab reinforced with deformed bars fails by splitting.

The results of the anchorage and splitting analyses are given in Table 17; the lower of the two calculated stresses from the anchorage or splitting analyses is given, and in a few cases, the higher value is also given in parentheses to allow a better comparison with the stresses, σ_t , predicted from the tied arch analogy. Some specimens which did not fail in anchorage are also included in Table 17 to further examine the accuracy of the anchorage and splitting analyses.

6.3.4 Discussion

6.3.4.1 Diagonal Tension

As shown in Table 16, CWC 7 was the only slab which failed to reach the allowable shear at the formation of the initial diagonal crack as defined by ACI-ASCE Committee 326 (Eq 22); no slab failed to reach the shear given by Eq 22 at ultimate. The distance between the critical section and the nearest support, which is equal to the ratio of moment to shear, M/V , at the critical section and which was measured from photographs of the slabs was normally close to the value given by Eq 23. However, in a few cases, the presence of a transverse wire a short distance away from the support aided the formation of a critical diagonal crack. For example, the diagonal crack formed at the outer transverse wire, 6 in. from the support in SFC 17 and failure occurred in the shear span. On the other hand, the diagonal crack formed 8 in. from the support in slab CWC 8 which had the same geometry and loading conditions as those of slab SFC 17 but was reinforced with deformed wires (no transverse wires). Redistribution of forces was possible in slab CWC 8 and failure resulted from a fracture of the reinforcement in the constant moment region. It appears that the presence of a transverse wire will seldom shift the location of the critical diagonal crack toward the support more than a distance equal to the effective depth of the slab.

The recommendations given by ACI-ASCE Committee 326 were based on beams which normally had a width-to-depth ratio of about 0.5. The slabs considered here had width-to-depth ratios of 4.0 to 6.0. Based on 79 beam and slab tests, de Cossio (20) found that the shear strength is related to the width-to-depth ratio. De Cossio placed a curve through

the available data by the method of least squares. For beams with a width-to-depth ratio equal to 0.5, it was found that diagonal cracks normally develop at a shear equal to about 110 per cent of the shear predicted by Eq 22; for slabs having width-to-depth ratios of 4.0 to 6.0, the diagonal crack normally formed at a shear equal to about 150 per cent of the shear predicted by Eq 22. The slabs considered here, which were reinforced with deformed wire and deformed wire fabric, developed critical diagonal tension cracks at a shear equal to about 130 per cent of the shear predicted by Eq 22.

6.3.4.2 Anchorage and Splitting

In Table 17, the calculated anchorage capacities of those specimens which failed in anchorage after the development of the diagonal tension crack are compared to the measured anchorage capacities which are based on the tied arch analogy. The computed anchorage stress of slab CDB 3 which was reinforced with #4 bars at 6 in. centers was greater than the actual yield strength of the steel; since the steel actually had yielded at failure, it is likely that the failure in the shear span was related to yielding. The agreement between calculated and measured anchorage stresses is good for slabs CWD 10, CWE 12, and CFE 20, fair for slabs SFC 17 and CWE 11 and poor for slab SFA 35. The bond stress expression, $U_u = 6 \sqrt{f'_c}/D$, is only approximate for the various wire sizes and deformation patterns considered. For a nominal concrete strength of 3000 psi, this expression predicts ultimate bond stresses from 540 psi for a D29 wire to 920 psi for a D10 wire; pull-out tests (16) have indicated that an ultimate bond stress of 920 psi is not unreasonable for a D10 deformed wire. Pull-out tests given in Appendix A1 indicate that the ultimate pull-out bond stress for a D29 wire is approximately 990 psi; this bond stress is greater than the computed anchorage stresses for slabs reinforced with D29 wire as shown in Table 17.

For slabs CWC 7, SFC 19, CFD 9 and CFA 20, the calculated steel stress at splitting was in good agreement with the stress at failure predicted by the tied arch analogy; the agreement is poor for slab SFA 39. When the depth-to-shear span ratio is increased, the apparent shearing strength of the concrete appears to increase above the value, $5.25 \sqrt{f'_c}$, used in the analysis. If this ratio is increased, the compressive stresses acting perpendicular to the splitting failure plane increase;

this increase in the compressive stresses tends to increase the apparent shearing strength. The shearing strength used in the analysis was approximately equal to the splitting tensile strength.

In this study, two slabs experienced weld failures above the supports. Slab CFA 22 contained 5 weld failures along the same transverse wire; the sixth weld was broken at the time of casting. Slab SFA 39 contained 2 weld failures on the first and third longitudinal wires from the edge of the slab; other welds were deformed but intact. The steel stress, σ_B , given in parentheses in Table 17 is the steel stress calculated from Eq 29. This computed anchorage stress is more than sufficient to develop the actual stress, σ_t , at failure; failure of the slabs SFA 22 and SFA 39 above is attributed to splitting. The weld strengths of the fabric in both slabs were slightly less than that permitted by ASTM A 497. After a splitting failure occurred, a large piece of concrete at the outer end of a slab became completely unattached. It is possible that as collapse occurred, this piece of concrete was wedged between the outer transverse wire and the concrete adjacent to the point of application of the load. This wedging action may be the cause of the weld failures and may help explain why only the welds on the outer transverse wire were broken.

6.3.4.3 Smooth Wire Fabric

It is known that as deformed wires and deformed bars develop bond, tensile stresses are produced which may cause local splitting. It is also believed that these tensile stresses contribute to the general splitting considered here. If smooth wire fabric is considered, bond is developed largely by friction; this type of bond would produce negligible tensile stresses.

Four slabs tested in an earlier study (15) were reinforced with smooth wire fabric (2x6:2/0x2 and 2x6:6/0x3/0) which was lightly rusted. The outward characteristics of failure were the same as those observed in the slabs reinforced with deformed wire fabric considered here except that it was concluded that the failures were caused by shear-compression followed by splitting. Each slab had an anchorage length, ℓ , of 8 in.; concrete strengths ranged from 2155 to 5400 psi. Inspection of the test results indicated that using Eq 28a with β equal to 6.3 provides a good estimate

of the steel stress at failure obtained experimentally. The results of this analysis are given below:

Slab	Reinforcement Style	p	f'_c	Stress at Failure, ksi	
				Experimental	Eq 28a & $\beta = 6.3$
SB2	2x6:2/0x2	0.0107	2155	54	54
SC2	2x6:2/0x2	0.0107	3075	64	65
SD2	2x6:6/0x3/0	0.0208	3350	36	35
SE2	2x6:6/0x3/0	0.0208	5400	44	44

It can be seen that excellent agreement is obtained for a large range of concrete strengths and steel percentages.

6.4 Anchorage Design Considerations

6.4.1 General

For adequate anchorage, the steel stress, f_s , at a critical section must be transferred into and out of the steel by suitable anchorage on either side of the critical section. The results presented here indicate that one of two mechanisms, splitting or bond plus weld failure, limit anchorage in slabs reinforced with deformed wires and deformed wire fabric.

The above analysis of anchorage using a bond stress of $U_u = 6 \sqrt{f'_c}/D$ permitted reasonable agreement between the experimental steel stress at failure, σ_t , at a critical section and the stress at failure predicted by Eq 27. Since the deformed wires used in this study exceeded the deformation requirements of ASTM A 496, it is desirable to develop expressions which are applicable to wire which just satisfies the deformation requirements. Based on the results presented in Appendix A1 and the discussion in Sec 5.4.1, a permissible bond stress of $10 \sqrt{f'_c}$ is assumed. Deformed wire fabric is assumed to have the minimum specified shear weld strength of 20,000 psi.

The expressions for development length were developed to be compatible with those for splice lengths developed in Chapter 5. Consequently the development lengths will be expressed in terms of the yield strength of the reinforcement and the compressive strength of the concrete. The expressions for development length will also be based on a lateral spacing of longitudinal reinforcement of less than 12 D which may produce early splitting and incomplete development of bond; to account for this

situation the development length is increased 20 per cent and a reduction factor is applied to situations where the longitudinal reinforcement has a spacing greater than 12 D. This type of splitting is not to be confused with the type of splitting which was found to occur when there was sufficient anchorage of the fabric by means of bond and welds, but the concrete possessed insufficient shearing strength to develop the wire.

6.4.2 Deformed Wires

The development length, L'' , for a deformed wire must be of sufficient length that the ultimate bond stress acting along L'' balances the force at the critical section, that is

$$L'' U_u \pi D = 1.2 A_w f_y$$

or

$$L'' = \frac{1.2 A_w f_y}{U_u \pi D}$$

Letting $U_u = 10 \sqrt{f'_c}$ and $A_w = \pi D^2/4$,

$$L'' = 0.03 f_y D / \sqrt{f'_c} \quad (32)$$

where:

L'' = development length, in.

f_y = yield strength of reinforcement, psi,

D = nominal diameter of reinforcement, in., and

f'_c = compressive strength of concrete, psi.

If the spacing of longitudinal wires is greater than 12 D, the length can be reduced one-sixth to $0.025 f_y D / \sqrt{f'_c}$.

To prevent a splitting failure, the force in the steel per inch of slab width must not exceed the force which can be transmitted by shear over the length L'' . Equating the force in the steel to the force which can be transferred by the concrete:

$$L'' f_v \geq p d f_y$$

If f_v equals $5.25 \sqrt{f'_c}$ per Sec 6.3.3, then the development length necessary to prevent a splitting failure must be at least:

$$L'' = \frac{p d f_y}{5.25 \sqrt{f'_c}} \quad (33)$$

where:

L'' = development length, in.

p = reinforcement ratio.

d = effective depth of reinforcement, in.

f_y = yield strength of reinforcement, psi, and

f'_c = compressive strength of concrete, psi.

For a typical strength of concrete used in floor slabs, 3000 psi, and a steel with a yield strength of 70,000 psi, this can be simplified to:

$$L'' = 250 p d \quad (33a)$$

Thus for design, the development length, L'' , must be greater than or equal to the larger of the two values given by Eqs 32 and 33.

6.4.3 Deformed Wire Fabric

To determine the necessary development length for deformed wire fabric it is necessary to consider the stress transferred by means of both the bond and the welds and it is also necessary to provide a development length sufficient to prevent splitting.

If the minimum specified weld strength of 20,000 psi is fully developed, the stress transferred by means of bond and welds can be expressed as:

$$10 \sqrt{f'_c} \times 5/6 \pi D L'' + 20,000 A_w N \geq f_y A_w$$

Simplifying and solving for the minimum development length,

$$L'' = 0.03 D (f_y - 20,000 N) / \sqrt{f'_c} \quad (34)$$

where:

L'' = development length, in.

D = nominal diameter of reinforcement, in.,

f_y = yield strength of reinforcement, psi.,

N = number of welds in the development length which are at least 2 in. from the critical section, and

f'_c = compressive strength of concrete, psi.

If the longitudinal reinforcement is spaced laterally greater than 12 D the length given by Eq 34 may be reduced one-sixth.

To prevent a splitting failure, Eq 33 applies.

6.5 Summary and Conclusions

The results obtained from a number of tests of slabs reinforced with deformed wire and deformed wire fabric and from pull-out tests indicate the following:

1. The transfer of stress between the reinforcement and concrete in an anchorage zone is complex, but can be related to the bond, the weld strengths of the fabric and the strength of the concrete.

2. The minimum development length for deformed wire may be computed from

$$L'' = 0.03 f_y D / \sqrt{f'_c} \quad (32)$$

3. The minimum development length for deformed wire fabric is

$$L'' = 0.03 D (f_y - 20,000 \text{ N}) / \sqrt{f'_c} \quad (34)$$

4. To prevent splitting type anchorage failures the development lengths in 2 and 3 must be at least

$$L'' = \frac{p d f_y}{5.25 \sqrt{f'_c}}, \text{ or} \quad (33)$$

$$L'' = 250 p d \quad (33a)$$

5. When the wires being developed are space 12 D or further apart, the development lengths required in 2 and 3 may be reduced by one-sixth.

6. When ultimate strength design procedures are used and the design strength is less than the specified yield the development length obtained from Eqs 32, 33, 33a and 34 may be proportionally reduced.

7. FLEXURAL STRENGTH

7.1 Background

7.1.1 Problem

In general structural elements must be designed to resist shears, moments and axial loads. For reinforced concrete beams and floor slabs, axial loading is normally negligible or ignored for design purposes and emphasis is placed on the design for shear and moment. The behavior of beams and slabs subjected to shear has been considered previously in Chapter 5.

As a section of an uncracked reinforced concrete beam or slab is subjected to an increasing moment, the steel plays a minor role; most of the moment is resisted by the concrete. Until cracking occurs, the flexural behavior can be considered identical to that of a plain concrete beam for most practical purposes. After cracking, the tensile strength contribution of the concrete decreases; when the tensile reinforcement has been stressed to its yield strength, the tensile strength contribution of concrete is negligible and often neglected entirely for purposes of analysis.

A number of comprehensive studies of the flexural mechanics of reinforced concrete have been conducted; Ref (15) give special attention to the problem of high strength reinforcements. A detailed review and development of flexural mechanics concepts is outside the scope of this paper, and the reader is referred to one of these studies for a more complete background on the subject.

7.1.2 Present Design Approaches

For the purposes of design, one-way slabs may be assumed to behave as wide beams and can be designed according to the provisions of Chapters 11 (working stress design) and 16 (ultimate strength design) of the ACI Building Code. This assumption corresponds to assuming that Poisson's ratio is equal to zero. However, the longitudinal compression of the concrete does produce some lateral expansion which, because of the Poisson's ratio effect, slightly increases the stiffness and strength.

Consideration will be limited here to the ultimate strength provisions of the code. In addition to the cross sectional dimension properties of a member, the code expresses flexural strength in terms of

the uniaxial compressive strength of the concrete, f'_c , and the yield strength of the reinforcement, f_y . Since the code assumes the concrete reaches its ultimate compressive strength at a strain of 0.003, for reinforcements having yield strengths in excess of 60,000 psi, the yield strength of the reinforcement is limited to 0.85 of the specified yield strength or 60,000 psi, whichever is greater unless the specified yield stress is obtained at a strain of 0.003 or less. For yield strengths above 60,000 psi special precautions are taken to insure that crack widths do not become excessive. Equation 16-1 is the basic ultimate strength moment expression.

$$M_u = \phi [A_s f_y (d - \frac{A_s f_y}{1.7 f'_c b})] \times 10^{-3} \quad (8)$$

where:

M_u = ultimate moment, in.-kips

ϕ = capacity reduction factor

A_s = area of tensile reinforcement, sq in.

f_y = yield strength of the reinforcement, psi.

d = effective depth, in.

f'_c = compressive strength of concrete, psi.

b = width of compressive face of flexural member, in.

To insure ductility, the area of the tensile reinforcement is limited to 0.75 of the balanced reinforcement ratio, p_b , which is the amount of steel which will produce a compression failure in the concrete at the same instant that the steel reaches the yield point. The balanced reinforcement ratio is expressed by Eq 16-2 of the ACI Building Code.

$$p_b = \frac{0.85 k_1 f'_c}{f_y} \frac{87,000}{87,000 + f_y} \quad (35)$$

where:

k_1 = factor relating the depth of the rectangular stress block to the strength of the concrete (defined in Sec 1503(g) of the ACI Building Code; taken as 0.85 for concrete

strengths up to 4000 psi and reduced continuously at the rate of 0.05 for each 1000 psi of strength in excess of 4000 psi.

For purposes of design and reasons of safety, the design ultimate moment capacity, for steel reinforced members, is based on the defined yield strength as opposed to the ultimate tensile strength of the reinforcement.

7.2 Experimental Results

Although 63 slabs were tested to failure, the majority of the slabs failed in the splice or in the shear span. Since the basic concepts of flexural strength are comparatively well defined, the study of flexural strength was considered secondary to the determination of crack control, splicing, and anchorage properties. Shear reinforcement was used in only a few slabs where necessary splicing or crack control information was lacking. As a consequence, only 11 slabs reinforced with deformed wire and deformed wire fabric are available to this phase of the investigation. Failure occurred by tensile fracture of the reinforcement except in one case where crushing of the concrete occurred.

Although Eq 8 is considered the ultimate moment for purposes of design, it does not provide an accurate estimate of the actual ultimate strength which can be obtained with beams and slabs reinforced with high strength reinforcement; for the purposes of analysis Eq 8 may be considered the yield moment. If the reinforcement fractures at ultimate, a more accurate estimate of the strength can be obtained by replacing the yield strength of the reinforcement, f_y , by the ultimate tensile strength, f'_s .

Table 18 gives the strength of slabs which failed by fracture of the reinforcement or by crushing of the concrete; also given are the moments predicted by Eq 8 based upon both the specified minimum yield strength of 70,000 psi and the actual ultimate tensile strength of the reinforcement. The capacity reduction factor, ϕ , was equal to unity for the purposes of analysis. For two specimens which contained splices, the actual effective depth at the critical section where failure occurred is given in place of the nominal effective depth.

7.3 Discussion of Results

As shown in Table 18, the experimental ultimate moments were slightly larger than the ultimate moments predicted by Eq 8, with f'_s

strengths up to 4000 psi and reduced continuously at the rate of 0.05 for each 1000 psi of strength in excess of 4000 psi.

For purposes of design and reasons of safety, the design ultimate moment capacity, for steel reinforced members, is based on the defined yield strength as opposed to the ultimate tensile strength of the reinforcement.

7.2 Experimental Results

Although 63 slabs were tested to failure, the majority of the slabs failed in the splice or in the shear span. Since the basic concepts of flexural strength are comparatively well defined, the study of flexural strength was considered secondary to the determination of crack control, splicing, and anchorage properties. Shear reinforcement was used in only a few slabs where necessary splicing or crack control information was lacking. As a consequence, only 11 slabs reinforced with deformed wire and deformed wire fabric are available to this phase of the investigation. Failure occurred by tensile fracture of the reinforcement except in one case where crushing of the concrete occurred.

Although Eq 8 is considered the ultimate moment for purposes of design, it does not provide an accurate estimate of the actual ultimate strength which can be obtained with beams and slabs reinforced with high strength reinforcement; for the purposes of analysis Eq 8 may be considered the yield moment. If the reinforcement fractures at ultimate, a more accurate estimate of the strength can be obtained by replacing the yield strength of the reinforcement, f_y , by the ultimate tensile strength, f'_s .

Table 18 gives the strength of slabs which failed by fracture of the reinforcement or by crushing of the concrete; also given are the moments predicted by Eq 8 based upon both the specified minimum yield strength of 70,000 psi and the actual ultimate tensile strength of the reinforcement. The capacity reduction factor, ϕ , was equal to unity for the purposes of analysis. For two specimens which contained splices, the actual effective depth at the critical section where failure occurred is given in place of the nominal effective depth.

7.3 Discussion of Results

As shown in Table 18, the experimental ultimate moments were slightly larger than the ultimate moments predicted by Eq 8, with f'_s

equal to f_y . Two slabs, CWC 8 and CWB 9, developed ultimate moments approximately ten per cent greater than the calculated ultimate moments; this error is not great and probably resulted from some restraint at the roller supports.

The calculated yield moments given in Table 18 are based on a yield stress of 70,000 psi which is the specified minimum yield stress. The deformed wire and deformed wire fabric reached the 70,000 psi stress at a strain of about 0.003. Since a design yield stress cannot exceed 60,000 psi, per the ACI Building Code, unless full-scale tests show crack widths are not excessive, most designers will use 60,000 psi. These tests indicate that the actual ultimate moment is governed by the ultimate tensile strength of the reinforcement. Since the minimum specified ultimate tensile strength for deformed wire and deformed wire fabric is 80,000 psi, a design based on a stress of 60,000 psi will result in actual strengths 33 per cent greater than the design strength.

7.4 Conclusions

The existing flexural computations in the ACI Building Code can be applied to members reinforced with deformed wire and deformed wire fabric. The use of a yield strength of 60,000 psi in the ultimate moment expression of the ACI Building Code, Eq 16-1, will produce members which have an actual ultimate strength at least 33 per cent greater than the design strength. With regard to strength it is safe to use the ASTM specified yield strength for deformed wire fabric of 70,000 psi in Eq 16-1.

LIST OF REFERENCES

1. Building Code Requirements for Reinforced Concrete, ACI Standard 318-63, American Concrete Institute, June 1963.
2. David Watstein and R. G. Mathey, "Width of Cracks in Concrete at the Surface of Reinforcing Steel Evaluated by Means of Tensile Bond Specimens," Proceedings, American Concrete Institute, Vol. 56, July 1959, pp. 47-56.
3. B. B. Broms, "Stress Distribution in Reinforced Concrete Members with Tension Cracks," Proceedings, American Concrete Institute, Vol. 62, September 1965, pp. 1095-1108.
4. "Rapport de Commission No. 4a, Fissuration (Report of Commission No. 4a on Cracking)," Comité Européen du Béton, Bulletin d'Information No. 12, C.E.B. Permanent Secretariat, Paris, France, February 1959.
5. Peter Gergely and L. A. Lutz, "Maximum Crack Width in Reinforced Flexural Members," to be published in Symposium on Cracking of Concrete, American Concrete Institute.
6. Eivind Hognestad, "High Strength Bars as Concrete Reinforcement, Part 2, Control of Cracking," Journal of the PCA Research and Development Laboratories, Vol. 4, No. 1, January 1962, pp. 46-62.
7. Amos Atlas, C. P. Siess and C. E. Kesler, "Behavior of One-Way Concrete Floor Slabs Reinforced with Welded Wire Fabric," Proceedings, American Concrete Institute, Vol. 62, May 1965, pp. 539-557.
8. Axel Efsen and H. Krenchel, "Flexural Cracks in Reinforced Concrete Beams," Discussion in the Journal of the American Concrete Institute, Proceedings, Vol. 54, December 1958, pp. 1356-1358.
9. European Committee for Concrete (C.E.B.), "Information Bulletin No. 24, 5th General Session, Vienna, April 1959," English translation issued by Cement and Concrete Association, London.
10. "Summary Report on Experiments Carried Out on Reinforced Concrete Slabs Reinforced with TOR-steel and Welded Wire Mesh," TORISTEG-Steel Corporation, Luxembourg, Technical Service, Vienna, February 1959.
11. P. M. Ferguson and F. N. Matloob, "Effect of Bar Cut-off on Bond and Shear Strength of Reinforced Concrete Beams," Proceedings, American Concrete Institute, Vol. 56, July 1959, pp. 5-24.
12. P. M. Ferguson and J. N. Thompson, "Development Length of High Strength Reinforcing Bars in Bond," Proceedings, American Concrete Institute, Vol. 59, July 1962, pp. 887-992.

13. David Watstein and R. G. Mathey, "Investigation of Bond in Beam and Pull-out Specimens with High Yield Strength Deformed Bars," Proceedings, American Concrete Institute, Vol. 57, March 1961, pp. 1071-1090.
14. Committee on Continuously Reinforced Concrete Pavement, "Test Investigation of Splices in Continuously Reinforced Concrete Pavement," Bulletin No. 3, Concrete Reinforcing Steel Institute.
15. Amos Atlas, C. P. Siess, A. C. Bianchini and C. E. Kesler, "Behavior of Concrete Floor Slabs Reinforced With Welded Wire Fabric," TAM Report No. 260, University of Illinois, August 1964.
16. L. M. Sur, R. S. Jensen, R. J. Reynolds, and C. E. Kesler, "WRI Study of Deformations on Wires," Mimeographed Paper, Theoretical and Applied Mechanics Department, University of Illinois, July 1965.
17. A. N. Talbot, "Tests of Reinforced Concrete Beams: Resistance to Web Stresses, Series of 1907 and 1908," Bulletin 29, Engineering Experiment Station, University of Illinois, 1909, pp. 85.
18. ACI-ASCE Committee 326, "Shear and Diagonal Tension," Proceedings, American Concrete Institute, Vol. 59, January, pp. 1-30, February, pp. 277-334, March, pp. 352-396, 1962.
19. Armas Laupa, C. P. Siess and N. M. Newmark, "Strength in Shear of Reinforced Concrete Beams," Bulletin 428, Engineering Experiment Station, University of Illinois, March 1955.
20. R. D. de Cossio, Discussion of Ref. 20, Proceedings, American Concrete Institute, Vol. 59, September 1962, pp. 1323-1349.

APPENDIX A1 PULL-OUT TESTS

A1.1 General

This investigation was conducted in conjunction with other studies concerned with the splicing and anchorage behavior of deformed wire and deformed welded wire fabric in concrete slabs. Because of the important role bond and weld strengths play in splicing and anchorage behavior, a limited number of pull-out tests were conducted with several sizes of deformed wires, with and without a transverse wire in the embedment length.

Four different sizes of deformed wire were considered; each of the wire sizes was supplied by a different manufacturer. A 6-in. effective embedment length, which was considered a common transverse wire spacing, was used for all specimens. The pull-out stress obtained with a deformed longitudinal wire, with a deformed longitudinal wire with a welded transverse wire, and with an unbonded deformed longitudinal wire with a welded transverse wire were considered. A total of 36 pull-out specimens were tested.

A1.2 Specimens

Pull-out specimens had a 9-in. square cross section and a 8-in. length. Four longitudinal wire sizes were studied: D10, D19, D21, and D29. Wire was also obtained from four fabric styles: D10xD4:6x6, D19xD9:6x12, D21xD7:6x12 and D29xD11:4x12. All but one transverse wire were removed from the longitudinal wire obtained from the fabric. The remaining transverse wire had a total length of approximately 8 in. The deformed wire and deformed wire fabric specimens were cast in concrete as shown in Fig. A.1 to provide three types of pull-out specimens.

Each specimen is presented by a series of numbers and letters. A typical specimen designation is:

DTG19-2

where "D" indicates deformed wire, "T" indicates the presence of a transverse wire welded to the longitudinal wire and "G" indicates that the longitudinal wire was unbonded. The number 19 is the cross sectional area of the longitudinal wire in hundreths of a square inch, and 2 indicates the specimen number. The absence of G or TG in a specimen designation indicates that the longitudinal wire was bonded, or that no

transverse wire existed and longitudinal wire was bonded, respectively. The designation is illustrated in Fig. A1.

Type I portland cement and Wabash sand and gravel, meeting relevant ASTM specifications, were used for all concrete. The mix proportions by weight of cement:sand:gravel were 1.00:3.38:4.29, respectively. The water to cement ratio was 0.69 by weight. The properties of the fresh and hardened concrete are given in Table A.1.

The deformed wires exceeded the requirements for Deformed Steel Wire for Concrete Reinforcement, A 496-64, for Material to be Used in the Fabrication of Welded Fabric. The deformed wire fabric exceeded the ASTM Standard Specification for Welded Deformed Steel Wire Fabric for Concrete Reinforcement, A 497-64, except the welds of the D29xD11: 4x12 fabric did not meet the minimum strength requirements. Low welds were especially requested for some of the fabric obtained for the comprehensive program in order that studies of splices and anchorage would be meaningful. The strength properties and geometry of the deformed wires and deformed wire fabric are given in Tables 7 and 8, respectively. Figure 1 shows the various types of deformed wires used in the study.

A lubricating gel was used to prevent bond on the first two inches at the loaded end of the longitudinal wire of D and DT specimens and destroy all bond along the longitudinal wire of DTG specimens. The gel was applied just prior to casting.

A1.3 Experimental Procedure

Pull-out specimens were cast in plywood forms, and 6 by 12-in. control cylinders were cast in steel forms in accordance with pertinent ASTM specifications. Nine pull-out specimens and seven control cylinders were cast from each batch of concrete. The pull-out specimens were comprised of three specimens each of types D, DT, and DTG with the same size longitudinal wire used with all three types; the specimens were cast with the longitudinal wires in a horizontal position.

Specimens were cured in the forms for 24 hours followed by 6 days in a 100 per cent relative humidity chamber at 70 F. After the removal of specimens from the moist room, two cylinders were tested in compression to provide an estimate of the age at which the strength would reach 3500 psi; specimens were tested at this age. Three control cylinders

were used to obtain the compressive strength and two cylinders were used to obtain the tensile splitting strength at the time of test.

Pull-out specimens were tested as shown in Fig. A.2. Specimens which contained D10 longitudinal wire were loaded in 400 lb increments; all other specimens were loaded in 500 lb increments. Slip was measured at the free and loaded ends of the longitudinal wire until failure occurred.

A1.4 Experimental Results

The load applied to the longitudinal wire was divided by the nominal cross sectional area of the wire to permit the results to be presented in terms of stress.

The slip at the loaded end was corrected to eliminate the error in the slip reading caused by the elongation of the wire between the location of dial gage measurement and the point where bonding began. DTG specimens were unbonded along the entire length; therefore, the slip of the wire at the loaded end was equal to the slip at the free end plus the elongation of the wire between the weld and the point where slip was measured at the loaded end.

A summary of the pull-out results with corrected slip values are given in Table A.2. The stress-slip curves for individual specimens are given in Figs. A.3 through A.14. Two specimens, DT10-1 and DT10-3, failed with a fracture of the longitudinal wire. All other specimens exhibited a pull-out mode of failure accompanied by a failure of the weld at the transverse wire with DTG and DT specimens. Splitting of the concrete occurred when DT21-3 reached failure. It was also observed that while the welds on D10, D19 and D29 failed leaving a small, almost smooth depression in the longitudinal wire; welds on D21 wire failed leaving a very jagged region on the longitudinal wire where a portion of the longitudinal wire remained attached to the transverse wire and was stripped away.

A1.5 Discussion of Results

The bond stress at failure was obtained by dividing the load at failure by bonded surface area of the steel, i.e.:

$$U_u = \frac{P_u}{\pi D \ell}$$

where:

U_u = ultimate bond stress, psi.

p_u = ultimate pull-out load, lb.

D = nominal diameter of wire, in.

ℓ = effective embedment length, 6 in.

The ACI Building Code (1) specifies that the ultimate bond stress for bars which meet the deformation requirements of ASTM A 305 can be expressed as follows:

$$U_u = \frac{\alpha \sqrt{f'_c}}{D} \quad (9)$$

where:

α = bond stress coefficient.

f'_c = compressive strength of concrete, psi.

D = nominal diameter of reinforcement, in.

For bars with less than 12 in. of bottom cover, $\alpha = 9.5$ but U_u cannot exceed 800 psi. Assuming that the ultimate bond stress for deformed wire reinforcement can be properly expressed by Eq 9, α can be determined as follows:

$$\alpha = \frac{p_u}{\pi \ell \sqrt{f'_c}} \quad (36)$$

Values of U_u and α are given in Table A.3. The average ultimate bond stress ranged from 70 to 124 per cent of the bond stress permitted for deformed bars. The bond stress coefficient, α , was smallest for smaller wires and was approximately equal to 9.5, the value permitted for deformed bars, for the D29 wire.

The average results obtained with the D, DTG and DT specimens are given below.

Specimens	Longitudinal Wire Size			
	D10	D19	D21	D29
	(Average Stress at Failure, ksi)			
D	40	27	41	39
DTG	47	49	33	21
D + DTG	87	76	74	60
DT	88	84	83	56

It can be seen that the strengths of the DTG specimens are slightly higher than the shear weld strengths given in Table 8. It can also be seen that the strengths of the DT specimens are approximately equal to the combined strength of the D and the DTG specimens. This indicates that if splitting is avoided, the pull-out stress is a combination of the stress developed by bond and the stress developed by the weld strengths.

The results given here are for the particular wires that were used in the other phases of the investigation. The wires exceeded the deformation requirements of ASTM A 496, and, therefore, the results cannot be applied directly to design procedures. A much larger series of pull-out tests (16) have been conducted with a number of deformed wire sizes and deformation patterns. It was found that the total shearing area was the most important factor affecting the pull-out strength. Figure A.15 was developed from the results of this study; it relates the diameters of embedment, necessary to develop a 70,000 psi pull-out stress, to the shearing area per inch. For a given wire size, the shearing area necessary to develop 70,000 psi in a given number of diameters of embedment can be found and related to the average ultimate bond stress acting along the embedment length. It was, therefore, possible to develop Fig. A.16 which relates the shearing area per inch to the ultimate pull-out bond stress for various wire sizes. ASTM A 496 requires that 25 per cent of the surface of the wire be deformed. Using Fig. A.16 it was found that for wires just meeting this 25 per cent shearing area requirement, the ultimate pull-out bond stress would be expected to vary between 700 psi for D29 wire to 800 psi for D4 wire.

It is not clear why the D10 and D19 wires tested here do not compare well with this prediction; pull-out data is subject to appreciable scatter and it may be that the three specimens each of D10 and D19 wire tested here did not give representative strengths. Figures A.15 and A.16 are based on 123 pull-out tests and are considered to give results more representative of what would be expected in general.

A1.6 Conclusions

1. Ultimate bond stresses for various sizes of deformed wires ranged from 70 to 124 per cent of the ultimate bond stress permitted for deformed bars by the ACI Building Code.

2. If welds fail, the ultimate pull-out stress can be approximated by combining the stresses transferred by means of welds and bond.

3. The ultimate pull-out bond stress can be related to the shearing area per inch as shown in Fig. A.16.

APPENDIX A2 MEANS OF CRACK CONTROL IN THE ACI BUILDING CODE

Subcommittee 9 of the American Concrete Institute Committee 318, Standard Building Code has tentatively recommended that when the design yield strength of the reinforcement exceeds 40,000 psi, the cross sections at maximum moments shall be proportioned so that the quantity Z given by

$$Z = f_s \sqrt[3]{t_b A} \quad (37)$$

shall not exceed 170 kips/in. for interior members and 130 kips/in. for exterior exposure.

In Eq 37

f_s = tensile steel stress at the service load level of dead load plus live load. In lieu of such computations, f_s may be taken as 60 per cent of the design yield strength, f_y .

t_b = thickness of concrete cover measured from the extreme tension fiber to the center of the bar located closest thereto.

A = effective tension area of concrete surrounding the main tension reinforcing bars and having the same centroid as that of the reinforcement, divided by the number of bars or bundles of bars. When the main reinforcement consists of several bar sizes, the number of bars shall be computed as the total steel area divided by the area of the largest bar used.

Equation 37 and the proposed upper limits of Z were developed from Eq 6 using an approximate value of 1.2 for R . The limits of Z of 170 kips/in. and 130 kips/in. correspond to limiting crack widths of 0.015 and 0.012 in.

Figure A.17 was plotted to determine how the maximum crack widths of the slabs tested in this investigation would compare to the values predicted by Eq 6 for different values of Z . This figure is similar to Fig. 8 except that the abscissa does not include R . The line for Eq 6, Gergely-Lutz, was computed using 1.2 for R , the value used by the Subcommittee. The average value of R for the one-way slabs in this

investigation was 1.35. Because of the differences in the values of R crack widths from this investigation are slightly higher than those given by Eq 6.

If a value of 1.2 for R represents average depth beams and a value of 1.35 for R represents average depth slabs, it will be appropriate to reduce the Z values by $1.2/1.35$ for slabs to obtain similar crack control capabilities, provided that it is desirable that cracks in slabs should be controlled to the same extent as those in beams. Then the upper limits of Z would be 170 and 130 kips/in. for beams and 150 and 115 kips/in. for slabs.

APPENDIX A3 EXAMPLES OF SPLICE DESIGNS

In Chapter 5, Eqs 17 and 18 were developed to permit the design of a splice of deformed wire fabric. These equations are based on slab tests and recent pull-out tests. Two typical splice designs will now be considered to illustrate the necessary calculations. The necessary length of lap for the splice of two identical sheets of fabrics and for the splice of two different fabric styles will be determined. A concrete strength of 3600 psi is assumed in both examples.

1. Two sheets of 6x6:D10xD4 are to be spliced to transfer the full yield strength load, $f_y = 70,000$ psi. The length of the splice is equal to the sum of the overhangs, assumed in this case to be 3 in. each, plus the distance between outermost transverse wires, Eq 18, or

$$\ell = \ell_o + \ell_s$$

$$\ell = 6 + p d \left[\frac{70,000}{3.5 \sqrt{3600}} - \frac{8 \times 6}{0.356} \right]$$

but

$$p d = A_w / S_\ell \text{ or } 0.10/6$$

then

$$\ell = 6 + 0.0167 (334 - 135)$$

$$\ell = 9.3 \text{ in.}$$

The length of lap must now be checked in Eq 17. Since the value of N for the lap calculated from Eq 18 is 1 (see Fig. 15), then,

$$\ell = 0.045 \times 0.356 (70,000 - 20,000 \times 1)/60$$

$$\ell = 13.4 \text{ in.}$$

Since the longitudinal reinforcement has a lateral spacing greater than 12 D, the splice length may be reduced 1/6; or,

$$\ell = 13.4 \times 5/6$$

$$\ell = 11.1 \text{ in.}$$

Equation 17 controls, and the required length of lap is 11.1 in.

2. A sheet of 5x6:D13xD5 is to be spliced with 6x8:D21xD7. Assume that the 5x6:D13xD5 has a 3-in. overhang and the 6x8:D21xD7 has a 4-in. overhang, then ℓ_o is 3 in. plus 4 in. or 7 in. The splice is to

APPENDIX A3 EXAMPLES OF SPLICE DESIGNS

In Chapter 5, Eqs 17 and 18 were developed to permit the design of a splice of deformed wire fabric. These equations are based on slab tests and recent pull-out tests. Two typical splice designs will now be considered to illustrate the necessary calculations. The necessary length of lap for the splice of two identical sheets of fabrics and for the splice of two different fabric styles will be determined. A concrete strength of 3600 psi is assumed in both examples.

1. Two sheets of 6x6:D10xD4 are to be spliced to transfer the full yield strength load, $f_y = 70,000$ psi. The length of the splice is equal to the sum of the overhangs, assumed in this case to be 3 in. each, plus the distance between outermost transverse wires, Eq 18, or

$$\ell = \ell_o + \ell_s$$

$$\ell = 6 + p d \left[\frac{70,000}{3.5 \sqrt{3600}} - \frac{8 \times 6}{0.356} \right]$$

but

$$p d = A_w / S_\ell \text{ or } 0.10/6$$

then

$$\ell = 6 + 0.0167 (334 - 135)$$

$$\ell = 9.3 \text{ in.}$$

The length of lap must now be checked in Eq 17. Since the value of N for the lap calculated from Eq 18 is 1 (see Fig. 15), then,

$$\ell = 0.045 \times 0.356 (70,000 - 20,000 \times 1)/60$$

$$\ell = 13.4 \text{ in.}$$

Since the longitudinal reinforcement has a lateral spacing greater than 12 D, the splice length may be reduced 1/6; or,

$$\ell = 13.4 \times 5/6$$

$$\ell = 11.1 \text{ in.}$$

Equation 17 controls, and the required length of lap is 11.1 in.

2. A sheet of 5x6:D13xD5 is to be spliced with 6x8:D21xD7. Assume that the 5x6:D13xD5 has a 3-in. overhang and the 6x8:D21xD7 has a 4-in. overhang, then ℓ_o is 3 in. plus 4 in. or 7 in. The splice is to

transfer the full yield strength, 70,000 psi, in the fabric with the smaller longitudinal cross sectional area, in this case the 5x6:D13xD5 fabric. The effectiveness, or the stress, in the 6x8:D21xD7 fabric must now be calculated. By equating the tensile force in the steel per inch of slab width:

$$Y (6x8:D21xD7) = \frac{6}{5} \times \frac{0.13}{0.21} = 0.74$$

Thus when the 5x6:D13xD5 fabric is stressed to 70,000 psi the 6x8:D21xD7 fabric will only be stressed to 52,000 psi.

From Eq 18, the length of lap for the 5x6:D13xD5 fabric is:

$$\ell = 7 + \frac{0.13}{5} \left[\frac{70,000}{3.5 \sqrt{3600}} - \frac{8 \times 7}{0.406} \right]$$

$$\ell = 7 + 0.026 (333-138)$$

$$\ell = 12.1 \text{ in.}$$

The outermost transverse wires in the lap are 5.1 in. apart with this length of lap, and the value of N for use in Eq 17 is 1 (see Fig. 15); then from Eq 17,

$$\ell = 0.045 \times 0.407 (70,000 - 20,000 \times 1) / \sqrt{3600}$$

$$\ell = 15.3 \text{ in.}$$

In this case, the length can be reduced by one-sixth since the lateral spacing of longitudinal wires is greater than 12 D. Thus,

$$\ell = (5/6) \times 15.3$$

$$\ell = 12.7 \text{ in.}$$

The length required for the lap of the 6x8:D21xD7 fabric for a Y value of 0.74 must now be calculated. From Eq 18,

$$\ell = 7 + 0.74 \times \frac{0.21}{6} \left[\frac{70,000}{3.5 \sqrt{3600}} - \frac{8 \times 7}{0.517} \right]$$

$$\ell = 12.8 \text{ in.}$$

Again, the value of N is 1 and from Eq 17,

$$\ell = 0.74 \times 0.045 \times 0.517 (70,000 - 20,000 \times 1) / \sqrt{3600}$$

$$\ell = 14.3 \text{ in.}$$

Since the lateral spacing of the longitudinal reinforcement is greater than 12 D, the length may be reduced by 1/6.

$$l = (14.5)(5/6)$$

$$l = 12.1 \text{ in.}$$

Therefore the necessary length of lap is 12.8 in.

The above examples illustrate the general procedure required to determine the length of splices for deformed wire fabric reinforcement and the necessary checks.

TABLE 1--OUTLINE OF CRACK CONTROL SPECIMENS

Slab	Reinforcement ^a Style	Steel Ratio, p	Total Slab Depth, in.	Effective Depth, d, in.	Length of Shear Span, a, in.	Distance ^b to Transverse wire, in.
<u>Deformed Bars</u>						
CDB 1	6:#2	0.0020	5.0	4.0	12	...
CDB 2	6:#3	0.0046	5.0	4.0	12	...
CDB 3	6:#4	0.0054	7.0	6.0	18	...
CDB 4	4:#5	0.0130	7.0	5.9	18	...
<u>Deformed Wires</u>						
CWA 5	6:D7	0.0029	5.0	4.0	12	...
CWB 6	6:D7	0.0029	5.0	4.0	12	...
CWC 7	2:D9	0.0075	7.0	6.0	18	...
CWC 8	4:D9	0.0056	5.0	4.0	12	...
CWB 9	6:D10	0.0042	5.0	4.0	12	...
CWD 10	6:D19	0.0079	5.0	4.0	12	...
CWE 11	6:D21	0.0088	5.0	4.0	12	...
CWE 12	6:D21	0.0065	7.0	5.4	18	...
CWA 13	4:D29	0.0121	7.0	6.0	18	...

(Continued)

^aStyle designation: 6:D7, number before colon is longitudinal wire or bar spacing and number after colon is longitudinal wire or bar size; 6x12:D7xD4, numbers ahead of colon are longitudinal and transverse wire spacings and numbers after colon are the longitudinal and transverse wire size.

^bDistance of outermost transverse wire from support.

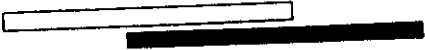
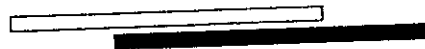
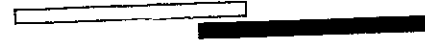

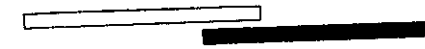
TABLE 1--OUTLINE OF CRACK CONTROL SPECIMENS (Concluded)

Slab	Reinforcement ^a Style	Steel Ratio, p	Total Slab Depth, in.	Effective Depth, d, in.	Length of Shear Span, a, in.	Distance ^b to Transverse wire, in.
<u>Deformed Wire Fabric</u>						
CFA 14	6x12:D7xD4	0.0029	5.0	4.0	12	0
CFB 15	6x12:D7xD4	0.0029	5.0	4.0	12	6
CFC 16	2x12:D9xD5	0.0075	7.0	6.0	18	0
CFC 17	4x12:D9xD5	0.0056	5.0	4.0	12	6
CFB 18	6x12:D10xD4	0.0042	5.0	4.0	12	6
CFD 19	6x12:D19xD9	0.0079	5.0	4.0	12	0
CFE 20	6x12:D21xD7	0.0088	5.0	4.0	12	0
CFE 21	6x6:D21xD7	0.0065	7.0	5.4	18	0
CFA 22	4x12:D29xD11	0.0121	7.0	6.0	18	0
CFA 23	4x6:D29xD11	0.0121	7.0	6.0	18	0

^aStyle designation: 6:D7, number before colon is longitudinal wire or bar spacing and number after colon is longitudinal wire or bar size; 6x12:D7xD4, numbers ahead of colon are longitudinal and transverse wire spacings and numbers after colon are the longitudinal and transverse wire size.

^bDistance of outermost transverse wire from support.

TABLE 2--OUTLINE OF SPLICE SPECIMENS

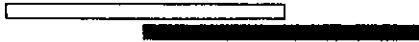

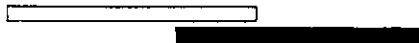
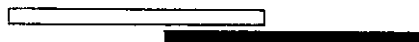
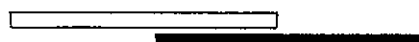
Slab	Reinforcement ^a Style	p ^b	Total Slab Depth, in.	d ^c	Clear Cover, in.	Length of Shear Span, a, in.	Amount of Overlap in. dia		Detail of Lap
<u>Deformed Bars</u>									
SDB 1	6:#4	0.0056	7	6.0	0.75	12	12.00	24.0	
SDB 2	4:#5	0.0130	7	5.9	0.75	12	15.00	24.0	
<u>Deformed Wires</u>									
SWB 3	6:D7	0.0028	5	4.1	0.75	12	3.58	12.0	
SWB 4	6:D7	0.0028	5	4.1	0.75	12	5.96	20.0	
SWC 5	2:D9	0.0074	7	6.1	0.75	18	4.05	12.0	
									(Continued)

^aStyle designation: 6:D7, number before colon is longitudinal wire or bar spacing and number following colon is longitudinal wire or bar size. 6x12:D7xD4, numbers ahead of colon are longitudinal and transverse wire spacing and numbers after colon are longitudinal and transverse wire size.

^bReinforcement ratio based on depth of lower reinforcement in lap.

^cEffective depth, in.

TABLE 2--OUTLINE OF SPLICE SPECIMENS (Continued)

Slab	Reinforcement ^a Style	p^b	Total Slab Depth, in.	d^c	Clear Cover, in.	Length of Shear Span, a, in.	Amount of Overlap in. dia		Detail of Lap
SWC 6	2:D9	0.0074	7	6.1	0.75	18	10.14	30.0	
SWB 7	6:D10	0.0041	5	4.1	0.75	12	4.27	12.0	
SWB 8	6:D10	0.0041	5	4.1	0.75	12	5.70	16.0	
SWB 9	6:D10	0.0041	5	4.1	0.75	12	7.12	20.0	
SWB 10	6:D10	0.0041	5	4.1	0.75	12	8.55	24.0	

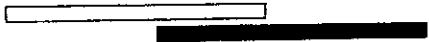

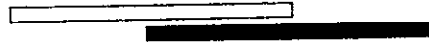


(Continued)

^aStyle designation: 6:D7, number before colon is longitudinal wire or bar spacing and number following colon is longitudinal wire or bar size. 6x12:D7xD4, numbers ahead of colon are longitudinal and transverse wire spacing and numbers after colon are longitudinal and transverse wire size.

^bReinforcement ratio based on depth of lower reinforcement in lap.

^cEffective depth, in.

TABLE 2--OUTLINE OF SPLICE SPECIMENS (Continued)

Slab	Reinforcement ^a Style	p^b	Total Slab Depth, in.	d^c	Clear Cover, in.	Length of Shear Span, a, in.	Amount of Overlap in. dia		Detail of Lap
SWD 11	6:D19	0.0079	5	4.0	0.75	12	7.86	16.0	
SWD 12	6:D19	0.0079	5	4.0	0.75	12	9.82	20.0	
SWE 13	6:D21	0.0088	5	4.0	0.75	12	10.34	20.0	
SWE 14	6:D21	0.0058	7	6.0	0.75	18	15.51	30.0	
SWA 15	4:D29	0.0122	7	6.0	0.75	12	12.16	20.0	




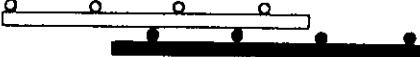

(Continued)

^aStyle designation: 6:D7, number before colon is longitudinal wire or bar spacing and number following colon is longitudinal wire or bar size. 6x12:D7xD4, numbers ahead of colon are longitudinal and transverse wire spacing and numbers after colon are longitudinal and transverse wire size.

^bReinforcement ratio based on depth of lower reinforcement in lap.

^cEffective depth, in.

TABLE 2--OUTLINE OF SPLICE SPECIMENS (Continued)

Slab	Reinforcement ^a Style	^b p	Total Slab Depth, in.	^c d	Clear Cover, in.	Length of Shear Span, a, in.	Amount of Overlap in. dia	Detail of Lap
SWA 16	4:D29	0.0122	7	6.0	0.75	12	14.59 24.0	
SWA 17	4:D29	0.0122	7	6.0	0.75	18	18.24 30.0	
<u>Deformed Wire Fabric</u>								
SFA 18	6x6:D7xD4	0.0028	5	6.1	0.75	12	8.00 26.8	
SFC 19	2x6:D9xD5	0.0074	7	6.1	0.75	18	14.00 47.0	
SFB 20	6x6:D10xD4	0.0041	5	4.1	0.75	12	5.70 16.0	

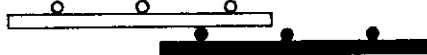
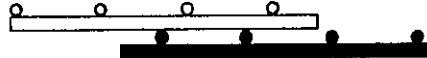

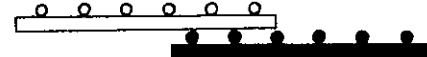
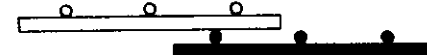
(Continued)

^aStyle designation: 6:D7, number before colon is longitudinal wire or bar spacing and number following colon is longitudinal wire or bar size. 6x12:D7xD4, numbers ahead of colon are longitudinal and transverse wire spacing and numbers after colon are longitudinal and transverse wire size.

^bReinforcement ratio based on depth of lower reinforcement in lap.

^cEffective depth, in.

TABLE 2--OUTLINE OF SPLICE SPECIMENS (Continued)

Slab	Reinforcement ^a Style	^b P	Total Slab Depth, in.	^c d	Clear Cover, in.	Length of Shear Span, a, in.	Amount of Overlap in. dia		Detail of Lap
SFB 21	6x6:D10xD4	0.0041	5	4.1	0.75	12	8.00	22.5	
SFB 22	6x6:D10xD4	0.0041	5	4.1	0.75	12	14.00	39.3	
SFD 23	6x12:D19xD9	0.0079	5	4.0	0.75	12	3.00	6.1	
SFD 24	6x3:D19xD9	0.0079	5	4.0	0.75	12	7.50	15.3	
SFD 25	6x6:D19xD9	0.0079	5	4.0	0.75	12	7.86	16.0	

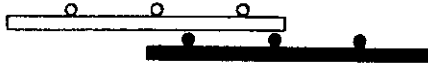
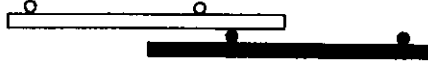
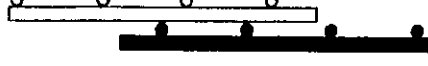
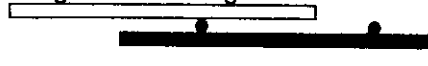
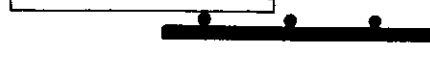
(Continued)

^aStyle designation: 6:D7, number before colon is longitudinal wire or bar spacing and number following colon is longitudinal wire or bar size. 6x12:D7xD4, numbers ahead of colon are longitudinal and transverse wire spacing and numbers after colon are longitudinal and transverse wire size.

^bReinforcement ratio based on depth of lower reinforcement in lap.

^cEffective depth, in.

TABLE 2--OUTLINE OF SPLICE SPECIMENS (Continued)

Slab	Reinforcement ^a Style	p^b	Total Slab Depth, in.	d^c	Clear Cover, in.	Length of Shear Span, a, in.	Amount of Overlap in. Dia		Detail of Lap
SFD 26	6x6:D19xD9	0.0079	5	4.0	0.75	12	9.82	20.0	
SFD 27	6x12:D19xD9	0.0079	5	4.0	0.75	12	9.82	20.0	
SFD 28	6x6:D19xD9	0.0079	5	4.0	0.75	12	14.00	38.5	
SFD 29	6x12:D19xD9	0.0079	5	4.0	0.75	12	14.00	38.5	
SFE 30	6x6:D21xD7	0.0058	7	6.0	0.75	12	8.00	15.5	

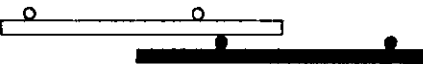

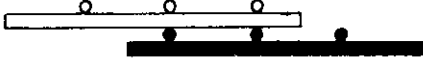
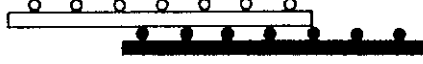
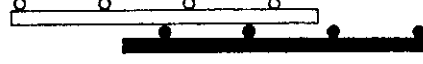
(Continued)

^aStyle designation: 6:D7, number before colon is longitudinal wire or bar spacing and number following colon is longitudinal wire or bar size. 6x12:D7xD4, numbers ahead of colon are longitudinal and transverse wire spacing and numbers after colon are longitudinal and transverse wire size.

^bReinforcement ratio based on depth of lower reinforcement in lap.

^cEffective depth, in.

TABLE 2--OUTLINE OF SPLICE SPECIMENS (Continued)

Slab	Reinforcement ^a Style	p^b	Total Slab Depth, in.	d^c	Clear Cover, in.	Length of Shear Span, a, in.	Amount of Overlap in. dia		Detail of Lap
SFE 31	6x12:D21xD7	0.0088	5	4.0	0.75	12	10.34	20.0	
SFE 32	6x6:D21xD7	0.0058	7	6.0	0.75	12	14.00	27.1	
SFA 33	4x6:D29xD11	0.0184	5	6.0	0.75	12	12.16	20.0	
SFA 34	4x3:D29xD11	0.0133	7	5.4	1.25	12	13.50	21.5	
SFA 35	4x6:D29xD11	0.0122	7	6.0	0.75	12	14.00	23.0	

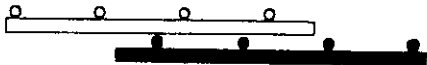
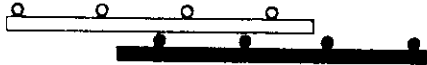
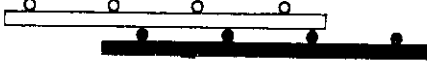
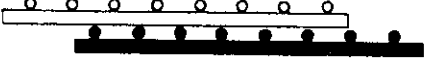
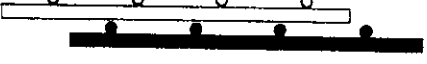
(Continued)

^aStyle designation: 6:D7, number before colon is longitudinal wire or bar spacing and number following colon is longitudinal wire or bar size. 6x12:D7xD4, numbers ahead of colon are longitudinal and transverse wire spacing and numbers after colon are longitudinal and transverse wire size.

^bReinforcement ratio based on depth of lower reinforcement in lap.

^cEffective depth, in.

TABLE 2--OUTLINE OF SPLICE SPECIMENS (Concluded)

Slab	Reinforcement ^a Style	ρ^b	Total Slab Depth, in.	d^c	Clear Cover, in.	Length of Shear Span, a, in.	Amount of Overlap in. dia		Detail of Lap
SFA 36	4x6:D29xD11	0.0122	7	6.0	0.75	18	14.00	23.0	
SFA 37	4x6:D29xD11	0.0133	7	5.4	1.25	18	14.00	23.0	
SFA 38	4x6:D29xD11	0.0122	7	6.0	0.75	18	16.00	26.3	
SFA 39	4x3:D29xD11	0.0133	7	5.4	1.25	12	19.50	32.1	
SFA 40	4x6:D29xD11	0.0133	7	5.4	1.25	18	20.00	32.9	

^aStyle designation: 6:D7, number before colon is longitudinal wire or bar spacing and number following colon is longitudinal wire or bar size. 6x12:D7xD4, numbers ahead of colon are longitudinal and transverse wire spacing and numbers after colon are longitudinal and transverse wire size.

^bReinforcement ratio based on depth of lower reinforcement in lap.

^cEffective depth, in.

TABLE 3--MIX PROPORTIONS

Source	Designation	Proportions by Wt			Water-Cement Ratio, by Wt
		Cement	Sand	Gravel	
Ready Mix	R1	1.00	3.40	4.44	0.55
Ready Mix	R2	1.00	3.94	5.91	0.81
Ready Mix	R3	1.00	4.10	5.21	0.81
Laboratory Mix	L	1.00	3.86	5.21	0.81

TABLE 4--CONCRETE PROPERTIES OF CRACK CONTROL SLABS

Slab	Mix*	Compressive Strength of Concrete, psi	Splitting Tensile Strength of Concrete, psi	Modulus of Rupture of Concrete, psi	Air Content, per cent	Slump, in.
<u>Deformed Bars</u>						
CDB 1	L	3100	314	407	5.7	3
CDB 2	L	3680	384	472	4.5	2
CDB 3	L	3300	326	395	4.0	3-3/4
CDB 4	L	3300	326	395	3.7	2-1/2
<u>Deformed Wires</u>						
CWA 5	L	3700	386	502	4.3	2-1/2
CWB 6	R1	3850	...	580	2.5	4-1/2
CWC 7	L	3100	322	458	4.6	2-1/4
CWC 8	R3	3100	297	430	2.8	2-1/2
CWB 9	R2	3750	237	561	4.9	3
CWD 10	R2	4150	...	475	5.4	2-1/2
CWE 11	R2	4200	...	475	5.4	2-1/2
CWE 12	L	3100	314	407	6.0	3
CWA 13	L	3100	322	458	5.0	3
<u>Deformed Wire Fabric</u>						
CFA 14	L	3000	324	410	5.6	2-1/4
CFB 15	R2	4800	405	434	3.3	2-1/2
CFC 16	L	3700	386	502	5.2	2-3/4
CFC 17	R3	3100	297	430	2.8	2-1/2
CFB 18	R2	4800	405	434	3.3	2-1/2
CFD 19	R2	4200	396	495	4.9	2-1/2
CFE 20	R2	4250	396	495	4.9	2-1/2
CFE 21	L	3200	325	458	5.2	2-1/2
CFA 22	L	3000	324	410	5.8	3
CFA 23	L	3400	340	468	5.0	2-3/4

* See Table 3 for definition of symbols and mix proportions.

TABLE 5--CONCRETE PROPERTIES OF SLABS WITH SPLICES

Slab	Mix*	Compressive Strength of Concrete, psi	Splitting Tensile Strength of Concrete, psi	Modulus of Rupture of Concrete, psi	Air Content per cent	Slump, in.
<u>Deformed Bars</u>						
SB 1	L	3530	333	448	4.6	3-1/2
SB 2	L	3570	333	448	4.6	3-1/2
<u>Deformed Wires</u>						
SWB 3	L	3750	337	506	4.8	1-3/4
SWB 4	L	3700	337	506	5.2	3-1/4
SWC 5	L	3270	328	446	5.1	3-1/4
SWC 6	L	3650	385	522	5.0	3
SWB 7	L	3460	346	481	3.2	3-1/2
SWB 8	R3	3480	314	449	4.6	3-1/4
SWB 9	R3	3100	320	463	6.7	5
SWB 10	L	3270	303	452	4.9	3-1/4
SWD 11	R3	3450	314	449	4.6	3-1/4
SWD 12	R3	3100	320	463	6.7	5
SWE 13	L	3320	268	509	6.1	3-1/4
SWE 14	L	3650	385	522	5.0	3
SWA 15	L	3430	346	481	4.8	4
SWA 16	L	3250	303	452	5.1	3-1/2
SWA 17	L	3400	343	497	5.3	3
<u>Deformed Wire Fabric</u>						
SFA 18	L	3640	377	454	5.0	3
SFC 19	L	3250	328	446	5.1	3-1/4

(Continued)

* See Table 3 for definition of symbols and mix proportions.

TABLE 5--CONCRETE PROPERTIES OF SLABS WITH SPLICES (Concluded)

Slab	Mix*	Compressive Strength of Concrete, psi	Splitting Tensile Strength of Concrete, psi	Modulus of Rupture of Concrete, psi	Air Content per cent	Slump, in.
SFB 20	R3	3580	337	421	5.5	3-1/4
SFB 21	L	3500	340	547	4.6	2
SFB 22	L	3500	340	547	5.1	3
SFD 23	L	3070	340	418	5.1	2-1/2
SFD 24	L	3400	340	468	5.4	3-1/2
SFD 25	R3	3600	337	421	5.5	3-1/4
SFD 26	L	3350	356	450	6.0	2-3/4
SFD 27	R3	2700	306	349	2.4	4
SFD 28	L	3480	340	468	5.4	3-1/4
SFD 29	L	3550	340	418	5.0	3
SFE 30	L	3450	337	488	5.1	2-3/4
SFE 31	L	3350	268	509	6.5	3-3/4
SFE 32	L	3470	337	488	5.2	2-3/4
SFA 33	L	3300	356	450	5.3	2-3/4
SFA 34	L	3650	364	444	4.7	2-1/2
SFA 35	L	3680	377	454	4.6	3-3/4
SFA 36	L	3680	384	472	5.2	2-3/4
SFA 37	L	3500	332	495	4.6	2-3/4
SFA 38	L	3150	325	458	5.2	2-1/2
SFA 39	L	3600	364	444	4.7	2-3/4
SFA 40	L	3530	332	495	5.1	3-1/2

* See Table 3 for definition of symbols and mix proportions.

TABLE 6--STRENGTH AND GEOMETRY OF BARS

No.	Strength, psi			Deformation, Height, in.		Shearing Area ^b sq in./in.	Bearing Area ^c sq in./in.
	Yield		Ultimate	Height, in.			
	0.003 ^a	0.005 ^a		A 305	Measured		
2	49,000	49,000	70,000	...	0.019	0.617	0.083
3	61,000	61,000	98,000	0.015	0.024	0.946	0.135
4	70,000	71,000	121,000	0.020	0.031	1.277	0.126
5	64,000	65,000	115,000	0.028	0.039	1.735	0.184

^a Strain

^b The shearing area is the surface area of an imaginary cylinder whose cross section is everywhere tangent to the top surface of the deformations - but not including the top surface area of the deformations.

^c The bearing area is the maximum projected area of the deformations on a plane perpendicular to the axis of the bar excluding the projected area of the ribs.

TABLE 7--STRENGTH AND GEOMETRY OF DEFORMED WIRE

Manufactur- er	Wire Size No.	Strength, psi			Deformations			Shearing Area ^c		Bearing Area ^d sq in./in.
		Yield		Ultimate	Number per inch per line ^b	Height, in.		sq in./in.		
		0.003 ^a	0.005 ^a			A 496	Measured	A 496	Measured	
A	D7	67,000	73,000	83,000	5.17	0.0134	0.017	0.234	0.318	0.033
B	D7	72,000	83,000	96,000	4.06	0.0134	0.017	0.234	0.294	0.025
C	D9	73,000	81,000	86,000	4.10	0.0152	0.019	0.265	0.312	0.031
B	D10	72,000	79,000	87,000	4.12	0.0160	0.019	0.279	0.310	0.033
D	D19	69,000	73,000	87,000	3.92	0.0245	0.026	0.386	0.454	0.061
E	D21	70,000	75,000	87,000	3.83	0.0259	0.050	0.406	0.640	0.085
A	D29	69,000	75,000	87,000	3.65	0.0304	0.040	0.478	0.695	0.121

^aStrain^bEach wire has 4 lines of deformations.^cShearing area is defined as the area removed from the surface of the wire when it is deformed.^dBearing area is defined as the maximum area removed from the cross sectional area of the wire or bar when it is deformed.

TABLE 8--STRENGTH PROPERTIES OF FABRIC

Manufacturer	Fabric Style	Yield Strength, psi				Ultimate Strength, psi	Measured Weld Shear ^b Strength, psi
		Across Welds		Between Welds			
		0.003 ^a	0.005 ^a	0.003 ^a	0.005 ^a		
A	6x6:D7xD4	70,000	75,000	70,000	75,000	85,000	19,000
A	6x12:D7xD4	69,000	74,000	69,000	74,000	84,000	19,400
B	6x12:D7xD4	70,000	77,000	72,000	78,000	85,000	50,000
C	2x6:D9xD5	73,000	87,000	73,000	86,000	92,000	32,200
C	2x12:D9xD5	74,000	85,000	73,000	85,000	90,000	33,800
C	4x12:D9xD5	76,000	86,000	71,000	89,000	92,000	51,400
B	6x6:D10xD4	75,000	87,000	70,000	85,000	96,000	36,800
B	6x12:D10xD4	74,000	87,000	73,000	87,000	96,000	20,600
D	6x3:D19xD9	79,000	90,000	79,000	91,000	98,000	35,100
D	6x6:D19xD9	78,000	91,000	79,000	90,000	96,000	44,100
D	6x12:D19xD9	79,000	89,000	79,000	89,000	96,000	41,300
E	6x6:D21xD7	78,000	87,000	76,000	86,000	93,000	30,400
E	6x12:D21xD7	78,000	88,000	79,000	90,000	93,000	29,100
A	4x3:D29xD11	70,000	76,000	76,000	76,000	86,000	18,900
A	4x6:D29xD11	68,000	74,000	69,000	74,000	85,000	12,000
A	4x12:D29xD11	69,000	74,000	68,000	74,000	85,000	15,800

^aStrain^bASTM A 497 requires a weld strength of 20,000 psi for deformed wire fabric.

TABLE 9--CRACK SPACING IN CONSTANT MOMENT REGION

Slab	Age of Concrete At Time of Test, days	Average Crack Spacing, in.			
		30,000 ^a	40,000 ^a	50,000 ^a	60,000 ^a
<u>Deformed Bars</u>					
CDB 1	33	b	b	19.2 ^d	6.0 ^c
CDB 2	27	b	4.8	4.6	4.2
CDB 3	27	6.0	6.0	6.0	6.0
CDB 4	29	3.8	3.8	3.8	3.8
<u>Deformed Wires</u>					
CWA 5	29	b	b	6.9	6.0
CWB 6	19	b	48.0	13.7	6.4
CWC 7	27	5.1	4.8	4.2	4.2
CWC 8	27	13.7	6.9	6.0	5.3
CWB 9	29	10.7	5.0	4.8	4.8
CWD 10	27	4.8	4.0	4.0	3.8
CWE 11	29	5.3	4.8	4.6	4.6
CWE 12	29	6.5	6.0	6.0	5.5
CWA 13	29	5.1	4.8	4.8	4.5 ^c
<u>Deformed Wire Fabric</u>					
CFA 14	27	b	9.6	6.4	6.4
CFB 15	28	b	8.7	6.4	5.3
CFC 16	27	5.1	4.5	4.0	4.0
CFC 17	29	5.1	5.1	4.4	4.0
CFB 18	32	9.6	6.0	6.0	5.1
CFD 19	25	5.3	4.8	4.6	4.6
CFE 20	27	4.4	3.8	3.8	3.8
CFE 21	33	6.0	6.0	6.0	6.0
CFA 22	29	4.8	4.0	3.8	3.8 ^c
CFA 23	28	4.5	4.2	4.2	4.2

^aCalculated steel stress, psi.^bNo cracking detected at this steel stress.^cCrack spacing at failure -- steel stress did not reach 60,000 psi.^dFor calculated steel stress of 49,000 psi, (yield point).

TABLE 10--CRACK WIDTHS IN SLABS AT THE LEVEL OF REINFORCEMENT

Slab	Average Crack Widths, in.				Maximum Crack Widths, in.			
	30,000 ^a	40,000 ^a	50,000 ^a	60,000 ^a	30,000 ^a	40,000 ^a	50,000 ^a	60,000 ^a
<u>Deformed Bars</u>								
CDB 1	b	b	0.0027 ^e	d	b	b	0.004 ^e	d
CDB 2	b	0.0030	0.0036	0.0044	b	0.005	0.006	0.006
CDB 3	0.0023	0.0040	0.0056	0.0073	0.003	0.005	0.007	0.010
CDB 4	0.0021	0.0034	0.0043	0.0053	0.004	0.005	0.007	0.008
<u>Deformed Wires</u>								
CWA 5	b	b	0.0052	0.0073	b	b	0.010	0.013
CWB 6	b	0.0030	0.0035	0.0053	b	0.005	0.008	0.010
CWC 7	0.0017	0.0028	0.0038	0.0045	0.002	0.004	0.005	0.006
CWC 8	0.0030	0.0048	0.0058	0.0066	0.004	0.007	0.010	0.014
CWB 9	0.0015 ^c	0.0023	0.0033	0.0035	0.002 ^c	0.005	0.006	0.007
CWD 10	0.0028	0.0035	0.0043	0.0050 ^c	0.006	0.007	0.007	0.008 ^c
CWE 11	0.0028	0.0036	0.0045	0.0053 ^c	0.004	0.005	0.008	0.013 ^c
CWE 12	0.0026	0.0044	0.0072	0.0075	0.004	0.007	0.012	0.013
CWA 13	0.0025	0.0059	0.0083	d	0.004	0.007	0.013	d

(Continued)

^a Calculated steel stress, psi.

^b No crack detected at this steel stress.

^c An extrapolated value of questionable magnitude--excluded from statistical calculations.

^d Failure occurred before this steel was reached.

^e For calculated steel stress of 49,000 psi (yield point).

TABLE 10--CRACK WIDTHS IN SLABS AT THE LEVEL OF REINFORCEMENT (Concluded)

Slab	Average Crack Widths, in.				Maximum Crack Widths, in.			
	30,000 ^a	40,000 ^a	50,000 ^a	60,000 ^a	30,000 ^a	40,000 ^a	50,000 ^a	60,000 ^a
<u>Deformed Wire Fabric</u>								
CFA 14	b	0.0029	0.0038	0.0058	b	0.006	0.008	0.012
CFB 15	b	0.0035 ^c	0.0047	0.0058	b	0.006 ^c	0.008	0.010
CFC 16	0.0015	0.0025	0.0040	0.0045	0.002	0.004	0.005	0.006
CFC 17	0.0019	0.0034	0.0038	0.0044	0.004	0.006	0.007	0.010
CFB 18	0.0021	0.0042	0.0063	0.0086 ^c	0.005	0.007	0.013	0.020 ^c
CFD 19	0.0023	0.0028	0.0033	0.0035	0.006	0.007	0.008	0.008
CFE 20	0.0022	0.0030	0.0038	0.0048 ^c	0.005	0.006	0.006	0.006 ^c
CFE 21	0.0029	0.0046	0.0055	0.0087	0.004	0.006	0.007	0.012
CFA 22	0.0025	0.0038	0.0044	d	0.004	0.006	0.007	d
CFA 23	0.0024	0.0037	0.0047	0.0063	0.004	0.005	0.006	0.010

^aCalculated steel stress, psi.^bNo crack detected at this steel stress.^cAn extrapolated value of questionable magnitude--excluded from statistical calculations.^dFailure occurred before this steel was reached.^eFor calculated steel stress of 49,000 psi (yield point).

TABLE 11--CRACK WIDTHS IN SLABS AT THE EXTREME TENSILE FIBER

Slab	Average Crack Widths, in.				Maximum Crack Widths, in.			
	30,000 ^a	40,000 ^a	50,000 ^a	60,000 ^a	30,000 ^a	40,000 ^a	50,000 ^a	60,000 ^a
<u>Deformed Bars</u>								
CDB 1	b	b	0.0040 ^f	e	b	b	0.007 ^f	e
CDB 2	b	0.0050	0.0060	0.0073	b	0.009	0.010	0.010
CDB 3	0.0043	0.0070	0.0103	0.0133	0.005	0.008	0.013	0.019
CDB 4	0.0030	0.0053	0.0071	0.0088	0.006	0.009	0.012	0.013
<u>Deformed Wires</u>								
CWA 5	b	b	0.0077	0.0108	b	b	0.014	0.018
CWB 6	c	c	c	c	c	c	c	c
CWC 7	0.0035	0.0048	0.0058	0.0058	0.005	0.007	0.009	0.011
CWC 8	0.0048	0.0076	0.0093	0.0101	0.007	0.012	0.017	0.021
CWB 9	0.0010 ^d	0.0030	0.0043	0.0046	0.003 ^d	0.006	0.008	0.009
CWD 10	0.0030	0.0043	0.0055	0.0071 ^d	0.007	0.008	0.011	0.013 ^d
CWE 11	0.0039	0.0046	0.0060	0.0082 ^d	0.006	0.007	0.009	0.013 ^d
CWE 12	0.0041	0.0065	0.0105	0.0123	0.006	0.012	0.018	0.023
CWA 13	0.0049	0.0073	0.0114	e	0.007	0.011	0.017	e
<u>Deformed Wire Fabric</u>								
CFA 14	b	0.0057	0.0067	0.0088	b	0.009	0.013	0.021
CFB 15	b	0.0047 ^d	0.0063	0.0080	b	0.008 ^d	0.010	0.010
CFC 16	0.0024	0.0040	0.0053	0.0066	0.004	0.005	0.007	0.009
CFC 17	0.0032	0.0057	0.0074	0.0082	0.006	0.010	0.013	0.017
CFB 18	0.0027 ^d	0.0056	0.0086	0.0116 ^d	0.005 ^d	0.013	0.017	0.025 ^d
CFD 19	0.0032	0.0037	0.0040	0.0044	0.006	0.007	0.008	0.008
CFE 20	0.0029	0.0041	0.0053	0.0067 ^d	0.005	0.007	0.009	0.012 ^d
CFE 21	0.0039	0.0070	0.0085	0.0123	0.006	0.009	0.011	0.019
CFA 22	0.0042	0.0056	0.0072	e	0.006	0.009	0.012	e
CFA 23	0.0039	0.0056	0.0070	0.0101	0.006	0.008	0.010	0.015

^aCalculated steel stress, psi

^bNo cracking detected at this steel stress.

^cCrack widths not measured at extreme tensile fiber.

^dAn extrapolated value of questionable magnitude, excluded from statistical calculations.

^eFailure occurred before this steel stress was reached.

^fFor calculated steel stress of 49,000 psi (yield point).

TABLE 12--EQUATIONS FOR MAXIMUM CRACK WIDTH

Source of Data	Maximum Crack Width at Extreme Tensile Fiber,		Maximum Crack Width at Level of Reinforcement,	
	$\sqrt[3]{t_b A} R f_s$		$\frac{\sqrt[3]{t_s A} f_s}{1 + 2t_s/3h_1}$	
	C^a	σ^b	C^a	σ^b
Deformed Wire Fabric	0.0732	2.88	0.0881	1.54
Deformed Wire	0.0826	3.51	0.0919	2.52
Smooth Wire Fabric	0.0895	1.21
Deformed Bars	0.0732	2.58	0.0700	1.81
<u>From Reference 5</u>				
Hognestad	0.0714	3.14
Rüsch-Rehm	0.0880	3.11	0.0880	2.26
Kaar-Mattock ^c	0.1047	2.54	0.1165	1.75
Clark	0.0767	1.65
Kaar-Hognestad ^c	0.0711	2.30
Hognestad and Broms	0.0743	1.81

$$^a w_c = C X, \text{ where } X = \sqrt[3]{t_b A} R f_s \times 10^{-3} \text{ or } \frac{\sqrt[3]{t_s A}}{1 + 2t_s/3h_1} f_s \times 10^{-3}$$

$$^b \sigma = \sqrt{\frac{\Sigma (w_o - w_c)^2}{n - 1}}, \text{ where } n \text{ is the number of observations}$$

^c Measured steel stress used in crack widths expressions.

TABLE 13--RESULTS OF STATIC TESTS OF SLABS WITH SPLICES

TABLE 13--RESULTS													
Slab	Amount of Overlap, in.	Long. Wire or Bar Size	Length Constant Moment Span, in.	Concrete Strength, psi	Max Test Load, kips	Max Test ^a Moment in.-kips	Type of Failure ^b	Calculated Yield Moment, in.-kips		Effectiveness			
								Max ^c	Min ^d	Test Mom		Cal	Max
<u>Deformed Bars</u>													
SB 1	12.00	No. 4	48	3530	46.1	276.6	S	318.4 ^e	290.0 ^e	0.87			0.95
SB 2	15.00	No. 5	48	3570	87.3	523.8	S	617.4 ^e	541.9 ^e	0.85			0.97
<u>Deformed Wires</u>													
SWB 3	3.58	D7	48	3750	7.7	46.2	S	77.9	72.0	0.59			0.64
SWB 4	5.97	D7	48	3700	11.1	66.6	S	77.8	72.0	0.86			0.92
SWC 5	4.05	D9	36	3270	20.0	180.0	S	416.9	391.3	0.43			0.46
SWC 6	10.14	D9	36	3650	44.3	398.7	S	421.3	395.8	0.95			1.01
SWB 7	4.27	D10	48	3460	11.0	66.0	S	108.5	98.5	0.61			0.67
SWB 8	5.70	D10	48	3480	10.5	63.0	S	108.5	98.5	0.58			0.64
SWB 9	7.12	D10	48	3100	12.0	72.0	S	107.8	97.9	0.67			0.74
SWB 10	8.55	D10	48	3270	16.0	96.0	S	108.1	98.2	0.89			0.98
SWD 11	7.86	D19	48	3450	14.0	84.0	S	192.9	166.8	0.44			0.50
SWD 12	9.82	D19	48	3100	16.0	96.0	S	190.6	164.5	0.50			0.58

(Continued)

^aDead load moment due to weight of slab neglected.^bS = Failure of the lap, F = flexural failure by tensile failure of steel, V = Shear failure outside constant moment region.^cCalculated yield moment based on effective depth of lower reinforcement in lap and yield strength of 70,000 psi.^dCalculated yield moment based on effective depth of upper reinforcement in lap and yield strength of 70,000 psi.^eCalculated yield moment based on actual yield strength of steel.

TABLE 13--RESULTS OF STATIC TESTS OF SLABS WITH SPLICES (Continued)

Slab	Amount of Overlap, in.	Long. Wire or Bar Size	Length Constant Moment Span, in.	Concrete Strength, psi	Max Test Load, kips	Max Test ^a Moment in.-kips	Type of ^b Failure	Calculated Yield Moment, in.-kips		Effectiveness			
								Max ^c	Min ^d	Test Mom		Test Mom	
										Cal	Max	Cal	Min
SWE 13	10.34	D21	48	3320	18.0	108.0	S	209.2	178.8	0.52		0.60	
SWE 14	15.51	D21	36	3650	30.0	270.0	S	329.0	298.6	0.82		0.90	
SWA 15	12.16	D29	48	3430	60.2	361.2	S	618.3	544.2	0.58		0.66	
SWA 16	14.60	D29	48	3250	70.2	421.2	S	612.4	538.4	0.69		0.78	
SWA 17	18.24	D29	36	3400	50.3	452.7	S	617.3	543.2	0.73		0.83	
<u>Deformed Wire Fabric</u>													
SFA 18	8.00	D7	48	3640	14.4	86.4	F	77.8	67.5	1.11		1.28	
SFC 19	14.00	D9	36	3250	44.8	403.2	V	146.6	372.0	0.97		1.08	
SFB 20	5.70	D10	48	3580	15.0	90.0	S	108.6	92.4	0.83		0.97	
SFB 21	8.00	D10	48	3500	21.9	131.4	S	108.5	92.3	1.21		1.42	
SFB 22	14.00	D10	48	3500	22.5	135.0	F	108.5	92.3	1.24		1.46	
SFD 23	3.00	D19	48	3070	9.0	54.0	S	190.4	146.3	0.28		0.37	
SFD 24	7.50	D19	48	3400	17.5	105.0	S	192.6	148.5	0.55		0.71	
SFD 25	7.86	D19	48	3600	18.0	108.0	S	193.8	149.6	0.56		0.72	
SFD 26	9.82	D19	48	3350	25.3	151.8	S	192.3	148.2	0.79		1.02	

(Continued)

^aDead load moment due to weight of slab neglected.^bS = Failure of the lap, F = flexural failure by tensile failure of steel, V = Shear failure outside constant moment region.^cCalculated yield moment based on effective depth of lower reinforcement in lap and yield strength of 70,000 psi.^dCalculated yield moment based on effective depth of upper reinforcement in lap and yield strength of 70,000 psi.^eCalculated yield moment based on actual yield strength of steel.

TABLE 13--RESULTS OF STATIC TESTS OF SLABS WITH SPLICES (Concluded)

Slab	Amount of Overlap,	Long. Wire or Bar Size	Length Constant Moment Span, in.	Concrete Strength, psi	Max Test Load,	Max Test ^a Moment in.-kips	Type of ^b Failure	Calculated Yield Moment, in.-kips		Effectiveness			
								Max ^c	Min ^d	Test Mom		Cal	Max
										Cal	Max	Cal	Min
SFD 27	9.82	D19	48	2700	16.0	96.0	S	187.3	143.2	0.51		0.67	
SFD 28	14.00	D19	48	3480	28.4	170.4	S	193.1	149.0	0.88		1.14	
SFD 29	14.00	D19	48	3550	27.1	162.6	S	193.5	149.4	0.84		1.09	
SFE 30	8.00	D21	48	3450	38.1	228.6	S	327.8	279.8	0.70		0.82	
SFE 31	10.34	D21	48	3350	24.7	148.2	S	209.4	161.5	0.71		0.92	
SFE 32	14.00	D21	48	3470	61.0	366.0	S	327.9	280.0	1.12		1.31	
SFA 33	12.16	D29	48	3330	32.5	195.0	S	371.5	251.9	0.52		0.77	
SFA 34	13.50	D29	48	3650	62.6	375.6	S	563.7	444.1	0.67		0.85	
SFA 35	14.00	D29	48	3680	64.1	384.6	V	625.4	505.8	0.61		0.76	
SFA 36	14.00	D29	36	3680	47.4	426.6	S	625.4	505.8	0.68		0.84	
SFA 37	14.00	D29	36	3500	48.5	436.5	S	559.4	439.8	0.78		0.99	
SFA 38	16.00	D29	36	3150	44.3	398.7	S	608.8	489.2	0.65		0.82	
SFA 39	19.50	D29	48	3600	69.0	414.0	V	562.4	442.7	0.74		0.94	
SFA 40	20.00	D29	36	3530	60.2	541.8	S	560.3	440.7	0.97		1.23	

^aDead load moment due to weight of slab neglected.


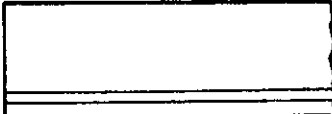
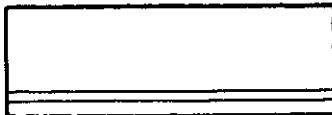
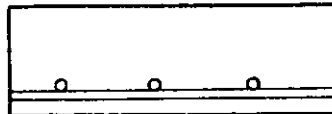
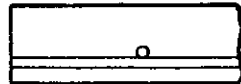
^bS = Failure of the lap, F = flexural failure by tensile failure of steel, V = Shear failure outside constant moment region.

^cCalculated yield moment based on effective depth of lower reinforcement in lap and yield strength of 70,000 psi.

^dCalculated yield moment based on effective depth of upper reinforcement in lap and yield strength of 70,000 psi.

^eCalculated yield moment based on actual yield strength of steel.

TABLE 14 --OUTLINE OF ANCHORAGE SPECIMENS

Slab	Reinforcement Style ^a	ρ^b	Total Slab Depth, in.	Effective Depth, in.	Length of Shear Span, in.	Detail of Shear Span
<u>Specimens Which Failed in the Shear Span</u>						
CDB 3	6:#4	0.0056	7	6.0	18	
CDB 4	4:#5	0.0130	7	5.9	18	
CWC 7	2:D9	0.0075	7	6.0	18	
SFC 19	2x6:D9xD5	0.0074	7	6.1	18	
CFC 17	4x12:D9xD5	0.0056	5	4.0	12	



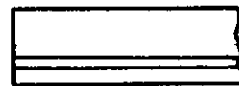
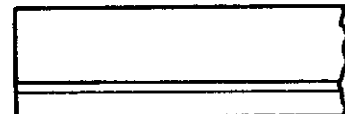

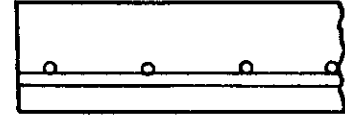
100

(Continued)

^aStyle designation: 6:D7, number before colon is longitudinal wire or bar spacing and number following colon is longitudinal wire or bar size; 6x12:D7xD4, numbers ahead of colon are longitudinal and transverse wire spacings, respectively. Numbers after colon are the longitudinal and transverse wire sizes, respectively.

^bReinforcement ratio.

TABLE 14--OUTLINE OF ANCHORAGE SPECIMENS (Continued)



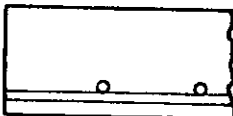
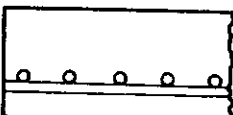
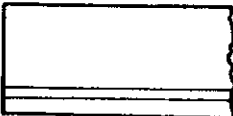
Slab	Reinforcement Style ^a	ρ ^b	Total Slab Depth, in.	Effective Depth, in.	Length of Shear Span, in.	Detail of Shear Span
CWD 10	6:D19	0.0079	5	4.0	12	
CFD 19	6x12:D19xD9	0.0079	5	4.0	12	
CWE 11	6:D21	0.0088	5	4.0	12	
CWE 12	6:D21	0.0065	7	5.4	18	
CFE 20	6x12:D21xD7	0.0088	5	4.0	12	
CFE 21	6x6:D21xD7	0.0065	7	5.4	18	

(Continued)

^aStyle designation: 6:D7, number before colon is longitudinal wire or bar spacing and number following colon is longitudinal wire or bar size; 6x12:D7xD4, numbers ahead of colon are longitudinal and transverse wire spacings, respectively. Numbers after colon are the longitudinal and transverse wire sizes, respectively.

^bReinforcement ratio.

TABLE 14--OUTLINE OF ANCHORAGE SPECIMENS (Continued)

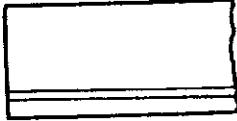
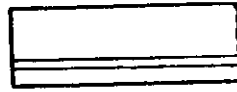
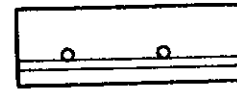
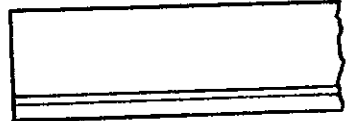
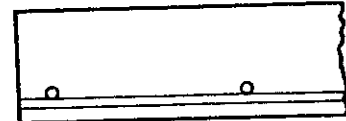
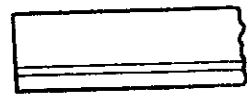
Slab	Reinforcement Style ^a	p^b	Total Slab Depth, in.	Effective Depth, in.	Length of Shear Span, in.	Detail of Shear Span
CWA 13	4:D29	0.0122	7	5.9	18	
CFA 22	4x12:D29xD11	0.0122	7	5.9	18	
SFA 35	4x6:D29xD11	0.0122	7	5.9	12	
SFA 39	4x3:D29xD11	0.0133	7	5.4	12	
<u>Specimens Which Did Not Fail in the Shear Span</u>						
SDB 1	6:#4	0.0056	7	6.0	12	

^aStyle designation: 6:D7, number before colon is longitudinal wire or bar spacing and number following colon is longitudinal wire or bar size; 6x12:D7xD4, numbers ahead of colon are longitudinal and transverse wire spacings, respectively. Numbers after colon are the longitudinal and transverse wire sizes, respectively.

^bReinforcement ratio.

(Continued)

TABLE 14--OUTLINE OF ANCHORAGE SPECIMENS (Continued)


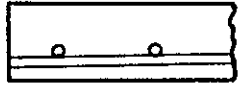



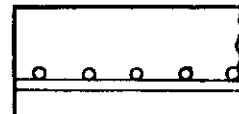
Slab	Reinforcement Style ^a	p^b	Total Slab Depth, in.	Effective Depth, in.	Length of Shear Span, in.	Detail of Shear Span
SDB 2	4:#5	0.0130	7	5.9	12	
CWB 6	6:D7	0.0029	5	4.0	12	
SFA 18	6x6:D7xD4	0.0029	5	4.1	12	
SWC 6	2:D9	0.0074	7	6.1	18	
CFC 16	2x12:D9xD5	0.0075	7	6.0	18	
CWC 8	4:D9	0.0056	5	4.0	12	

(Continued)

^aStyle designation: 6:D7, number before colon is longitudinal wire or bar spacing and number following colon is longitudinal wire or bar size; 6x12:D7xD4, numbers ahead of colon are longitudinal and transverse wire spacings, respectively. Numbers after colon are the longitudinal and transverse wire sizes, respectively.

^bReinforcement ratio.

TABLE 14--OUTLINE OF ANCHORAGE SPECIMENS (Concluded)

Slab	Reinforcement Style ^a	$\frac{b}{p}$	Total Slab Depth, in.	Effective Depth in.	Length of Shear Span, in.	Detail of Shear Span
CWB 9	6:D10	0.0042	5	4.0	12	
SFB 21	6x6:D10xD4	0.0041	5	4.1	12	
SFD 28	6x6:D19xD9	0.0079	5	4.0	12	
SFE 32	6x6:D21xD7	0.0058	7	6.0	12	
SFA 16	4:D29	0.0122	7	5.9	12	
SFA 34	4x3:D29xD11	0.0133	7	5.4	12	

^aStyle designation: 6:D7, number before colon is longitudinal wire or bar spacing and number following colon is longitudinal wire or bar size; 6x12:D7xD4, numbers ahead of colon are longitudinal and transverse wire spacings, respectively. Numbers after colon are the longitudinal and transverse wire sizes, respectively.

^bReinforcement ratio.

TABLE 15--SPECIMENS WHICH FAILED IN THE SHEAR SPAN

Slab	Max. Test Moment, in.-kips	Cal. Yield Moment, in.-kips	Cal. Ultimate Moment, in.-kips	Type of Failure and Notes
CDB 3	340	313	313	Diagonal tension followed by anchorage. After a diagonal crack had formed a crack grew down to reinforcement and failure occurred immediately.
CDB 4	597	640	640	Diagonal tension. Both edges of slab contained a diagonal crack about 6 in. from the point of application of the load at 55 kips. At failure a second diagonal crack formed near the support on one face only.
CWC 7	465	408	502	Diagonal tension followed by splitting. Just prior to failure small diagonal cracks developed at the level of the reinforcement; splitting was rapid and collapse violent.
SFC 19	403	416	547	Diagonal tension followed by splitting. Almost immediately after a diagonal tension crack had formed at a transverse wire 7 in. from the support, a splitting failure occurred.
SFC 17	157	140	180	Diagonal tension followed by anchorage. A diagonal crack developed gradually at the outer transverse wire, 6 in. from the support until anchorage failure occurred.
CWD 10	217	196	244	Diagonal tension followed by anchorage. A diagonal tension crack formed approximately midway between the load increments; failure occurred while the load was being held constant.

(Continued)

TABLE 15--SPECIMENS WHICH FAILED IN THE SHEAR SPAN (Continued)

Slab	Max. Test Moment, in.-kips	Cal. Yield Moment, in.-kips	Cal. Ultimate Moment, in.-kips	Type of Failure and Notes
CFD 19	277	196	269	Diagonal tension followed by splitting. After a diagonal crack had become fully inclined a crack grew downward to the reinforcement. Failure occurred after the load was increased by 6 kips.
CWE 11	245	215	267	Diagonal tension followed by anchorage. Failure occurred almost immediately after diagonal cracks had become fully inclined on both sides of slab.
CWE 12	317	296	367	Diagonal tension followed by anchorage. After diagonal cracks had developed, failure occurred by gradual slipping of reinforcement.
CPE 20	235	215	286	Diagonal tension followed by anchorage. After diagonal cracking had developed, secondary cracking developed at the level of reinforcement and steel began to slip.
SFE 21	395	296	393	Diagonal tension. A diagonal crack initially formed at a transverse wire 12 in. from the support. Violent failure occurred when a diagonal crack developed at a transverse wire 6 in. from the support.
CWA 13	490	607	755	Diagonal tension. Slightly inclined flexural cracks were developed when critical diagonal crack formed passing through earlier cracks.

(Continued)

TABLE 15--SPECIMENS WHICH FAILED IN THE SHEAR SPAN (Concluded)

Slab	Max. Test Moment, in.-kips	Cal. Yield Moment, in.-kips	Cal. Ultimate Moment, in.-kips	Type of Failure and Notes
CFA 22	487	604	733	Diagonal tension followed by splitting. A diagonal crack formed at a transverse wire 12 in. from support and splitting occurred.
SFA 35	385	626	760	Diagonal tension followed by anchorage. A diagonal crack formed at the outer transverse wire 4 in. from the support and anchorage failure occurred after the crack was developed.
SFA 39	414	563	691	Diagonal tension followed by splitting. Diagonal cracks developed at the first 2 transverse wires between the applied load and the support. Large crack widths were present at failure.

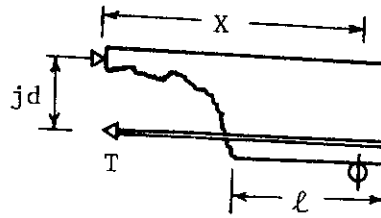
TABLE 16--RESULTS OF DIAGONAL TENSION ANALYSIS

Slab	Reinforcement Style	p ^a	d, in.	$\sqrt{f'_c}$, psi	V _{cr} , kips	V _t , kips	Results with M/V as Defined in Ref.(20)				Results with M/V Measured on Slab			
							M/V, in.	V ^b , kips	V _{cr} /V	V _t /V	M/V, in.	V ^b , kips	V _{cr} /V	V _t /V
CDB 3	6:#4	0.0056	6.0	57	...	18.9	12.0	16.7	...	1.13	10.5	16.9	...	1.12
CDB 4	4:#5	0.0130	5.9	57	33.2	33.2	12.1	17.7	1.88	1.88	10.5	18.0	1.84	1.84
CWC 7	2:D9	0.0075	6.0	56	15.0	25.8	12.0	16.6	0.91	1.56	9.0	17.0	0.88	1.52
SFC 19	2x6:D9xD5	0.0074	6.1	57	22.4	22.4	11.9	17.2	1.30	1.30	7.0	18.2	1.23	1.23
CFC 17	4x12:D9xD5	0.0056	4.0	56	11.0	13.1	8.0	10.8	1.02	1.21	6.0	11.0	1.00	1.19
CWD 10	6:D19	0.0079	4.0	64	17.0	18.1	8.0	12.7	1.34	1.43	10.0	12.5	1.47	1.45
CFD 19	6x12:D19xD9	0.0079	4.0	65	17.0	23.0	8.0	12.8	1.33	1.80	7.0	12.9	1.32	1.78
CWE 11	6:D21	0.0088	4.0	64	19.0	20.4	8.0	12.8	1.48	1.59	8.5	12.7	1.49	1.60
CWE 12	6:D21	0.0065	5.4	56	16.0	17.6	12.6	14.6	1.10	1.21	10.0	14.8	1.08	1.19
CFE 20	6x12:D21xD7	0.0088	4.0	65	16.0	19.6	8.0	12.9	1.24	1.51	7.0	13.3	1.20	1.47
CFE 21	6x6:D21xD7	0.0065	5.4	56	22.4	22.4	12.6	14.7	1.52	1.52	6.0	15.7	1.43	1.43
CWA 13	4:D29	0.0122	5.9	56	27.2	27.2	12.1	17.1	1.59	1.59	10.5	17.4	1.56	1.56
CFA 22	4x12:D29xD11	0.0122	5.9	55	...	27.0	12.1	16.8	...	1.60	11.0	17.0	...	1.59
SFA 35	4x6:D29xD11	0.0122	5.9	61	25.0	32.0	12.1	18.4	1.36	1.74	4.0	22.7	1.10	1.41
SFA 39	4x3:D29xD11	0.0133	5.4	61	22.0	34.5	6.6	18.3	1.20	1.89	5.0	19.6	1.12	1.76

^aReinforcement Ratio

$$b_V = bd\sqrt{f'_c} \left[1.9 + 2500 \frac{pdV}{M\sqrt{f'_c}} \right]$$

TABLE 17--RESULTS OF ANCHORAGE ANALYSIS



Slab	Reinforcement Style	V_t , kips	jd , ^a in.	X , in.	l , in.	$\sqrt{f'_c}$, psi	T , kips	Stress at Failure, ksi		Ratio of Cal. to Measured Stress	Type of ^b Failure
								Test σ_t	Calculated σ_B^c σ_S^d		
Specimens Which Failed in the Shear Span											
CDB 3	6:#4	18.9	5.6	17.0	12.5	57	58	72	78	...	DT, A
CDB 4	4:#5	33.2	4.9	17.0	12.5	57	115	62	(51)	49	DT
CWC 7	2:D9	25.8	5.4	16.0	11.0	56	76	71	...	71	DT, S
SFC 19	2x6:D9xD5	22.4	5.5	16.5	9.0 ^e	57	67	62	...	60	DT, S
CFC 17	4x12:D9xD5	13.1	3.7	11.0	7.0	56	39	72	82	...	DT, A
CWD 10	6:D19	18.1	3.7	12.0	12.0	64	59	77	82	...	DT, A
CFD 19	6x12:D19xD9	23.0	3.7	12.0	9.0 ^e	65	75	98	...	97	DT, A
CWE 11	6:D21	20.4	3.6	11.0	10.5	64	62	73	61	...	DT, S
CWE 12	6:D21	17.6	5.0	14.0	12.0	56	49	58	60	...	DT, A
CFE 20	6x12:D21xD7	19.6	3.7	12.0	9.0 ^e	65	64	76	81	(88)	DT, A
CFE 21	6x6:D21xD7	22.4	5.0	15.0	8.0 ^e	56	66	78	64	(67)	DT, A
										0.86	DT

^aBased on Eq 16-1, ACI 318-63, $jd = d - A_s f_y / (1.7 b f'_c)$.

^bA = anchorage; DT = diagonal tension; S = splitting; F = flexural failure with fracture of reinforcement; L = failure of splice.

^cFrom Eq 29.

^dFrom Eq 30.

^eOne transverse wire in the anchorage length l .

^fTwo transverse wires in the anchorage length l .

(Continued)

TABLE 17--RESULTS OF ANCHORAGE ANALYSIS (Concluded)

Slab	Reinforcement Style	V_t , kips	jd , ^a in.	x , in.	ℓ , in.	$\sqrt{f'_c}$, psi	T , kips	Stress at Failure, ksi			Ratio of Cal. to Measured Stress	Type of Failure ^b
								Test σ_t	Calculated σ_B^c	σ_S^d		
CWA 13	4:D29	27.2	5.0	16.0	12.5	56	87	50	45	...	0.90	DT
CFA 22	4x12:D29xD11	27.0	5.0	16.5	13.0 ^e	55	90	52	(60)	52	1.00	DT, S
SFA 35	4x6:D29xD11	32.0	5.1	10.5	6.0	61	65	38	24	...	0.63	DT, A
SFA 39	4x3:D29xD11	34.5	4.6	10.0	7.5 ^f	61	75	43	(68)	31	0.72	DT, S

Specimens Which Did Not Fail in the Shear Span

SDB 1	6:#4	23.0	5.61	12.0	14.0	59	49	62	88	L
SDB 2	4:#5	43.8	5.11	12.0	7.5	60	103	55	30	(30)	...	L
CWB 6	6:D7	9.2	3.88	12.0	10.5	62	28	102	175	...	2.81	F
SFA 18	6x6:D7xD4	7.2	3.97	8.0	9.0 ^e	60	14	52	146	...	1.71	F
SWC 6	2:D9	22.2	5.51	12.0	11.0	60	48	45	...	78	...	L
CFC 16	2x12:D9xD5	32.8	5.50	14.5	18.0 ^e	61	86	80	...	99	1.24	F
CWC 8	4:D9	16.3	3.70	11.0	10.0	56	48	90	116	...	1.29	F
SFB 21	6x6:D10xD4	11.0	3.88	10.0	9.0 ^e	58	28	71	99	L
CWC 9	6:D19	12.1	3.82	12.0	11.5	61	38	95	133	...	1.40	F
SFD 28	6x6:D19xD9	14.2	3.63	9.5	9.0 ^e	59	37	49	...	88	...	L
SFE 32	6x6:D21xD7	30.4	5.58	12.0	11.0 ^e	59	65	78	89	L
SFA 16	4:D29	35.1	5.03	12.0	10.0	57	84	48	...	41	...	L
SFA 34	4x3:D29xD11	31.3	4.63	10.0	8.5 ^f	60	68	39	...	37	...	L

^aBased on Eq 16-1, ACI 318-63, $jd = d - A_s f_y / (1.7 b f'_c)$.

^bA = anchorage; DT = diagonal tension; S = splitting; F = flexural failure with fracture of reinforcement; L = failure of splice.

^cFrom Eq 29.

^dFrom Eq 30.

^eOne transverse wire in the anchorage length ℓ .

^fTwo transverse wires in the anchorage length ℓ .

TABLE 18--SPECIMENS WHICH FAILED IN FLEXURE

Slab	Reinforcement Style	Effective Depth, in.	p	p/p _b		M ^a _{test} , in.-kips	M ^b _y , in.-kips	M ^c _u , in.-kips
				p _b based on Eq 38 with: f _y = 70,000	with: f _y = f' _s			
CWA 5	6:D7	4.0	0.0029	0.14	0.18	90	76	89
CWB 6	6:D7	4.0	0.0029	0.13	0.21	110	76	103
CWC 8	4:D9	4.0	0.0056	0.32	0.43	195	140	174
CWB 9	6:D10	4.0	0.0042	0.20	0.27	145	107	131
CFA 14	6x12:D7xD4	4.0	0.0029	0.17	0.22	93	75	90
SFA 18	6x6:D7xD4	3.6	0.0032	0.15	0.20	86	67	82
CFB 15	6x12:D7xD4	4.0	0.0029	0.11	0.15	96	76	92
CFB 13	6x12:D10xD4	4.0	0.0042	0.16	0.26	152	108	146
SPB 22	6x6:D10xD4	3.5	0.0048	0.24	0.38	135	92	124
CFC 16	2x12:D9xD5	6.0	0.0075	0.35	0.52	531	416	521
CFA 23	4x12:D29xD11	6.0	0.0121	0.62	0.83	732	619	725

^aAll slabs except CFA 23 failed by fracture of the longitudinal reinforcement; CFA 23 failed by crushing of the concrete.

^bBased on Eq 8 with $\phi = 1.00$ and $f_y = 70,000$ psi.

^cBased on Eq 8 with $\phi = 1.00$ and $f_y = f'_s$, the ultimate tensile strength of the reinforcement.

TABLE A.1--PROPERTIES OF CONCRETE

Longitudinal Wire Size	Age at Test Days	Compressive Strength, psi	Splitting Tensile Strength, psi	Air Content per cent	Slump, in.
D10	7	3650	397	4.7	3
D19	14	3210	322	5.5	3-1/4
D21	8	3630	375	5.3	3
D29	13	3750	396	5.6	3-1/4

TABLE A.2--PULL-OUT DATA

Specimen	Load at Failure, lb	Steel Stress at Failure, psi	Stress at Loaded End Slip of 0.005 in., psi	Stress at Loaded End Slip of 0.01 in., psi	Stress of Free End Slip of 0.01 in., psi
D10-1	3,850	38,500	15,000	24,000	30,000
D10-2	4,420	44,200	22,000	31,000	36,000
D10-3	3,720	37,200	16,000	22,000	24,000
DTG10-1	5,440	54,400	11,000	20,000	20,000
DTG10-2	5,300	53,000	13,000	21,000	21,000
DTG10-3	3,440	34,400	19,000	27,000	27,000
DT10-1	9,540 ^a	95,400	29,000	47,000	80,000
DT10-2	7,680	76,800	30,000	46,000	56,000
DT10-3	9,160 ^a	91,600	30,000	47,000	74,000
D19-1	6,120	32,430	19,000	25,000	27,000
D19-2	4,840	25,650	14,000	18,000	20,000
D19-3	4,460	23,630	14,000	17,000	18,000
DTG19-1	9,260	49,080	11,000	19,000	19,000
DTG19-2	9,840	52,150	14,000	22,000	22,000
DTG19-3	8,440	44,730	10,000	18,000	18,000
DT19-1	16,000	84,800	21,000	35,000	48,000
DT19-2	17,600	93,280	24,000	38,000	52,000
DT19-3	13,700	72,610	24,000	38,000	52,000
D21-1	9,360	44,550	32,000	40,000	42,000
D21-2	9,780	46,550	30,000	41,000	45,000
D21-3	6,920	32,940	21,000	28,000	31,000
DTG21-1	4,300	20,470	11,000	18,000	18,000
DTG21-2	7,080	33,700	13,000	20,000	20,000
DTG21-3	9,440	44,930	16,000	22,000	22,000
DT21-1	19,400	92,340	28,000	... ^b	61,000
DT21-2	15,300	72,830	33,000	47,000	56,000
DT21-3	17,300 ^c	82,350	28,000	41,000	53,000
D29-1	11,520	39,740	24,000	32,000	36,000
D29-2	9,920	34,220	19,000	28,000	31,000
D29-3	12,600	43,470	30,000	37,000	39,000
DTG29-1	4,500	17,250	10,000	15,000	15,000
DTG29-2	7,480	25,800	12,000	19,000	19,000
DTG29-3	5,540	19,110	13,000	19,000	19,000
DT29-1	18,500	63,820	26,000	40,000	48,000
DT29-2	15,000	51,750	25,000	38,000	47,000
DT29-3	15,500	53,470	26,000	40,000	49,000

^aTensile failure of wire.^bInaccurate slip measurement.^cSplitting of concrete occurred at failure.

TABLE A.3--ULTIMATE BOND STRESS

Specimen	Compressive Strength of Concrete, psi	Ultimate Bond Stress, psi	Bond Coefficient, α^*
D10-1	3650	574	3.38
D10-2	3650	659	3.88
D10-3	3650	555	3.20
		ave 596	ave 3.49
D19-1	3210	662	5.74
D19-2	3210	523	4.54
D19-3	3210	482	4.18
		ave 556	ave 4.82
D21-1	3630	961	8.25
D21-2	3630	1004	8.62
D21-3	3630	710	6.11
		ave 892	ave 7.66
D29-1	3750	1005	10.00
D29-2	3750	866	8.60
D29-3	3750	1100	10.92
		ave 991	ave 9.84

* From Eq 36

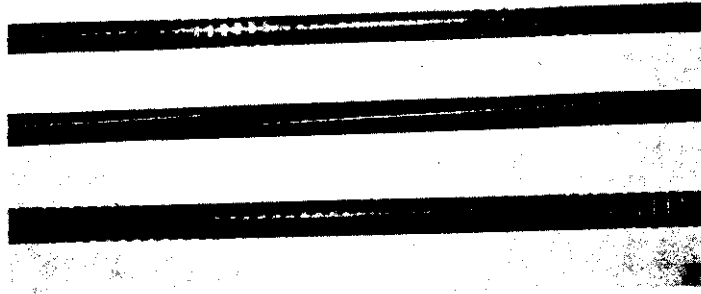


Fig.1 Typical Deformed Wires

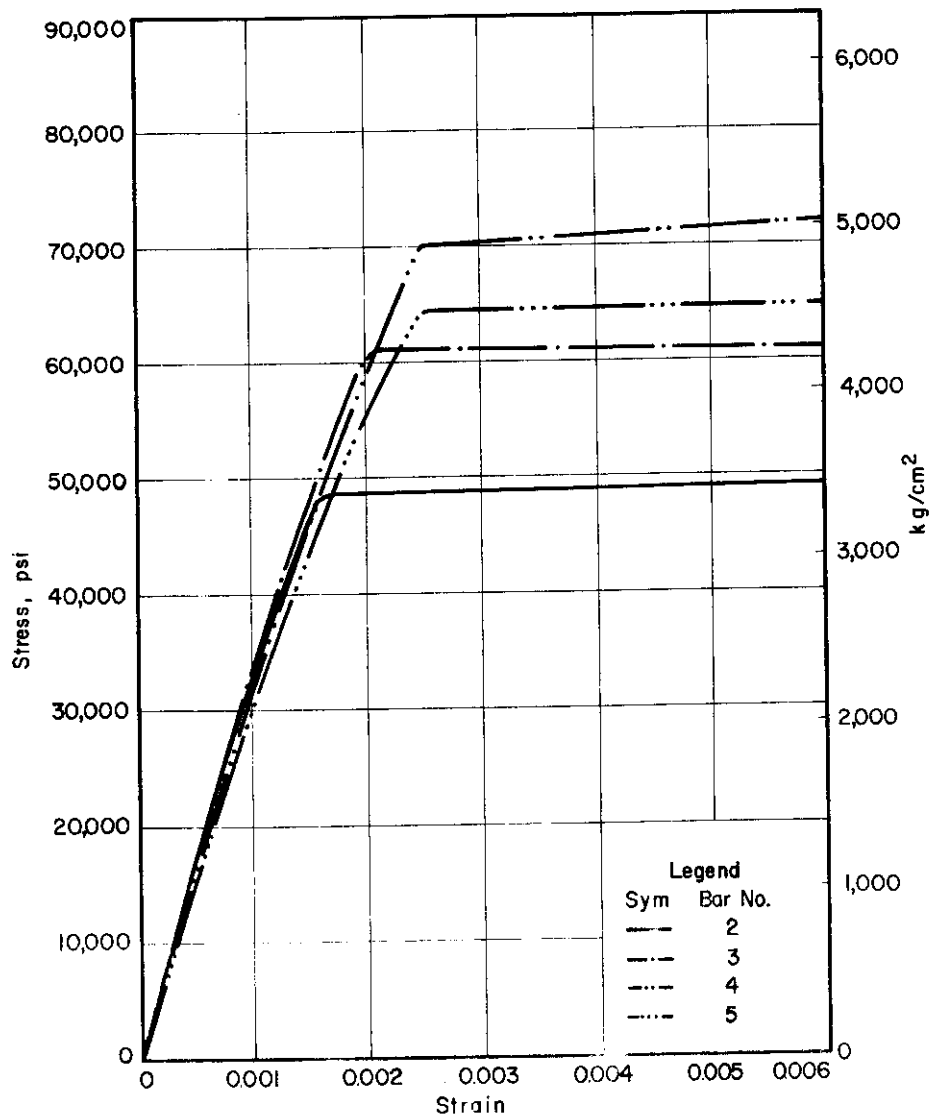


Fig. 2 Average Stress-Strain Curves for Deformed Bars

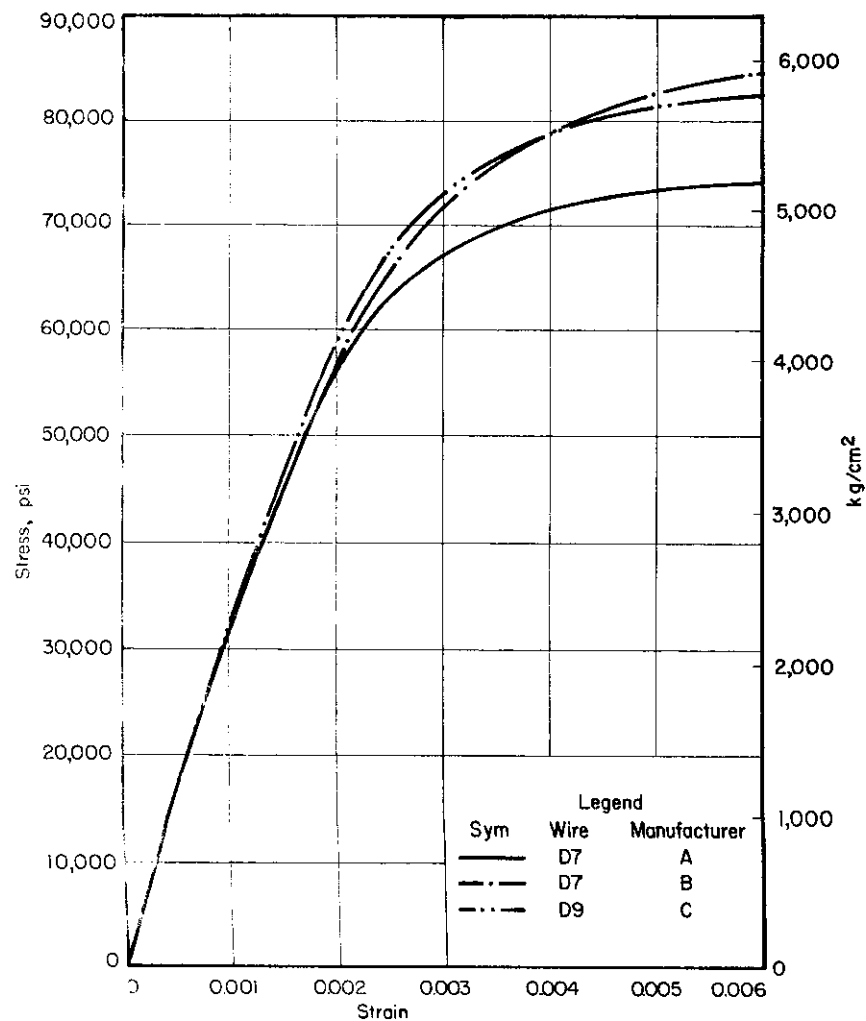


Fig. 3 Average Stress-Strain Curves for Deformed Wires

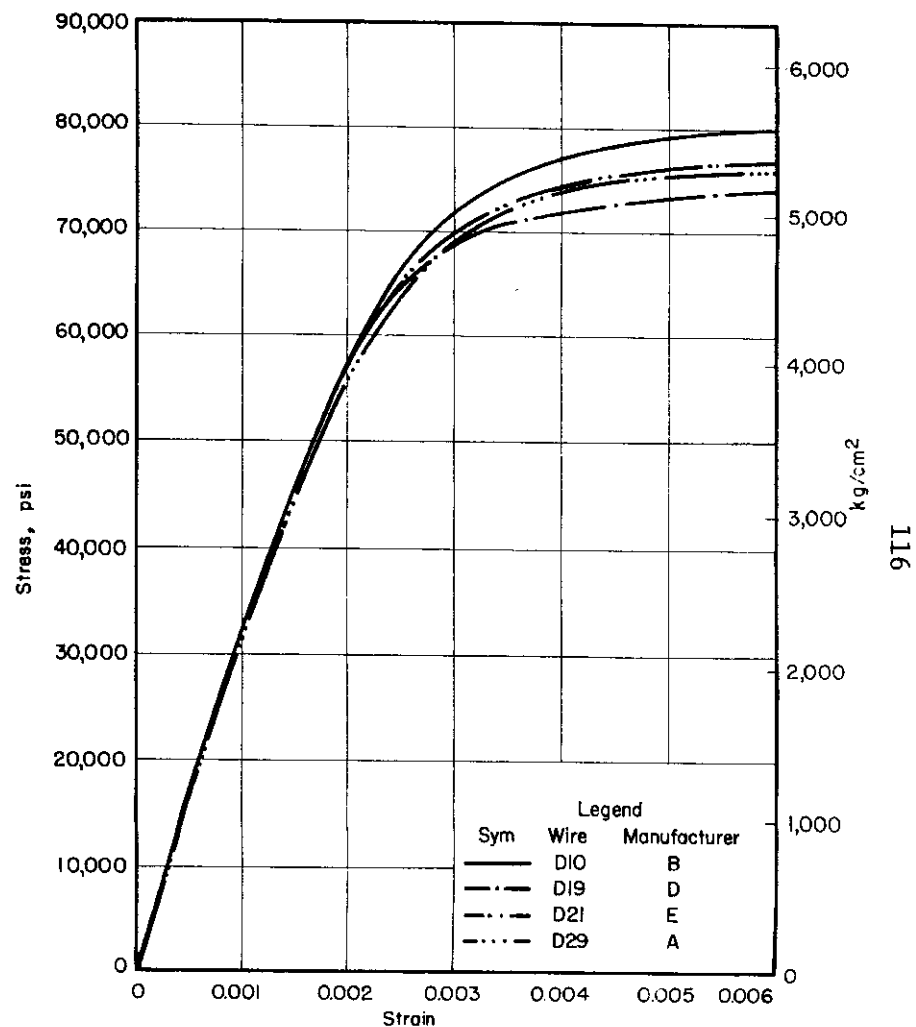


Fig. 4 Average Stress-Strain Curves for Deformed Wires

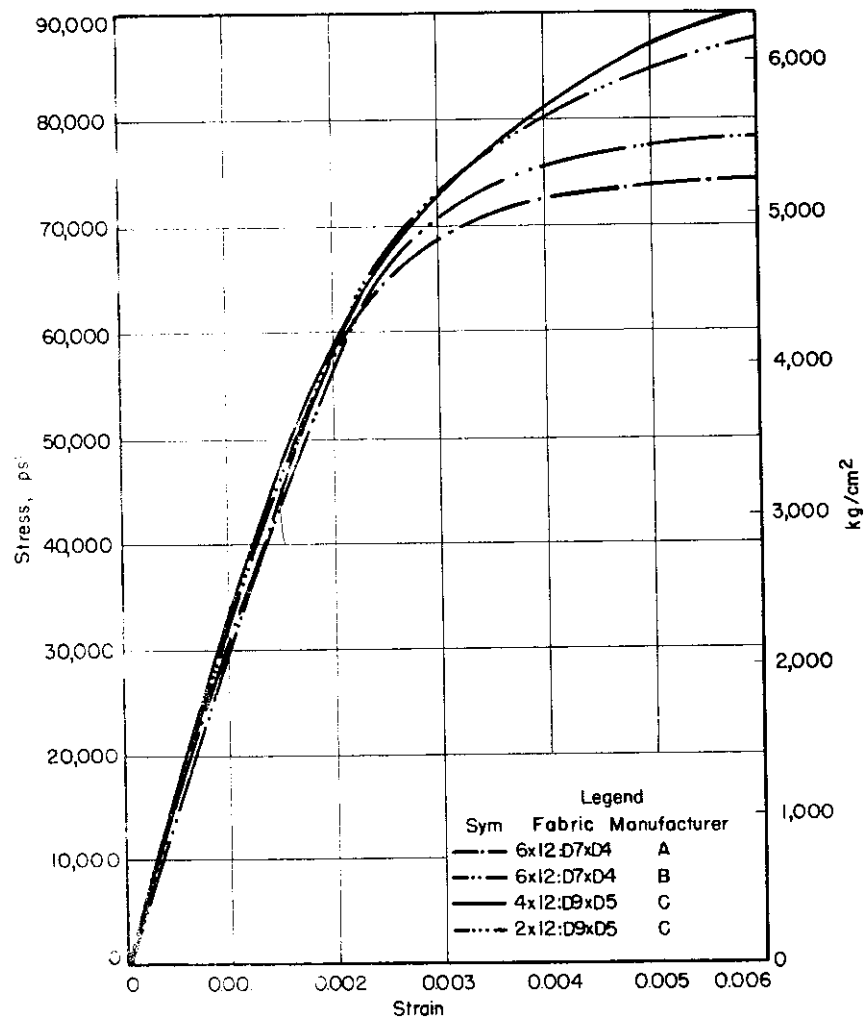


Fig. 5 Average Stress-Strain Curves for Longitudinal Wires from Fabric

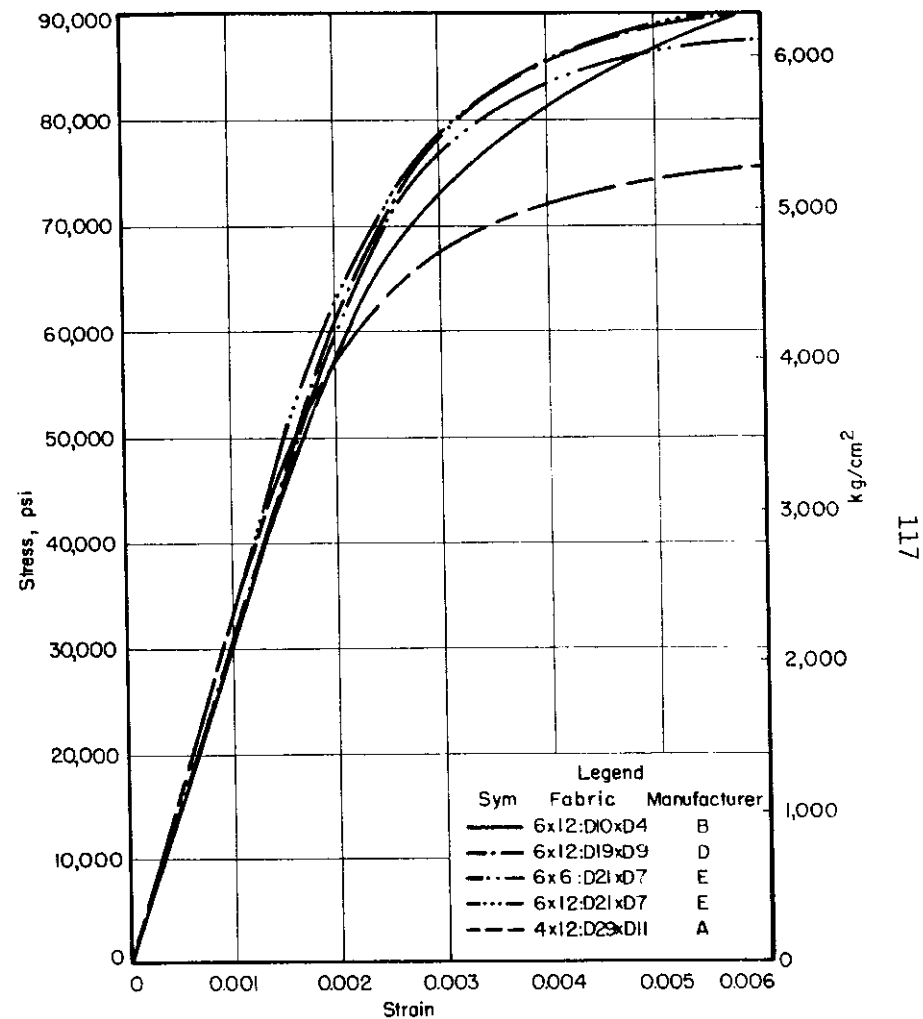


Fig. 6 Average Stress-Strain Curves for Longitudinal Wires from Fabric

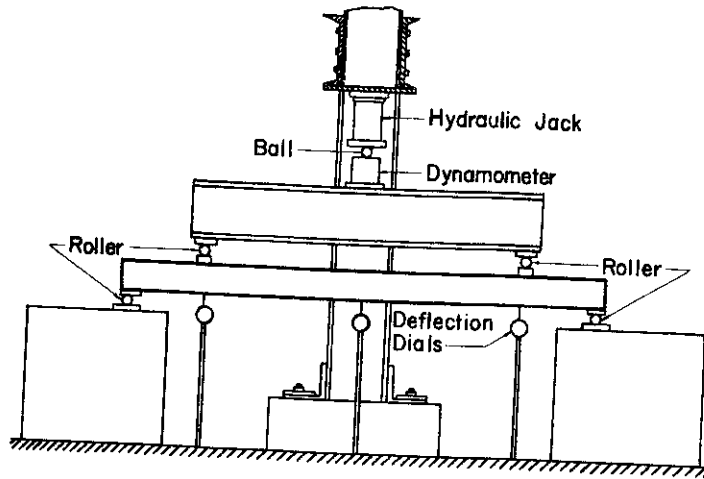


Fig. 7 Schematic of Test Setup

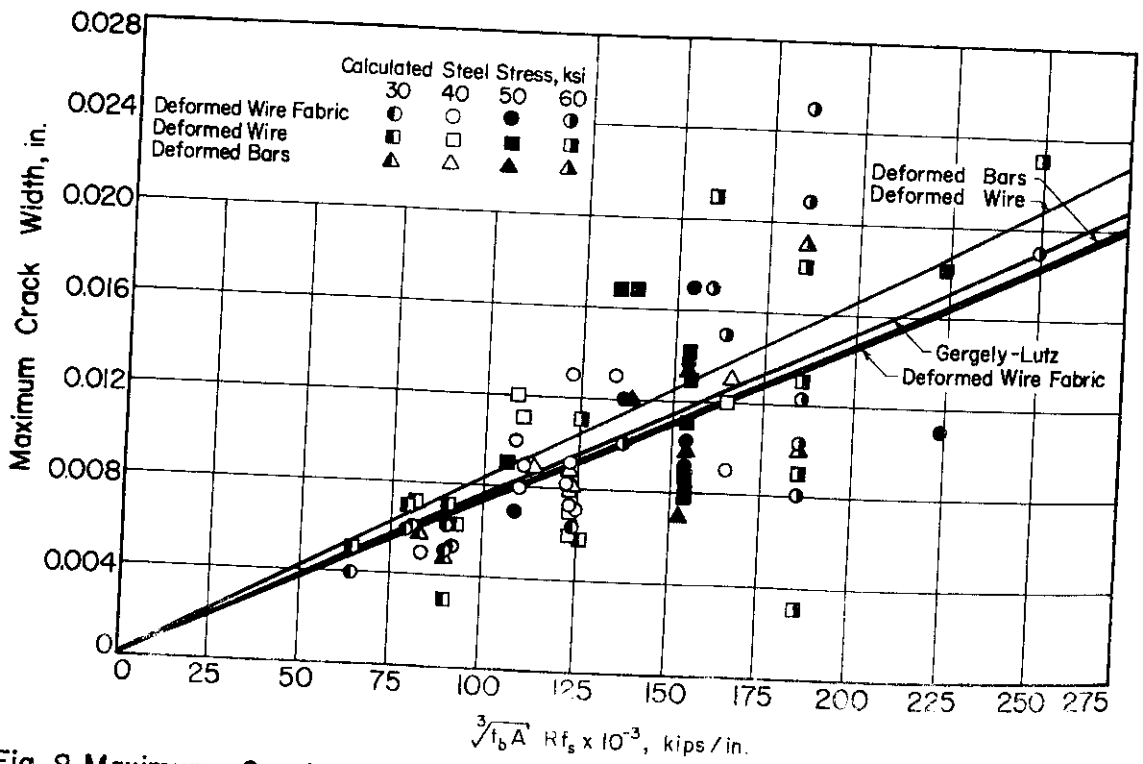


Fig. 8 Maximum Crack Widths at the Extreme Tensile Face

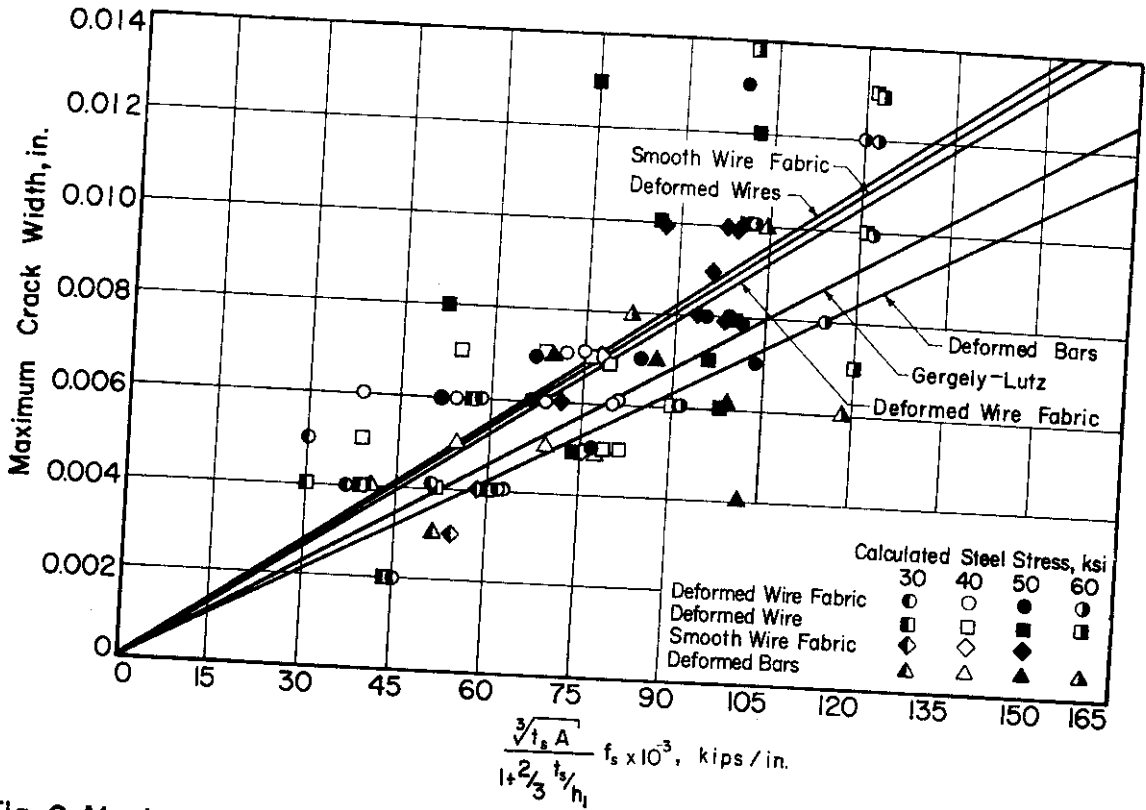


Fig. 9 Maximum Crack Widths at the Level of Reinforcement

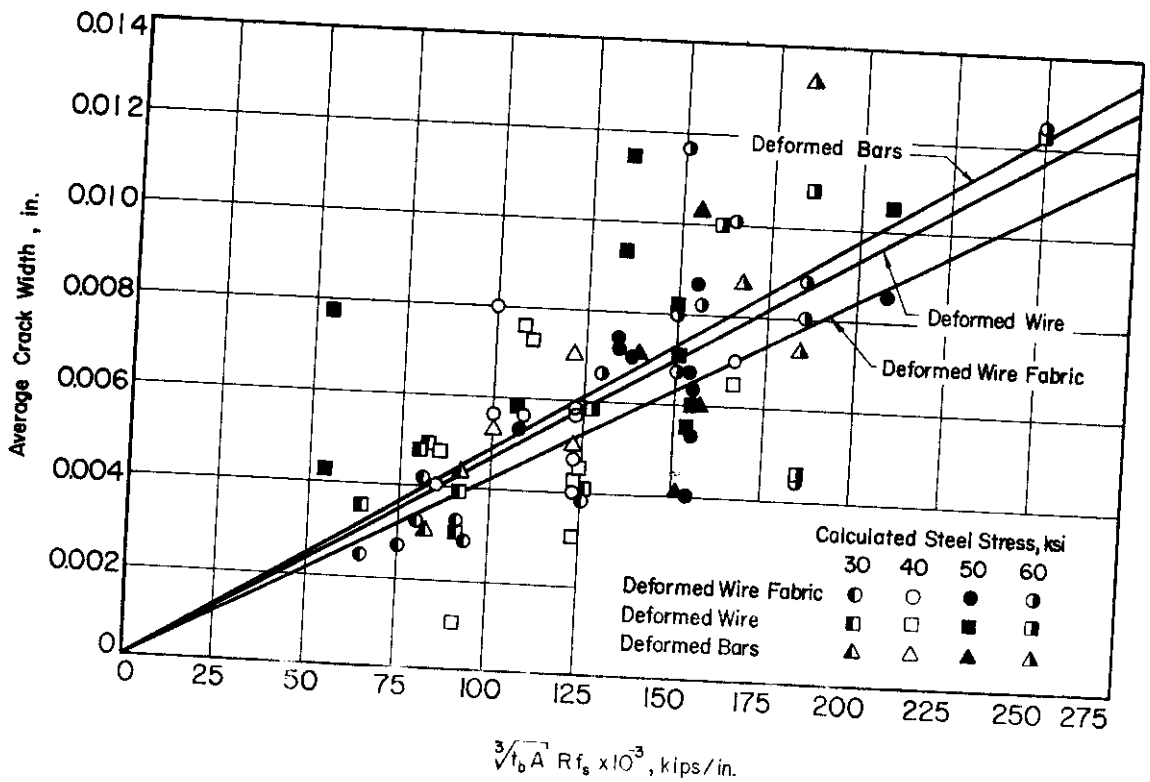


Fig. 10 Average Crack Widths at the Extreme Tensile Face

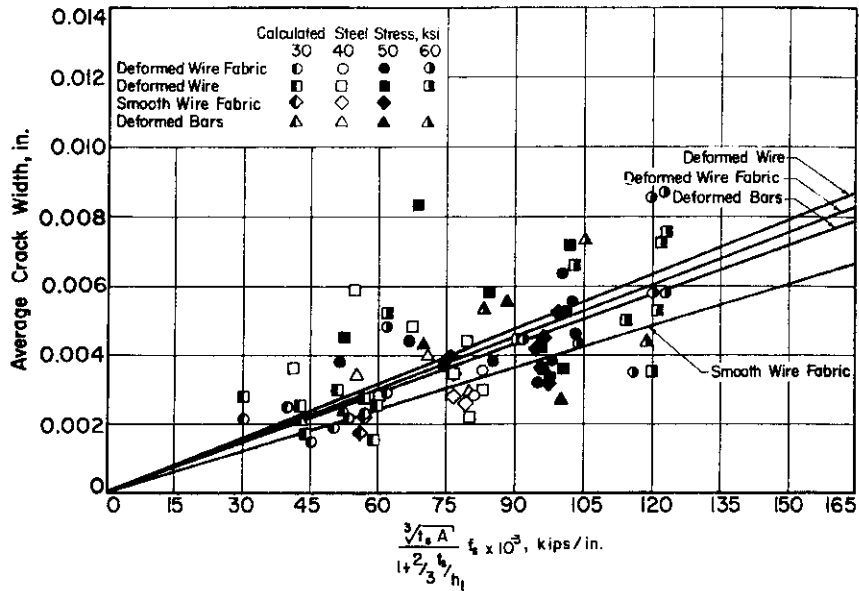


Fig. 11 Average Crack Widths at the Level of the Reinforcement

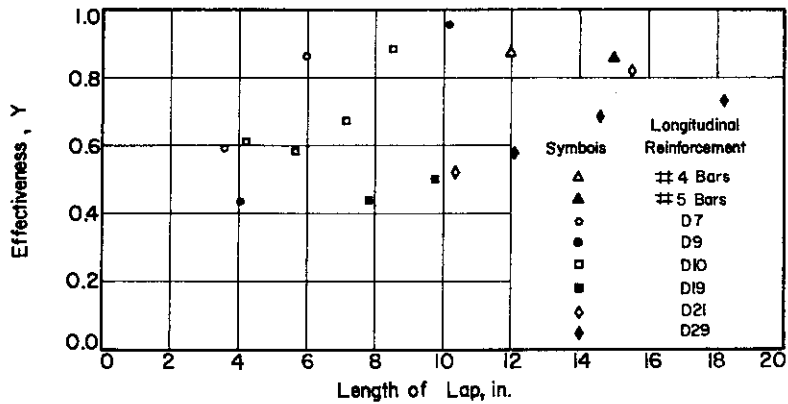


Fig. 12 Effectiveness of Laps in Slabs Reinforced with Deformed Wire and Deformed Bars

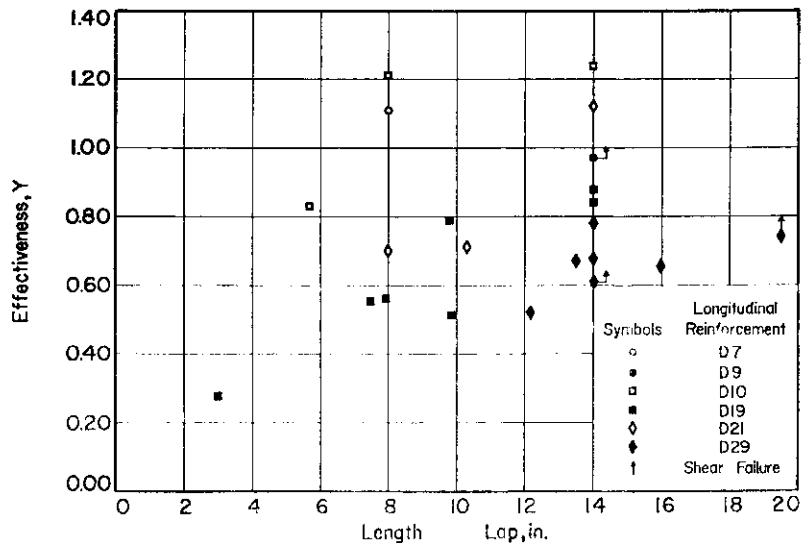


Fig. 13 Effectiveness of Laps in Slabs Reinforced with Deformed Wire Fabric

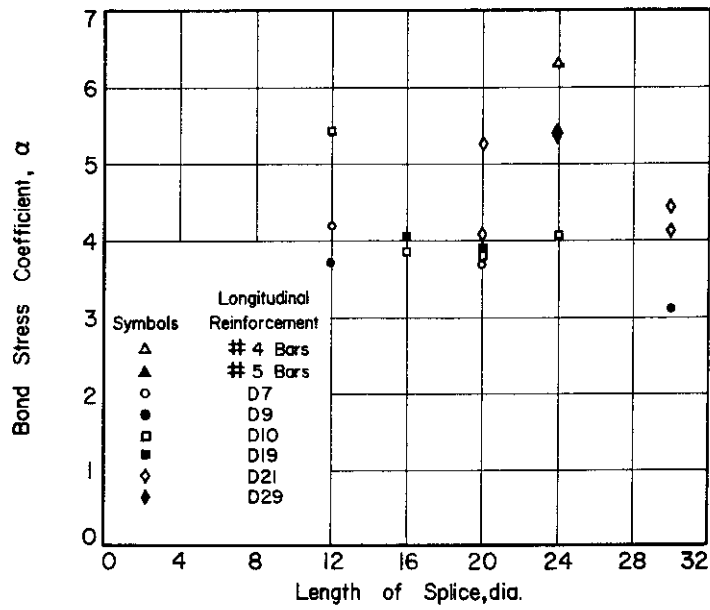


Fig. 14 Bond Stress Coefficient Obtained with Splices of Deformed Wires and Deformed Bars

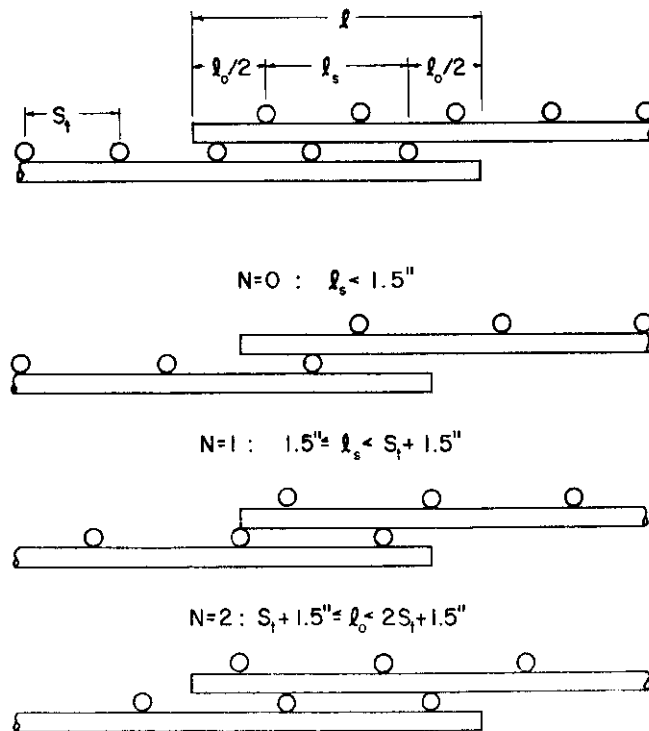


Fig. 15 Splice Details

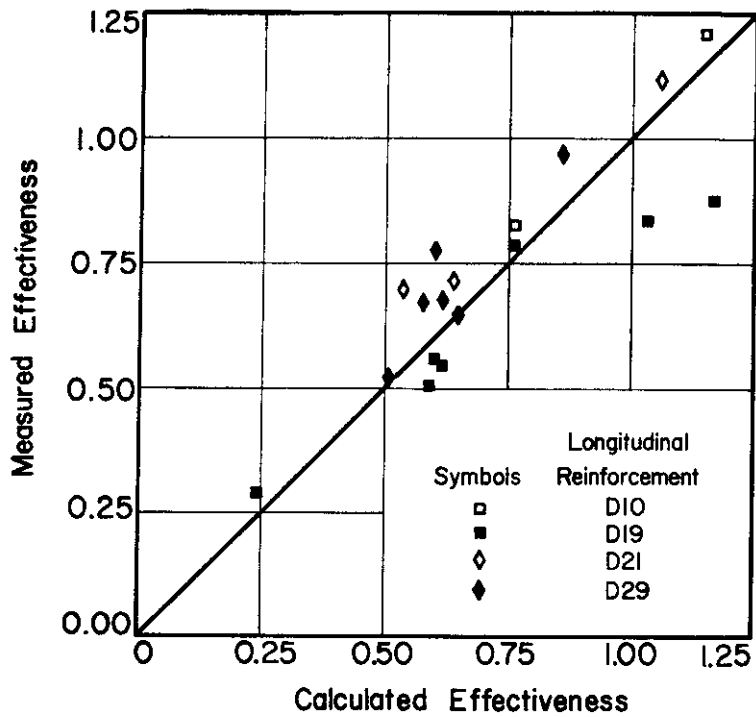


Fig. 16 Comparison of Measured and Calculated Effectiveness

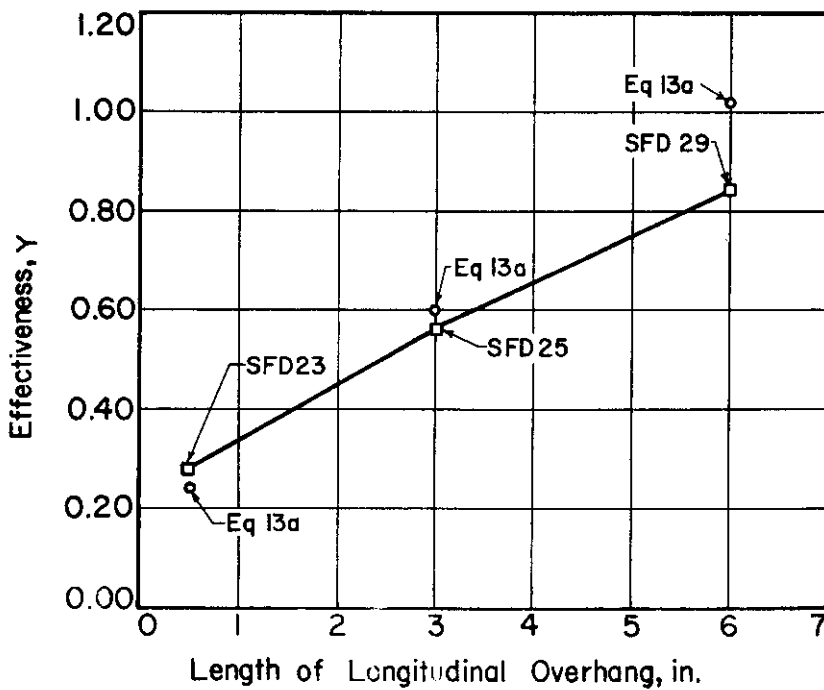


Fig. 17 Influence of Longitudinal Overhang on Splice Effectiveness

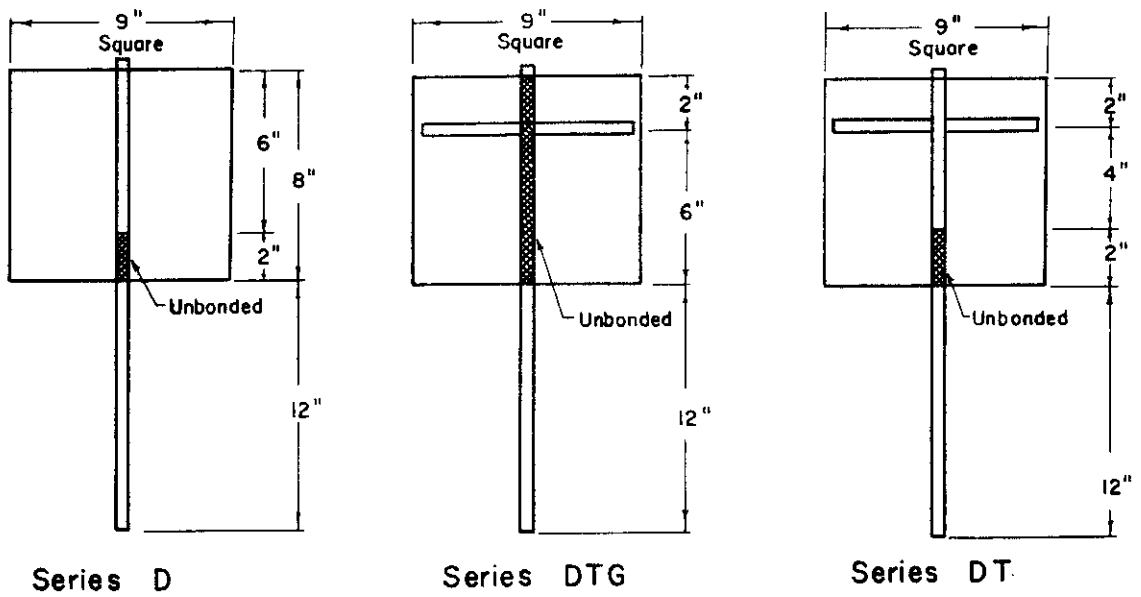


Fig. A.1 Pull Out Specimens

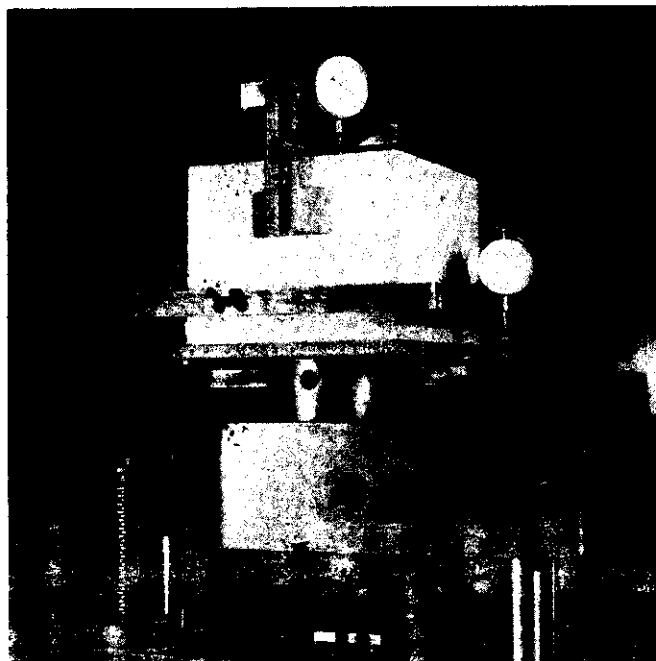


Fig.A.2 Test Setup

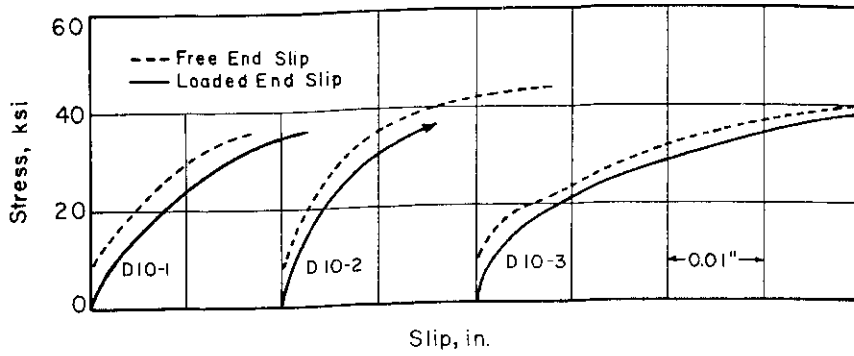


Fig.A.3 Stress-Slip Curves for Specimens with D10 Longitudinal Wire

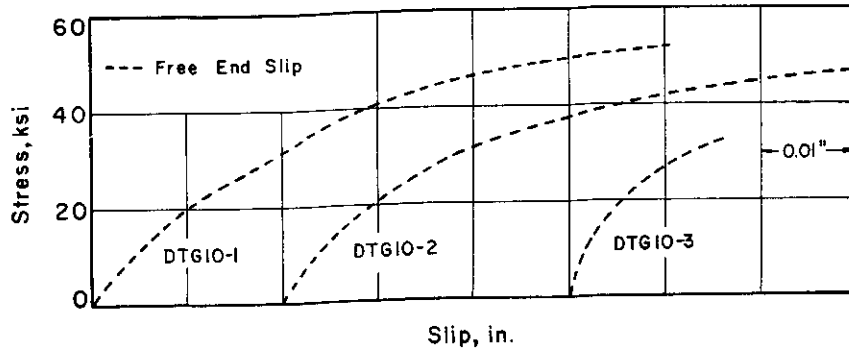


Fig.A.4 Stress Slip Curves for Specimens with Unbonded D10 Longitudinal Wire and D4 Transverse Wire

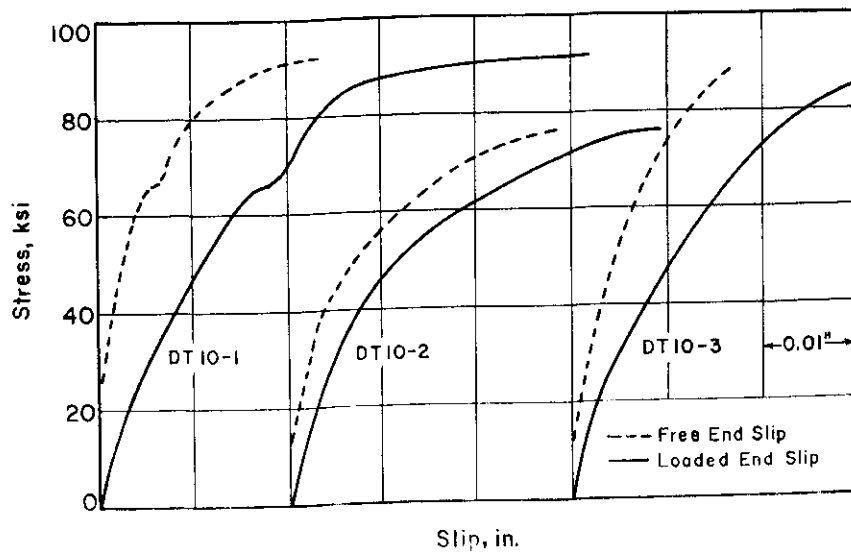


Fig.A.5 Stress-Slip Curves for Specimens with D10 Longitudinal Wire and D4 Transverse Wire

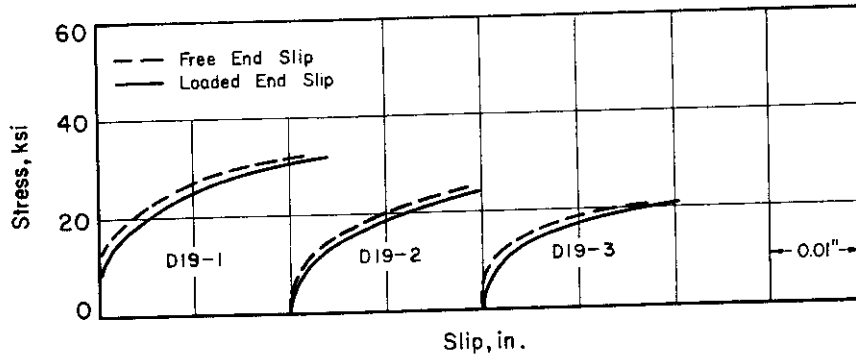


Fig.A.6 Stress-Slip Curves for Specimens with D19 Longitudinal Wire

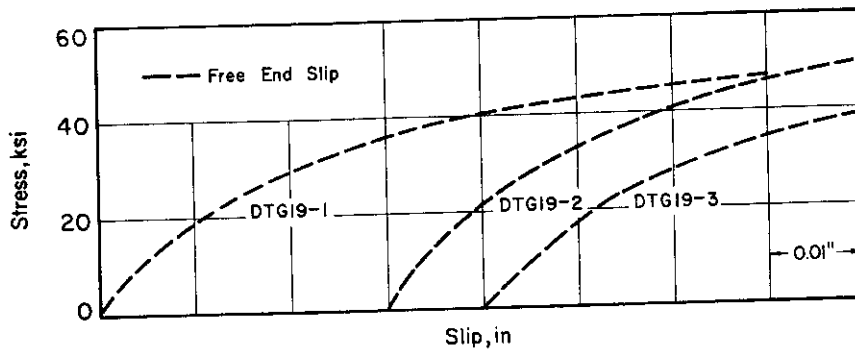


Fig.A.7 Stress-Slip Curves for Specimens with Unbonded D19 Longitudinal Wire and D9 Transverse Wire

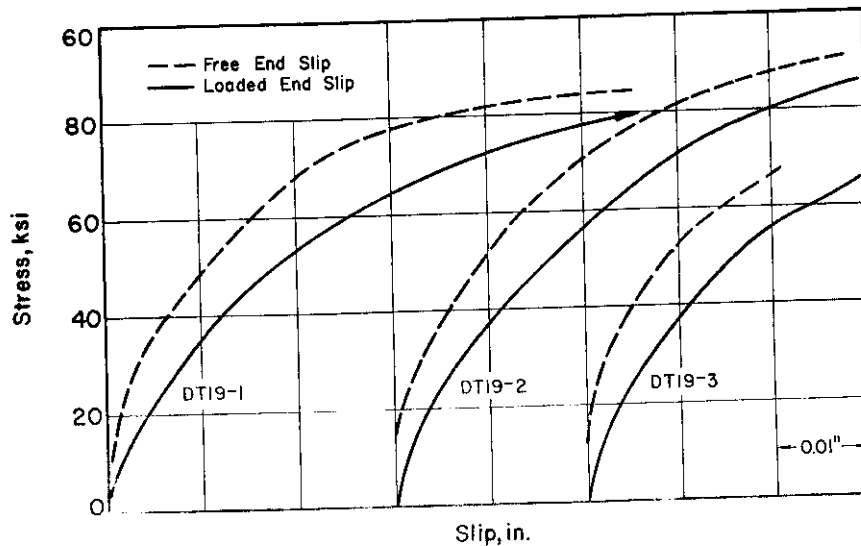


Fig.A.8 Stress-Slip Curves for Specimens with D19 Longitudinal Wire and D9 Transverse Wire

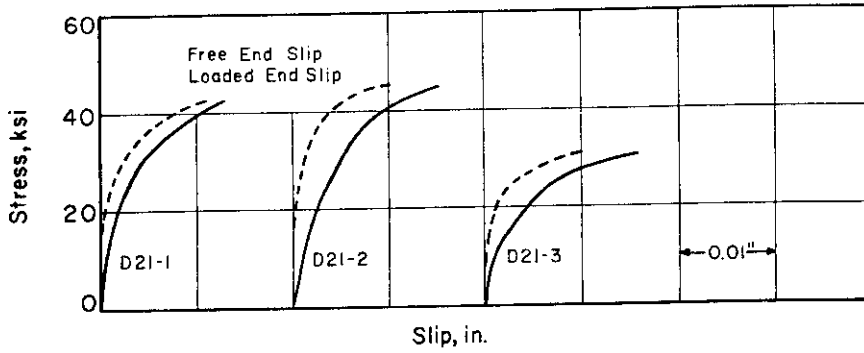


Fig.A.9 Stress - Slip Curves for Specimens with D 21 Longitudinal Wire

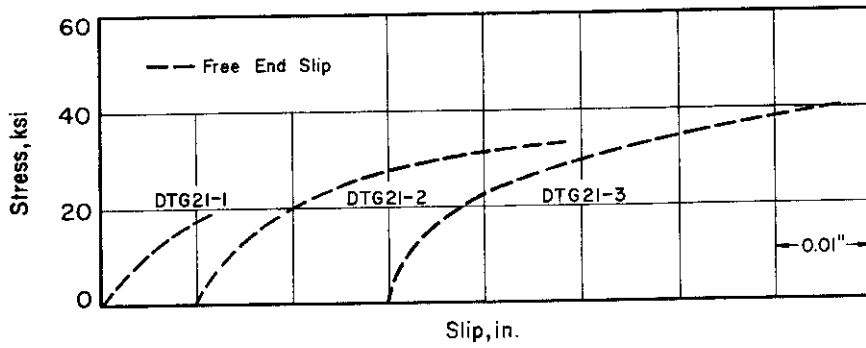


Fig.A.10 Stress-Slip Curves for Specimens with Unbonded D21 Longitudinal Wire and D7 Transverse Wire

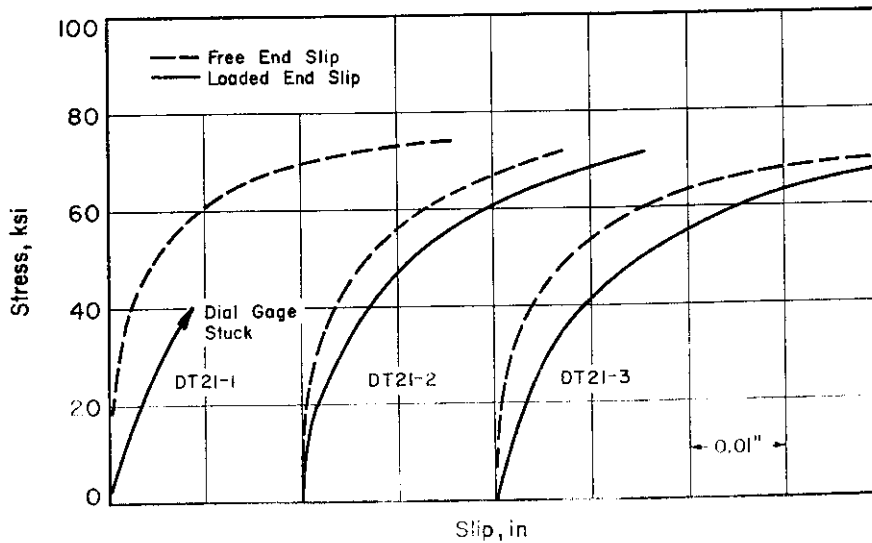


Fig.A.11 Stress-Slip Curves for Specimens with D21 Longitudinal Wire and D7 Transverse Wire

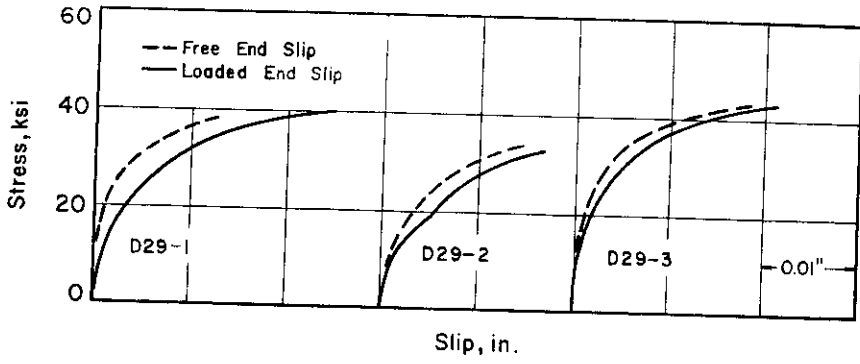


Fig.A.12 Stress-Slip Curves for Specimens with D29 Longitudinal Wire

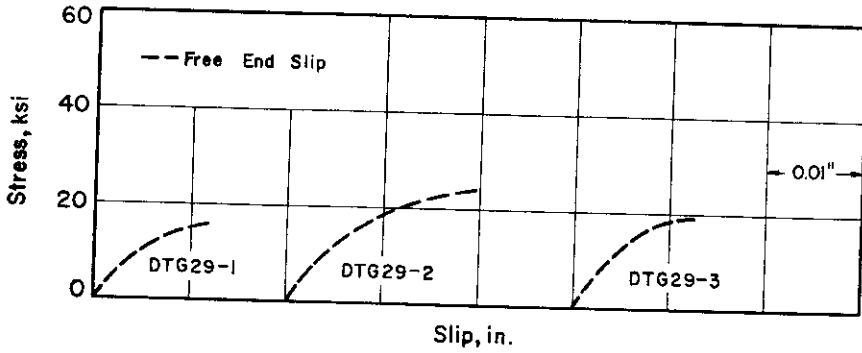


Fig.A.13 Stress-Slip Curves for Specimens with Unbonded D29 Longitudinal Wire and D11 Transverse Wire

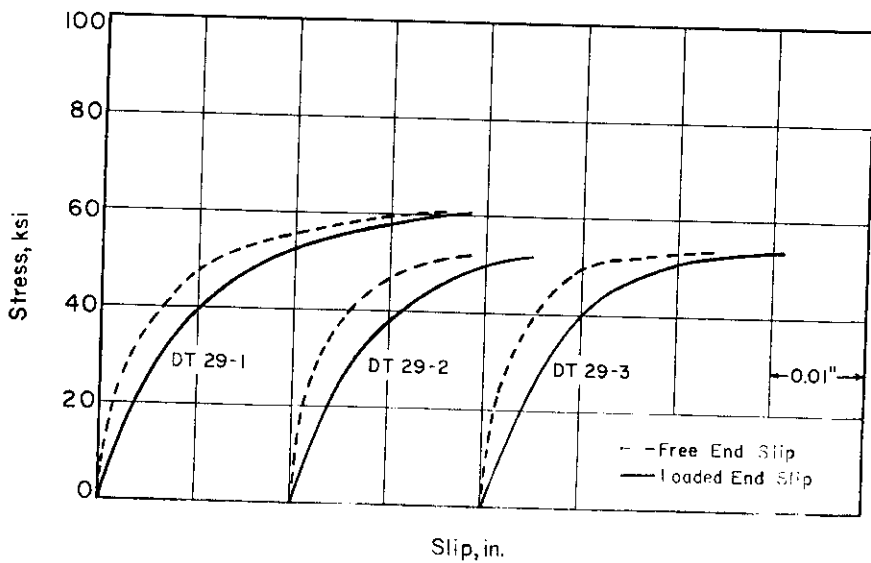


Fig.A.14 Stress-Slip Curves for Specimens with D29 Longitudinal Wire and D11 Transverse Wire

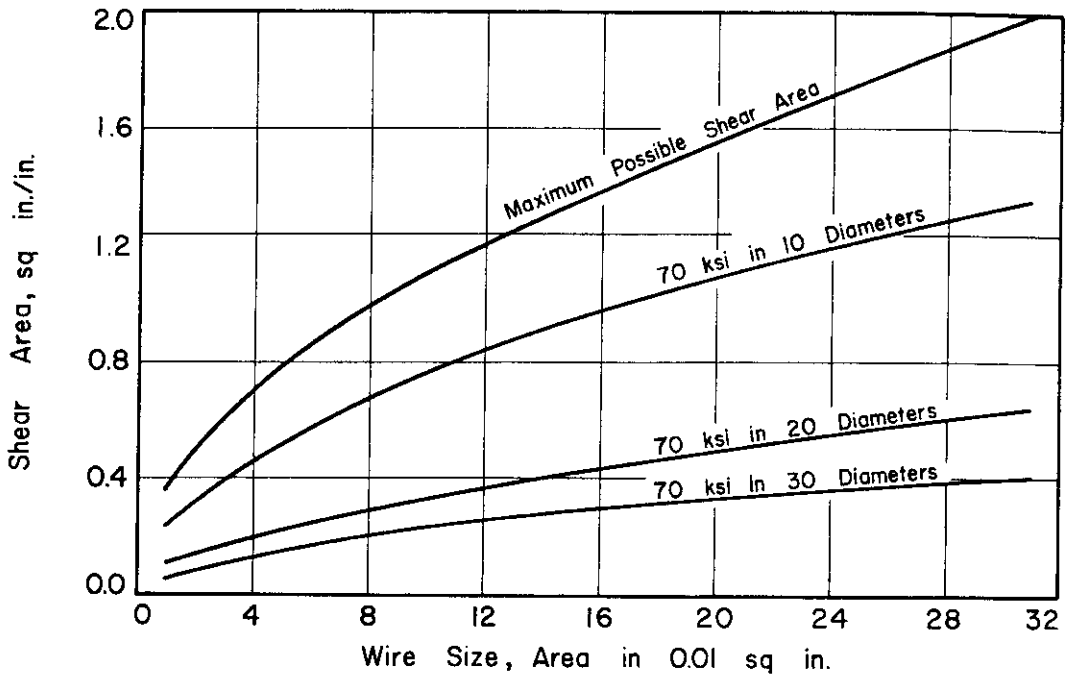


Fig.A.15 Shear Area per Inch Necessary for 70,000 psi at Various Embedment Lengths

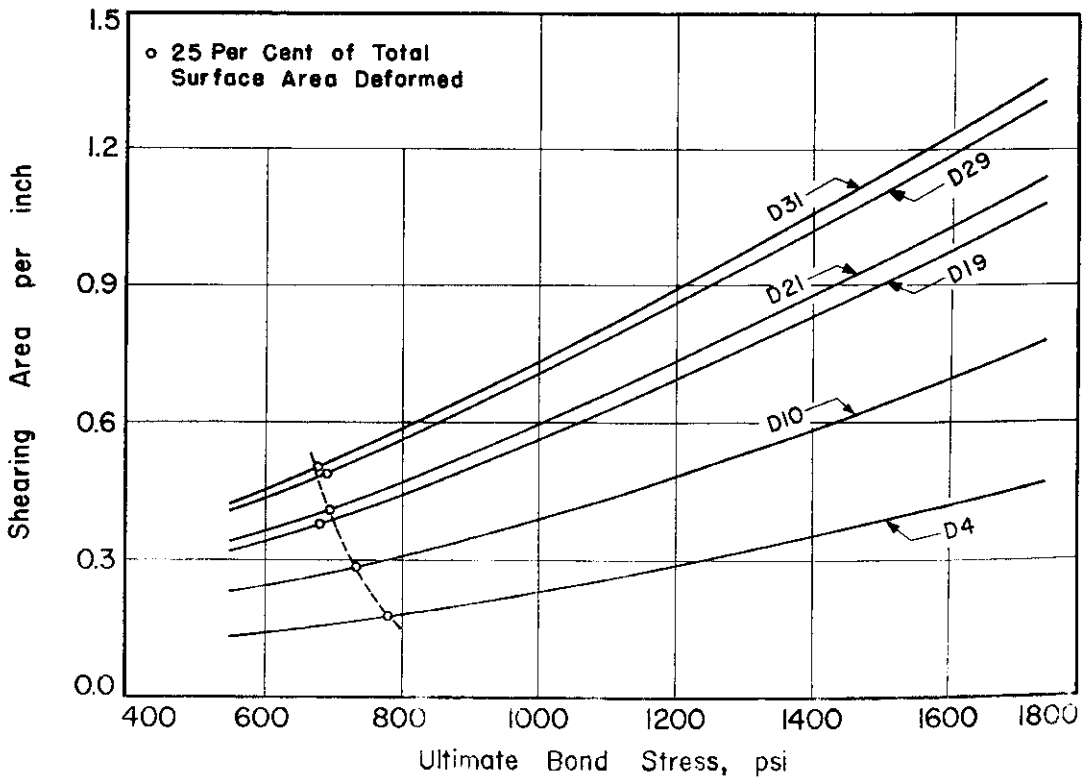


Fig.A.16 Relationship Between Shearing Area per Inch and Ultimate Bond Stress

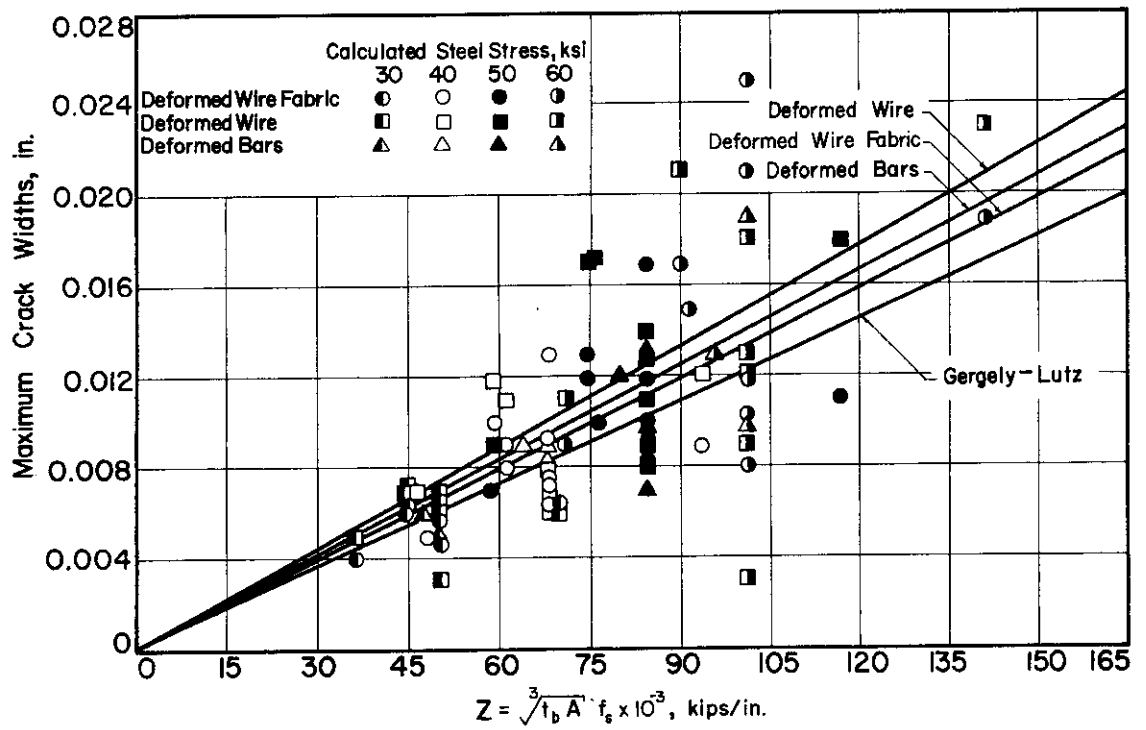


Fig.A.17 Maximum Crack Widths at the Extreme Tensile Fiber versus Z